SPATIAL PROBABILISTIC EVALUATION OF SEA BOTTOM SOIL PROPERTIES AND ITS EFFECT ON FOUNDATION DESIGN

A THESIS SUBMITTED TO
THE GRADUATE SCHOOL OF NATURAL AND APPLIED SCIENCES
OF
MIDDLE EAST TECHNICAL UNIVERSITY

BY

EMİR AHMET OĞUZ

IN PARTIAL FULFILLMENT OF THE REQUIREMENTS
FOR
THE DEGREE OF MASTER OF SCIENCE
IN
CIVIL ENGINEERING

DECEMBER 2017

Approval of the thesis:

SPATIAL PROBABILISTIC EVALUATION OF SEA BOTTOM SOIL PROPERTIES AND ITS EFFECT ON FOUNDATION DESIGN

submitted by **EMİR AHMET OĞUZ** in partial fulfillment of the requirements for the degree of **Master of Science in Civil Engineering Department, Middle East Technical University** by,

Prof. Dr. Gülbin DURAL ÜNVER _____
Dean, Graduate School of **Natural and Applied Sciences**

Prof. Dr. İsmail Özgür YAMAN _____
Head of Department, **Civil Engineering**

Asst. Prof. Dr. Nejan HUVAJ SARIHAN _____
Supervisor, **Civil Engineering Dept., METU**

Examining Committee Members:

Prof. Dr. Ayşen DENER AKKAYA _____
Statistics Dept., METU

Asst. Prof. Dr. Nejan HUVAJ SARIHAN _____
Civil Engineering Dept., METU

Asst. Prof. Dr. Onur PEKCAN _____
Civil Engineering Dept., METU

Assoc. Prof. Dr. Zeynep GÜLERCE _____
Civil Engineering Dept., METU

Assoc. Prof. Dr. Sami Oğuzhan AKBAŞ _____
Civil Engineering Dept., Gazi University

Date: 27.12.2017

I hereby declare that all information in this document has been obtained and presented in accordance with academic rules and ethical conduct. I also declare that, as required by these rules and conduct, I have fully cited and referenced all material and results that are not original to this work.

Name, Last Name: Emir Ahmet OĞUZ

Signature:

ABSTRACT

SPATIAL PROBABILISTIC EVALUATION OF SEA BOTTOM SOIL PROPERTIES AND ITS EFFECT ON FOUNDATION DESIGN

OĞUZ, Emir Ahmet

M.Sc., Department of Civil Engineering

Supervisor: Asst. Prof. Dr. Nejan HUVAJ SARIHAN

December 2017, 127 pages

The spatial correlation length (SCL), or the scale of fluctuation, is a parameter for describing the spatial variability of a soil property and is one of the important parameters used in random field theory. Studies reporting the SCL of soil properties of offshore/nearshore soils are rather limited in the literature. In this study, the vertical SCL is determined using site investigation data from two nearshore and one large offshore sites in Turkish waters. In nearshore sites, a total of 41 boreholes and Standard Penetration Tests (SPT) reaching to 35 m depth from seabed, in water depths of up to 26 m; and in the large offshore site, 65 cone penetration test (CPT) soundings (having 10-200 m lengths in seabed) in water depths of up to 64 m, are utilized. Based on extensive data, the vertical SCL is calculated using four different autocovariance functions. Among these four functions, the squared exponential function gives the highest and cosine exponential function gives the smallest SCL values. The vertical SCL values based on SPT-N value, CPT tip resistance, friction ratio and sleeve friction

are observed to be within typical ranges reported in the literature for similar soil groups, both onshore and offshore. The vertical SCL based on SPT-N value is larger than the SCL based on CPT tip resistance, friction ratio and sleeve friction. The vertical SCL based on SPT-N is slightly larger in sandy mixture soils as compared to clayey soils (about 2 m in sand mixtures and about 1.7 m in clays). In CPT data, deep water (greater than 10 m water depths) clays and sands have greater SCL than shallow water clays and sands. In both SPT and CPT cases, "constant mean with depth" approach always gives larger SCL as compared to "depth-dependent mean (or trend)" approach. The effects of SCL and coefficient of variation of soil parameters on settlement and bearing capacity of a shallow strip foundation are demonstrated by using random finite element analysis tools; RSETL2D and RBEAR2D, where all soil parameters are assumed to be lognormally distributed. The results of this study add to the limited database of spatial correlation lengths based on real data and could be useful for future studies on reliability assessment of nearshore and offshore foundations. Moreover, the results of random finite element analyses indicate that the variability of soil parameters, in terms of coefficient of variation and spatial correlation length, has a significant effect on settlement and bearing capacity of shallow strip footings.

Keywords: variability, spatial correlation length, scale of fluctuation, nearshore-offshore soils, reliability

ÖZ

DENİZ TABANI ZEMİN ÖZELLİKLERİNİN MEKANSAL OLASILIKSAL DEĞERLENDİRMESİ VE TEMEL TASARIMINDA ETKİSİ

OĞUZ, Emir Ahmet

Yüksek Lisans, İnşaat Mühendisliği Bölümü

Tez Yöneticisi: Yrd. Doç. Dr. Nejan HUVAJ SARIHAN

Aralık 2017, 127 sayfa

Mekansal korelasyon mesafesi (MKM), diğer bir adıyla dalgalanma ölçeği, zeminin değişkenliğini tanımlayan bir parametredir ve rastsal alan teorisinde kullanılan önemli parametrelerden biridir. Açık ve sığ denizlerde deniz tabanı zeminlerinin MKM değerini bildiren çalışmalar literatürde oldukça sınırlı sayıdadır. Bu çalışmada, Türkiye karasularında iki sığ deniz ve bir açık deniz sahasında deniz tabanı zemin etüd verileri kullanılarak düşey yönde MKM değerleri belirlenmiştir. Sığ deniz sahalarında maksimum 26 m su derinliklerinde ve deniz tabanından 35 m zemin derinliklerine inen 41 adet sondaj ve Standard Penetrasyon Deneyi (SPT) verisi, açık deniz sahasında ise deniz tabanından itibaren derinlikleri 10-200 m olan, ve maksimum 64 m su derinliklerinde 65 adet koni penetrasyon deneyi (CPT) ölçümleri kullanılmıştır. Kapsamlı verilere dayanarak, düşey yönde MKM dört farklı otokovaryans fonksiyonu kullanılarak elde edilmiştir. Bu dört fonksiyon arasında kare üssel fonksiyon en yüksek MKM değerlerini verirken, kosinüs üssel fonksiyon ise en düşük MKM değerlerini

vermiştir. SPT-N değeri, CPT uç direnci, yanal sürtünme ve sürtünme oranından elde edilen MKM değerleri, hem karada hem deniz tabanı zeminlerinde benzer zemin grupları için literatürde belirtilen tipik aralıklardadır. SPT-N değerinden elde edilen MKM, CPT uç direnci, yanal sürtünme ve sürtünme oranından elde edilen MKM değerinden büyüktür. SPT-N değerinden elde edilen düşey yönde MKM değeri kumlu karışım zeminlerde killi zeminlere göre biraz daha yüksektir (kumlarda yaklaşık 2 m, killerde ise 1.7 m). CPT verilerinde, açık deniz (10 m'den fazla su derinliğinde) killer ve kum karışımları, sığ deniz killeri ve kum karışımlarına göre daha yüksek MKM değerine sahiptir. SPT ve CPT verilerinin her ikisi kullanıldığı durumda da MKM bulunmasında "derinlikle sabit ortalama değer" yöntemi, "derinlikle değişen ortalama (trend)" yöntemine kıyasla daha fazla MKM değeri vermiştir. Bu istatistiksel çalışmanın sonuçları, literatürdeki, az sayıdaki, gerçek saha verilerine dayalı sığ ve açık deniz tabanı mekansal korelasyon mesafesi veri tabanına eklenecek ve bu tip sahalarda yapılacak yapıların güvenilirlik değerlendirmelerinde yararlı olacaktır. Buna ek olarak, rassal sonlu elemanlar yöntemi analizlerinin sonuçları, zemin parametrelerindeki değişkenliğin (varyasyon katsayısı ve mekansal korelasyon mesafesi) sığ sürekli temellerde oturma miktarına ve taşıma kapasitesine önemli etkileri olduğunu göstermektedir.

Anahtar kelimeler: değişkenlik, mekansal korelasyon mesafesi, dalgalanma ölçeği, sığ-açık deniz tabanı zeminler, güvenilirlik

To my Family,

ACKNOWLEDGEMENTS

I would like to express my sincere gratitude to my advisor, Asst. Prof. Dr. Nejan Huvaj Sarıhan. Her continuous support in my undergraduate and graduate educations, endless guidance and always believing in me helped me so much that I could not describe.

I would also like to thank Prof. Dr. Ayşen Dener Akkaya for her guidance and comments throughout my study. I am really grateful to her for sharing her knowledge and helping me.

I would like to thank the members of my thesis examining committee; Assoc. Prof. Dr. Zeynep Gülerce, Asst. Prof. Dr. Onur Pekcan, Assoc. Prof. Dr. Sami Oğuzhan Akbaş for their interests on my thesis topic and valuable contributions to this study.

I am grateful to my colleagues for their support and suggestions about the thesis progress. They have always helped me to overcome the obstacles.

I would like to thank and express my gratitude to my mother Mahmude Güldür, my sisters Rabia Oğuz and Hümeyra Merve Oğuz for their continuous support and always believing in me. I am grateful for their love and patience.

I would like to thank my life partner, my friend and beloved Nihan Öngay for her support and patience throughout my life. Her believing in me always encouraged me in my studies.

TABLE OF CONTENTS

LIST OF TABLES

LIST OF FIGURES

LIST OF ABBREVIATIONS

ACF	Sample Autocorrelation Function
Autoreg	Second Order Autoregressive
CH	High Plasticity Clay
CL	Low Plasticity Clay
CosExp	Cosine Exponential
COV	Coefficient of Variation
CPT	Cone Penetration Test
CPTu	Piezocone Penetration Test
cu	Undrained Shear Strength
CU	Consolidated Undrained
DPL	Dynamic Probing
Dr	Relative Density
E	Elastic Modulus
Exp	Exponential
FEM	Finite Element Method
FORM	First Orders Reliability
FOSM	First Order Second Moment Approximation
FR	Friction Ratio

FS	Factor Of Safety
MH	High Plasticity Silt
ML	Low Plasticity Silt
N	Number Of Blow Count of Standard Penetration Test
Pf	Probability Of Failure
q_c	Cone Tip Resistance
RBEAR2D	Random Finite Element Method Bearing Capacity Software
RFEM	Random Finite Element Method
RSETL2D	Random Finite Element Method Settlement Software
SC	Clayey Sand
SCL	Spatial Correlation Length (Scale of Fluctuation)
SCL_{CPT-FR}	Spatial Correlation Length Based on CPT Friction Ratio
SCL_{CPT-Fs}	Spatial Correlation Length Based on CPT Side Friction
SCL_{CPT-q_c}	Spatial Correlation Length Based on CPT Tip Resistance
SCL_{SPT-N}	Spatial Correlation Length Based on SPT-N Blowcount
SFEM	Stochastic Finite Element Method
SLS	Serviceability Limit State
SM	Silty Sand
SP	Poorly Graded Sand

SPT	Standard Penetration Test
SPT-N	Standard Penetration Test N Value
SqrExp	Squared Exponential
Std	Standard Deviation
SW	Well-Graded Sand
UC	Unconfined Compression
ULS	Ultimate Limit State
USCS	Unified Soil Classification System
UU	Unconsolidated-Undrained
w	Water Content
δ	Spatial Correlation Length (Scale of Fluctuation)

CHAPTER 1

INTRODUCTION

1.1.Problem Statement

Deterministic approaches are known to have some limitations, especially in modern geotechnical engineering practice, since they are not taking into account the heterogeneous and variable nature of the soils. The soil has both point variability and spatial variability which should be included in the reliability based designs and risk assessments. In the last two decades, probabilistic (stochastic) approaches are becoming more popular, where the variability of the soil can be considered by representing soil parameters via statistical distributions, using Monte Carlo simulations or creating random fields to represent the heterogeneity of the soil volume. Although deterministic approaches provide only a single result, such as the factor of safety, settlement amount, or ultimate bearing capacity etc., probabilistic approaches provide results with a range, which can be used in reliability based design allowing the engineers and decision-makers to quantify the probability of failure and risk.

Variability and uncertainties in soil properties have been a topic of interest for geotechnical engineers, especially in the recent decades. In conventional geotechnical design, characteristic/representative value of soil parameters are used leading often to a Factor of Safety which is unable to give any guidance on variability (Li and Lumb, 1987, Cherubini 2000). Because of the inherent variability of soil properties from site to site (and within a site), Baecher and Christian (2003) suggested that it is “neither easy nor wise to apply typical values of soil property … for a reliability analysis”. The key issue here is that a single characteristic value is unable to model variability, which

needs at least two numbers (e.g. a mean and a standard deviation). The importance and the effects of determining the variability in soil properties have been illustrated by various researchers with examples from actual case studies (Lacasse and Nadim 1996, Cho and Park 2009, Cho 2010, Zhang and Chen 2012, Carswell et al. 2013, Sarma et al. 2014, Liu et al. 2015, Jha 2016). Parameters of soil used in any design, such as foundations, dams, natural slopes, road cuts, embankments, and levees, have significant uncertainties due to limited site investigations and laboratory tests in addition to the uncertainties and limitations involved in empirical correlations (Figure 1. 1). Furthermore, there is no way to make enough soil investigations to get deterministic values for soil parameters at every point (Vanmarcke 1977). For this reason, in stochastic methods, the variability of soil parameters is defined by a mean, a standard deviation; and a spatial correlation length (SCL). The importance of SCL in soils and effects on foundation design problems was brought to the attention of the geotechnical engineering community in the mid 1990's by Griffiths and colleagues (e.g. Griffiths and Fenton 1993, Paice et al. 1996, Griffiths and Fenton 2007, Fenton and Griffiths 2008, Griffiths et al. 2009) with the development of the Random Finite Element Method (RFEM). The SCL is the distance over which the soil parameters tend to be spatially correlated. The SCL may be anisotropic (Cherubini 2000) with a higher value in the horizontal direction. In this study, however, only the vertical SCL is studied.

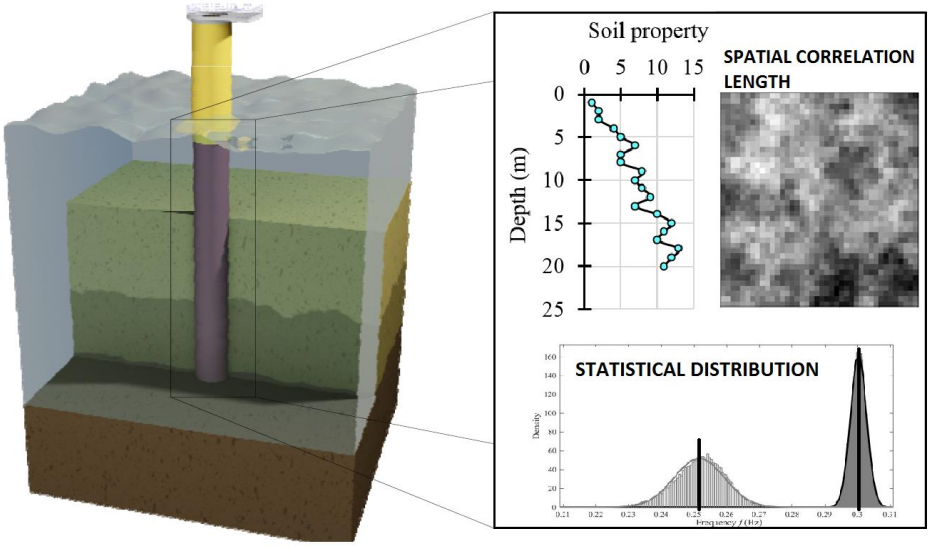

Figure 1. 1 Schematic presentation of variability in seabed soil properties along an offshore monopile

Lacasse (2013) emphasized that a single value of factor of safety (FS) cannot represent the safety level of the slopes. The slopes with larger FS may have a greater probability of failure than the ones with low FS. Figure 1. 2 shows probability density functions of two slopes with different FS values, and it is seen that higher FS value does not mean a less probability of failure. There is no direct relationship between FS and probability of failure for a slope. Likewise, Oguz et al. (2017) reported that deterministically calculated FS greater than 1.0 does not always mean a "safe slope", rather, the safety level is influenced by the level of uncertainty in soil properties, influenced by the extent and the quality of geotechnical data available. For the critical failure surface as well, the failure surfaces with higher FS values may have a greater probability of failure (lower reliability indexes) than deterministically critical failure surface if soil parameters have high uncertainty (Oguz et al. 2017).

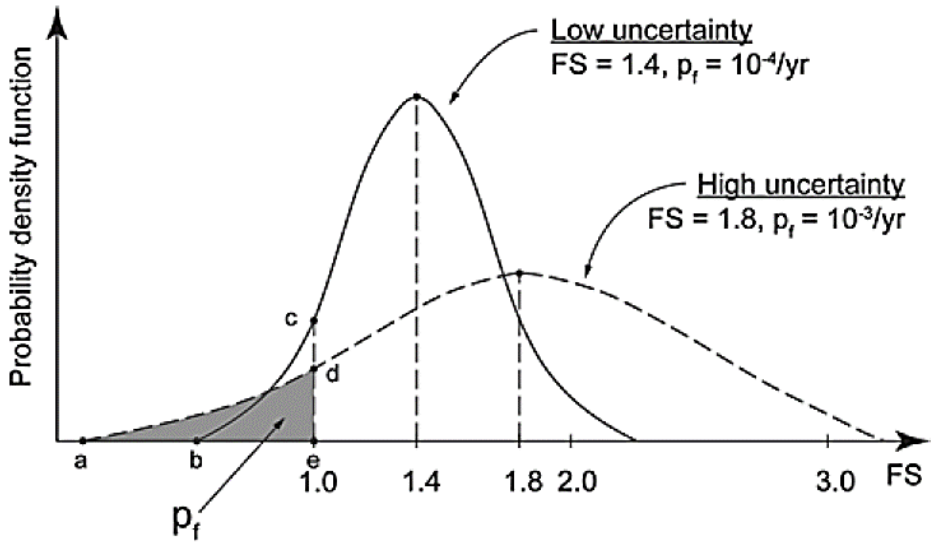

Figure 1. 2 Probability density functions of two slopes with different FS values Lacasse (2013)

1.2.Research Objectives

The objectives of this study can be listed as follows:

i. Identifying the typical characteristics, statistical information and variability of nearshore/offshore sea bottom soils.
ii. Determination of the spatial correlation length in the vertical direction based on field tests (SPT and CPT).
i. Investigation of the effects of variability and SCL of soil parameters on geotechnical design problems such as settlement, and ultimate bearing capacity using random finite element method.

The results of the present study add to the database of spatial correlation lengths based on real data and could be useful for future studies on reliability assessment of offshore foundations using advanced tools such as the random finite element method. In addition, this study clearly indicates that spatial variability in soils have significant effects on the design of foundations.

1.3. Scope

Chapter 2 presents a literature review on spatial correlation length and effects on design problems. In Chapter 3, the methodology of data evaluation is explained in details. In addition, treatment of raw data and assumptions made in the analyses are explained. In Chapter 4, the description of sites, calculated spatial correlation lengths and soil characteristics are provided. In Chapter 5, the effects of variability of sea bottom soil are investigated by using software RBEAR2D and RSETL2D (Fenton and Griffiths 2008) utilizing Random Finite Element Method (RFEM), a combination of finite element methodology and random field theory. Finally, in Chapter 6, the main conclusions of this study are drawn, and some recommendations are provided for future studies.

CHAPTER 2

LITERATURE REVIEW

Dealing with variability and uncertainty is more critical when the site is offshore because of the high cost of the site investigation in the offshore comparing to the cost of onshore investigations. The uncertainties of soil are considered in two parts, aleatory and epistemic uncertainty. The aleatory uncertainty is the inherent soil variability (natural randomness of soil parameters) and cannot be eliminated while epistemic uncertainty (measurement errors, statistical uncertainties, model uncertainties) due to lack of knowledge can be reduced by collecting more data. To represent the inherent variability of the soil, the mean, variance and scale of fluctuation of the data can be used to generate a random field in the reliability based approaches. In other words, a complete representation of the inherent variability of the soil can be achieved by defining mean, variance (with a proper statistical distribution) and scale of fluctuation. The mean and variance of the soil parameters are defined as the point variability and the scale of the fluctuation is the distance over which the soil parameters are similar to each other.

Lacasse and Nadim (2007) present the geotechnical risk and hazard assessment in their study and illustrate the importance of probabilistic approach. The risk includes hazard and corresponding consequences and is formulated as:

$$R = H * C \tag{2.1}$$

where R is risk, H is hazard and C is the consequence.

The more realistic framework in the risk assessment can be achieved by considering all uncertainties related to the soil and the structure with a probabilistic approach. By doing this, the probability of failure or risk can be evaluated and decisions on the projects can be taken. Figure 2. 1 illustrates that the deterministic factor of safety cannot be a measure for risk assessment. That is, higher FS (mean FS value of 1.5 in Figure 2. 1) may have a higher probability of failure when compared to lower FS, if it has high uncertainty (for example in shear strength) represented by high coefficient of variation, COV, value.

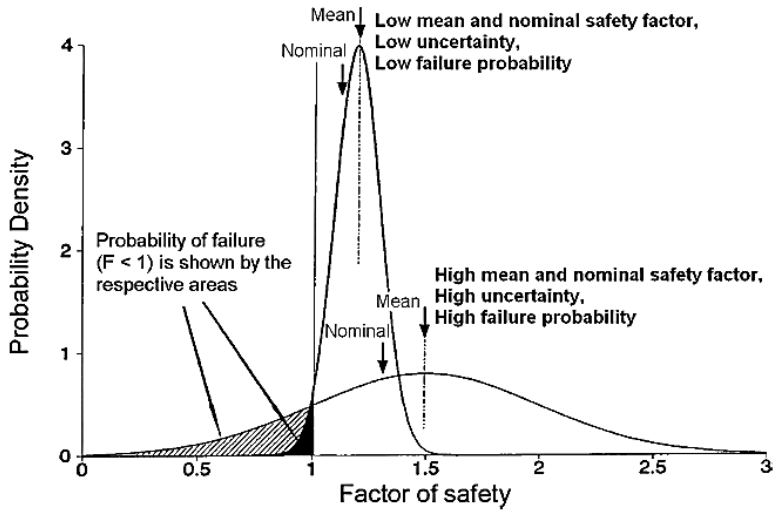

Figure 2. 1 Factor of safety and probability of failure regions (Lacasse and Nadim 2007)

There are several methods for probabilistic analyses to consider the variability of soil parameters, such as the first order second-moment approximation (FOSM), first order reliability method (FORM), Monte Carlo simulation etc. In the study of Lacasse and Nadim (2007), FOSM method is utilized to calculate the mean and standard deviation of the factor of safety which is a function of varying input parameters. The general overview of the processes in both deterministic and probabilistic approaches are provided in Figure 2. 2. It is seen that, while deterministic approach provides only factor of safety, probabilistic approach provides probability of failure, reliability index and parameters which can indicate failure.

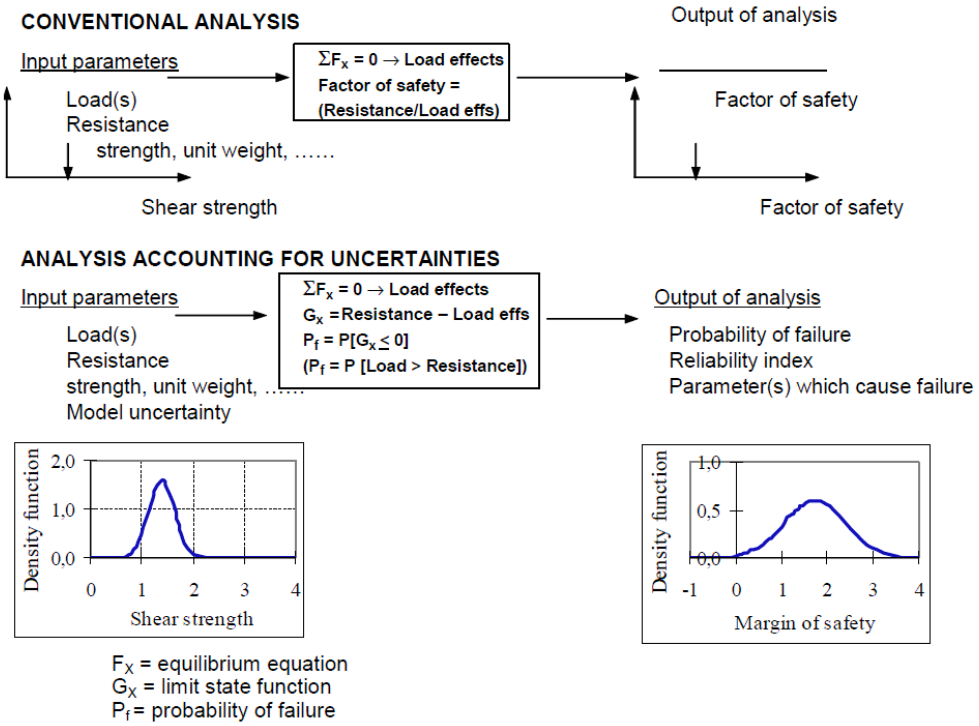

Figure 2. 2 Processes of both deterministic and probabilistic approach (Lacasse and Nadim 2007)

Lacasse and Nadim (2007) indicated that depending on the variation of the natural soil properties, aleatory uncertainties may have greater importance than epistemic uncertainties and handling them may require knowledge of the spatial variation of the soil parameters. The soil parameters can be described by summation of a trend and residuals (random component) about the trend. The residuals are assumed to have a spatial structure. The degree of the spatial structure (correlation) can be estimated by autocovariance function C(r) where r is the separation distance between two observation points. Autocorrelation function, the normalized form of autocovariance function, can be also used to define the degree of correlation. Exponential, squared exponential and spherical autocovariance functions are widely used in the literature in soil modelling; however, the second-order autoregressive and cosine of exponential autocorrelation functions are also utilized in the literature (DeGroot and Baecher 1993, Akkaya and Vanmarcke 2003, Lacasse and Nadim 2007, Huber 2013).

Probabilistic models considering spatially-varying soil properties are being used in studies on general foundations of structures (Paice et al. 1996, Griffiths and Fenton 2000, 2001, Griffiths et al. 2002, Popescu et al. 2005, Griffiths et al. 2006, Cassidy et al. 2013) as well as in offshore foundations, especially in the recent years (Andersen et al. 2011, Vahdatirad et al. 2011, Andersen et al. 2012, Vahdatirad et al. 2013, Liu et al. 2015, Nadim 2015, Overgard 2015). Significant economical and risk-associated benefits, and/or optimized design in terms of higher reliability index, and lower probability of failure for offshore foundations are provided with the use of spatial correlation length approach (Lacasse and Nadim 1996, Cho and Park 2009, Cho 2010, Zhang and Chen 2012, Carswell et al. 2013, Sarma et al. 2014, Liu et al. 2015, Jha 2016). For example, Liu et al. (2015) compared the annual probability of failure obtained for axial pile capacity with and without accounting for the vertical SCL_{CPT-q_c} for undrained shear strength for clays and relative density for sands. Based on CPT cone tip resistance at an offshore piled jacket foundation site in Western Australia, Liu et al. (2015) calculated the vertical SCL_{CPT-q_c} in the range of 0.1-0.5 m for sands, and 0.05-1.0 m for clays. Taking into account the vertical SCL gave higher annual reliability index and a lower probability of failure, which led to a more optimal and cost-effective pile penetration depth. The reduction is reported to be by a factor of 2 or 3 on the annual probability of failure (Liu et al. 2015). Therefore, the quantification of the vertical SCL is important and useful for reliability-based design of offshore structures (Cho and Park 2009, Carswell et al. 2013, Liu et al. 2015, Jha 2016). Although there exist numerous studies investigating the value of vertical SCL of soil properties (Chiasson et al. 1995, Jaska et al. 1999, Akkaya and Vanmarcke 2003, Firouzianbandpey et al. 2014), their number is rather limited for offshore / nearshore sediments (Phoon et al. 2003, Huber 2013, Liu et al. 2015, Zhang et al. 2016).

2.1 Random Finite Element Method

The inherent heterogeneous structure, i.e. the variability of soil can be defined by a statistical distribution (such as normal distribution, lognormal distribution etc.) at a point and SCL through distance. While most probable (average) parameter values are

selected and analyses are performed in deterministic approach, large number of simulations are performed in a single analysis in probabilistic approach. In each simulation, a soil parameter is randomly selected within its defined range of values. By doing so, large number of numerical analysis results can be obtained and these results can be utilized in assessment of probability of failure in reliability-based design. The above mentioned probabilistic approach can simply be integrated with the finite element method (FEM) and probabilistic results can be utilized to evaluate reliability of structures. However, selecting random variables within the statistical distribution and performing large number of simulations do not represent spatial heterogeneity of soil volume. To represent the heterogeneity through distance, a random field should also be created using spatial correlation length and a correlation function.

In the random finite element method, random field for soil properties (such as unit weight, cohesion, friction angle, Young's Modulus, Poisson's ratio etc.) is generated by utilizing statistical properties; a correlation function with a SCL and then the model is matched with finite element meshes. Statistical properties utilized in RFEM are the mean, standard deviation with a distribution model (such as normal, lognormal distributions) and SCL with a correlation function (Fenton and Griffiths 2008, Elachachi et al. 2012, Luo et al. 2014, Jha 2016). In this method, probabilistic analyses are conducted by performing large number of simulations (e.g. Monte Carlo Simulations) where also heterogeneity of soil is accounted in the analyses. In Figure 2. 3, random fields with different SCL values can be seen, where darker colors indicate larger values of a soil property compared to the mean value. In Figure 2. 3a, a single deterministic value of a soil parameter is assigned to the whole finite element model and SCL is not considered. In Figures 2.3 b-f, random fields are created with different vertical SCL values in the range of 0.25 m to 10 m (having ratio of horizontal to vertical SCL of 10) and matched with the finite element model. The random fields with small SCL values in Figure 2. 3 have rough and frequent changes, and it is seen that as the SCL value increase, the field starts to have more smooth changes.

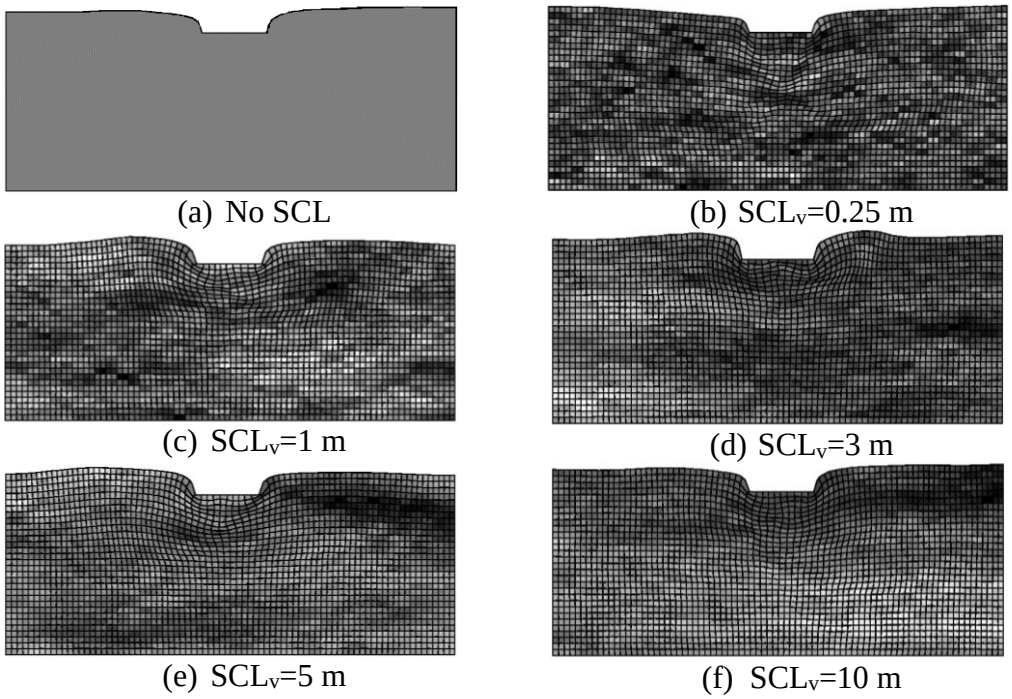

Figure 2. 3 Effect of small and large vertical SCL values on the random field for a bearing capacity of a foundation generated by RBEAR2D software (Fenton and Griffiths 2008), where the ratio of horizontal SCL to vertical SCL is 10 (darker colors indicate larger values of elastic modulus).

2.2 Spatial Variability in Soils and Evaluation of Spatial Correlation Length

SCL, which is also called as the scale of fluctuation, is the distance over which the soil parameters are positively correlated. That is, the two points in that distance will be both on the same side, above or below, of the mean. Likewise, SCL is defined as the distance beyond which soil parameters show no correlation (Hommels et al. 2010). In this chapter, a brief summary of the studies in the literature is provided.

The SCL concept is first proposed by Vanmarcke (1977) who studied the deviation from the average which is a part of three major sources of uncertainty; inherent soil heterogeneity, a limited number of soil samples and measurement error. The inherent

soil variability can be described by using mean, standard deviation (or coefficient of variation) and scale of fluctuation instead of treating the soil layer as homogeneous material with deterministic soil properties. The soil properties, like undrained shear strength (c_u) may show depth-dependent behavior, i.e. having trend with depth. It is advised that it is better to standardize the soil data which has trend behavior to investigate the fluctuation around depth-dependent mean. Vanmarcke (1977) provides spatial averaging process to evaluate the scale of fluctuation where the soil parameter is averaged through distance and the standard deviation of the averages decreases as the distance of averaging increases. This decrease is defined by reduction function and defined by:

$$\Gamma_u(\Delta z)=\frac{\tilde{u}_{\Delta z}}{\bar{u}} \tag{2.2}$$

where $\tilde{u}_{\Delta z}$ is the standard deviation of spatially averaged parameters while $\bar{u}$ is the standard deviation of the data. The square of reduction function is called variance function and as the averaging interval increases, the variance function becomes inversely proportional to the interval (Vanmarcke 1977). The above mentioned relationship brings us the scale of fluctuation, δ_u, as follows:

$$\Gamma_u^2(\Delta z) = \frac{\delta_u}{\Delta z} \tag{2.3}$$

Vanmarcke (1977) also states that the scale of fluctuation may be evaluated by correlation functions used to fit to the correlation coefficients. Four different correlation functions and corresponding scale of fluctuations are provided (Table 2. 1).

Table 2. 1 Autocovariance functions used in this study (Vanmarcke, 1977)

Autocovariance Function	**Scale of Fluctuation**
Exponential : $e^{-(\Delta z/a)}$	2a
Squared exponential: $e^{-(\Delta z/b)^2}$	$\sqrt{\pi}b$
Cosine exponential: $e^{-\frac{\Delta z}{c}}\cos(\Delta z/c)$	c
Second order autoregressive: $e^{-(\Delta z/d)}\ [1+(\Delta z/d)]$	4d

Additionally, a practical method to find the scale of fluctuation has been provided in the study of Vanmarcke (1977) where the scale of fluctuation is found by the average distance between the intersections of fluctuation and mean. The relation is given by:

$$\bar{\bar{d}}_u \approx 1.25 * \delta_u \quad (2.4)$$

where $\bar{\bar{d}}_u$ is the average distance between the intersections of fluctuation and mean.

DeGroot and Baecher (1993) divide the uncertainty of the soil parameters into two; inherent variability and measurement (sampling and testing) errors. The variability of the soil can be described by the summation of trend and residual about the trend. The parameters of the soil at the untested (unsampled zones) locations can be predicted by understanding the correlation structure of the soil parameters which is not applicable in the traditional methods. The variability of the soil, the trend and waviness about trend (fluctuation) is defined as:

$$Y(x) = T(x) + \varepsilon_{\mathrm{r}}(x) \quad (2.5)$$

where $Y(x)$ is the soil parameters, the $T(x)$ is the trend (mean), and $\varepsilon_{\mathrm{r}}(x)$ is the residual which has zero mean. The covariance between two observation points can be described by covariance function:

$$C_{ij} = E[\{(Y(X_i) - T(X_i)\} * \{(Y(X_j) - T(X_j)\}] \quad (2.6)$$

where E[] is the expected value. The value of C_{ij} is 1 when the separation distance is zero and then decreases towards zero with increasing separation distance. In Figure 2. 4, examples of the most commonly used autocovariance functions, and the effect of autocovariance distance, r_0, and variance is illustrated.

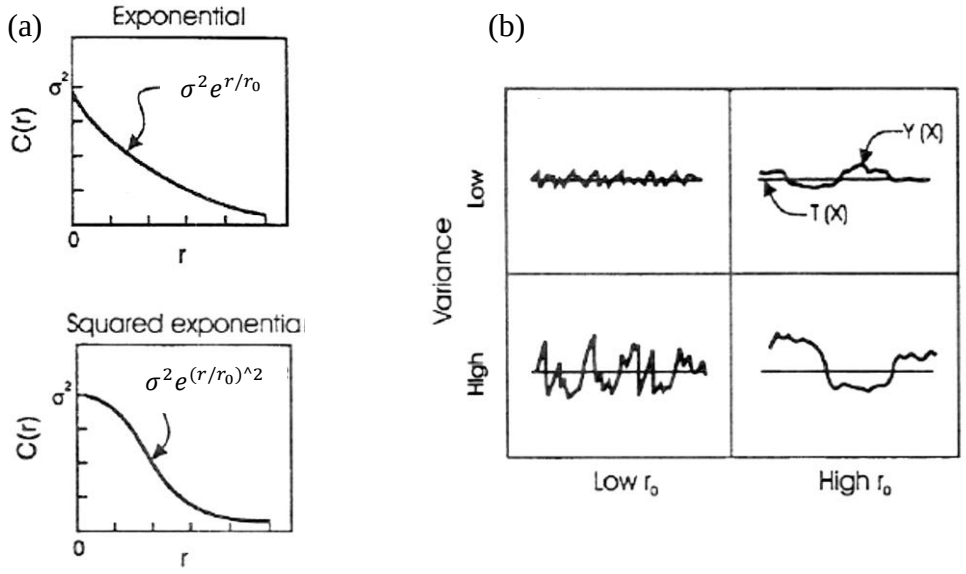

Figure 2. 4 (a) Commonly used autocovariance functions, (b) effect of autocovariance distance, $\boldsymbol{r_0}$, and variance (Lacasse and Nadim 1996, DeGroot and Baecher 1993)

DeGroot and Baecher (1993) state three methods to estimate correlation structure of the soil which are moment estimator (Equation 2.7), inverse estimator from probabilistic interpolation and maximum likelihood method (Equation 2.8). The last method, ML, is reported to be the most efficient and best way to obtain the correlation structure of the soil. Therefore, maximum likelihood method is utilized in order to estimate trend and autocovariance structure of residuals about trend.

One of the three methods, the method of moments is used to assess the correlation structure of the soil parameters and defined as:

$$C(r) = \frac{1}{n-r}\sum_{i=1}^{n-r}\left(Y_i - m_y\right) * (Y_{i+r} - m_y) \qquad (2.7)$$

where Y_i is the value of soil parameter at point i, the m_y is the mean of detrended data and n is the number of points.

Another and most efficient method, the maximum likelihood estimators (MLEs), are evaluated by maximizing the likelihood function:

$$L(x/\phi) = \frac{1}{(2\pi)^{n/2}|C|^{1/2}} \exp\{-\frac{1}{2}(\mathrm{x}-\mu)^{\mathrm{T}}\mathrm{C}^{-1}(\mathrm{x}-\mu)\} \qquad (2.8)$$

where C is covariance between points, μ is the mean vector at the point of interest, $X^T = \{x_1, x_2, x_3 \ldots\ldots, x_n\}$ is the observations and $\phi^T = \{\mu, \sigma, \theta\}$ is the distribution parameter vector.

Phoon and Kulhawy (1999a) state that the statistical variability values reported in the literature result from different sources of uncertainty although the studies assume only a single source of uncertainty. It is indicated that there are three major sources of uncertainty which are illustrated in Figure 2. 5; inherent soil variability (natural soil formation process), measurement errors (equipment, human effects etc.) and transformation uncertainty (empirical, or other correlation models). The reported statistical results can be used for the cases where the same conditions (uncertainties) are applicable. The measurement errors are removed from the field data in the study of Phoon and Kulhawy (1999a) and the remaining measurement represents the inherent soil variability. The study provides scale of fluctuation and coefficient of variation of the inherent variability, and measurement errors. Statistically evaluated parameters are undrained shear strength, friction angle, natural water content, Atterberg limits, dry-saturated unit weights and relative density, and evaluated field tests are cone penetration test, vane shear test and dilatometer test. Phoon and Kulhawy (1999a) indicate that the statistical data like COV in the literature includes not only the inherent variability but also other uncertainties and therefore the reported COV values are greater than the COV of inherent soil variability.

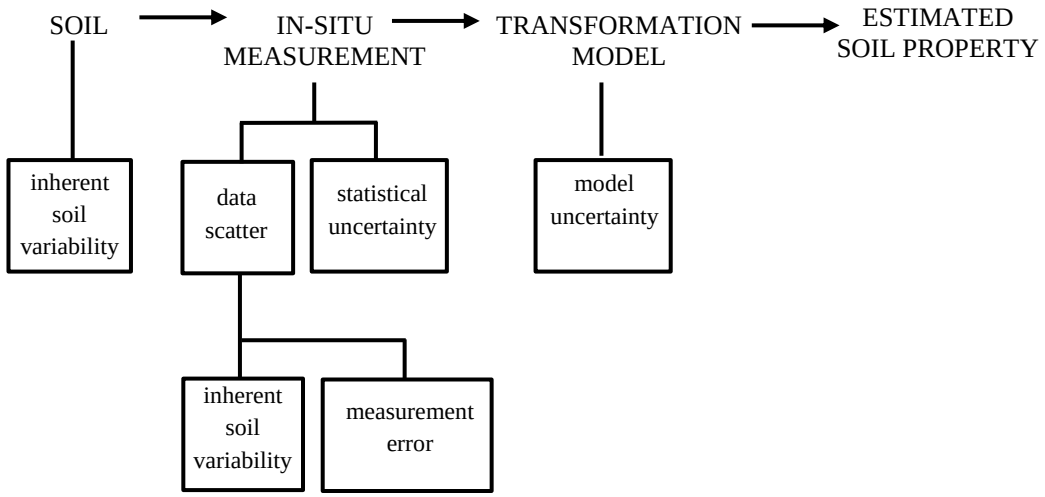

Figure 2. 5 Uncertainty of soil parameters (Phoon and Kulhawy,1999a)

The soil variability (Figure 2. 6) is divided into two; trend $t(z)$ and deviation from the trend $w(z)$ (Phoon and Kulhawy 1999a) and the soil property, $\xi(z)$, becomes:

$$\xi(z) = t(z) + w(z) \tag{2.9}$$

The fluctuation is considered as statistically homogenous which means that the mean and standard deviation are constant and the correlation between two measurements is only related to the distance of separation. The measurements should be detrended to satisfy statistical homogeneity. It is also highlighted that the duration of the testing (time frame) is also very important and as time passes, the soil may include additional variability with time (Phoon and Kulhawy 1999a).

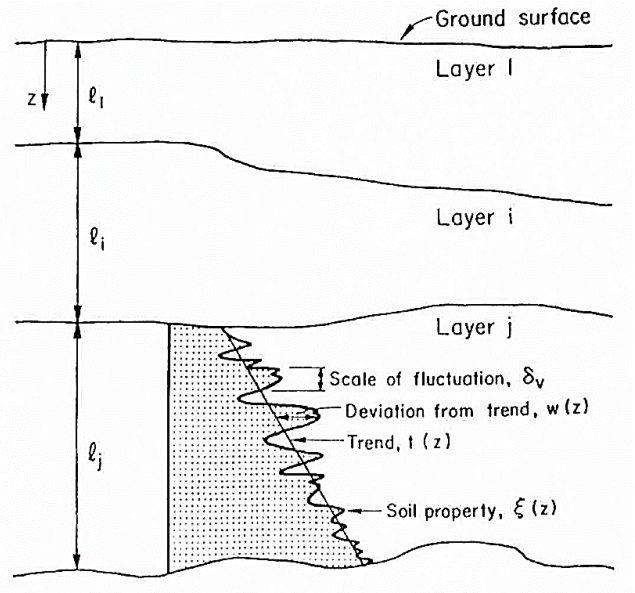

Figure 2. 6 Inherent soil variability (Phoon and Kulhawy,1999a)

Phoon and Kulhawy (1999a) provide an extensive literature review (Table 2. 2) consisting of ranges and means of scale of fluctuations based on different data sets of different studies. It is seen that there is only one study for SPT-N blowcount, effective unit weight and natural water content of clay while several studies exist for others. It is stated that the sampling distance has a significant effect on scale of fluctuation. The literature review also shows that the horizontal scale of fluctuation is much greater than the vertical.

Table 2. 2 Literature review of spatial correlation length (Phoon and Kulhawy 1999a)

			Scale of fluctuation (m)	
Property	**Soil type**	**# of studies**	**Range**	**Mean**
Vertical fluctuation				
c_u (Undrained Shear Strength)	Clay	5	0.8-6.1	2.5
q_c	Sand, clay	7	0.1-2.2	0.9
q_T	Clay	10	0.2-0.5	0.3
c_u (Vane Shear Stress)	Clay	6	2.0-6.2	3.8
N	Sand	1	-	2.4
w_n	Clay, loam	3	1.6-12.7	5.7
w_L	Clay, loam	2	1.6-8.7	5.2
$\overline{\gamma}$	Clay	1	-	1.6
γ	Clay, loam	2	2.4-7.9	5.2
Horizontal fluctuation				
q_c	Sand, clay	11	3.0-80.0	47.9
q_T	Clay	2	23.0-66.0	4.5
s_u (Undrained Shear Strength)	Clay	3	46.0-60.0	50.7
w_n	Clay	1	-	170.0

In the study of Jaksa et al. (1999), scale of fluctuation in both vertical and horizontal direction based on CPT (with 5 mm depth interval) data has been studied. Two field studies, 222 vertical CPT (5 m depth) and CPT (horizontal) under an embankment, have been considered. The scale of fluctuations of two different sites, where there exists stiff overconsolidated clay, have been evaluated by correlation function proposed by (Vanmarcke 1977) and Bartlett's approximation. Jaksa et al. (1999) state that the real correlation structure of the soil cannot be known but can be estimated from the limited measurements. The autocovariance, c_k , (Equation 2.10) and autocorrelation, ρ_k, (Equation 2.11) are used to obtain correlation structure and defined as follow:

$$c_k = Cov(X_i, X_{i+k}) = E[(X_i - \bar{\bar{X}})(X_{i+k} - \bar{\bar{X}})] \quad (2.10)$$

$$\rho_k = \frac{c_k}{c_0} \quad (2.11)$$

where k is the lag distance, X_i is the value of parameter X at the location of i and c_0 is the autocovariance at zero separation distance. In addition, sample autocorrelation function (Equation 2.12) which is an important parameter showing the correlation structure is defined as:

$$r_k = \frac{\sum_{i=1}^{N-k}(X_i-\bar{\bar{X}})(X_{i+k}-\bar{\bar{X}})}{\sum_{i=1}^{N}(X_i-\bar{\bar{X}})^2} \quad (2.12)$$

where k=0, 1, 2, …, K are the lags, K is the max number of lags and N is the number of measurement data. After calculation of correlation coefficient, correlation functions can be utilized to calculate spatial correlation length. Jaksa et al. (1999) also present an easier method, Bartlett's approximation to evaluate scale of fluctuation where Bartlett's Limit (Equation 2.13) is defined as:

$$|r_k| = \pm\frac{1.96}{\sqrt{N}} \quad (2.13)$$

Jaksa et al. (1999) state that if the data is not stationary, it can be easily converted to the stationary by standardizing (zero mean and unit standard deviation) or detrending. Only stiff overconsolidated clay, Keswich Clay, is taken for the evaluation process. Then, the trend behavior is extracted from the cone tip resistance data which means that data is converted to stationary data which is then used to evaluate sample autocorrelation function (ACF). After all, the scale of fluctuation is calculated by fitting correlation functions and by Bartlett's approximation (Figure 2. 7). Exponential (Markov) and squared exponential (Gaussian) are utilized to fit the correlation coefficient data, r_k. In addition, the intersection of ACF and Bartlett's limits is investigated and it is reported that the distance of intersection and evaluated scale of fluctuation with function fitting method have strong relation (Figure 2. 8) and following relation is provided:

$$\delta_v = 0.939 * r_B + 14.05 \quad (2.14)$$

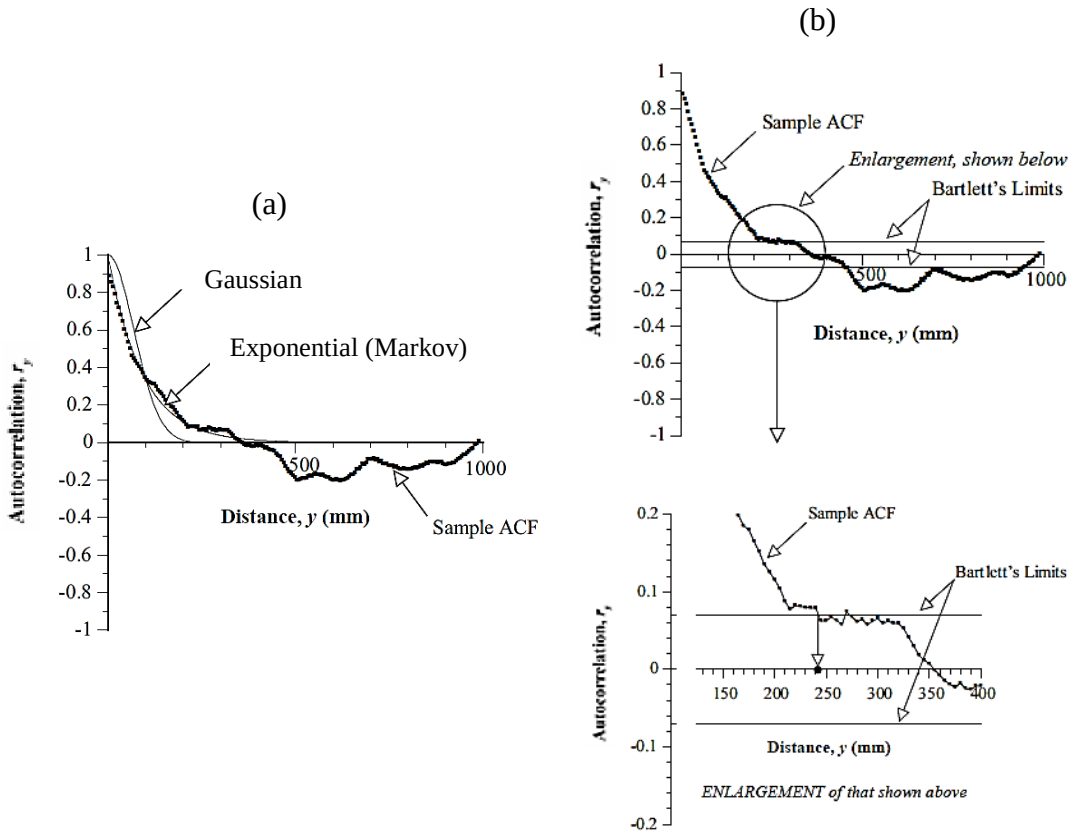

Figure 2. 7 (a) Fitting autocovariance functions, (b) utilizing Bartlett's limits (Jaksa et al. 1999)

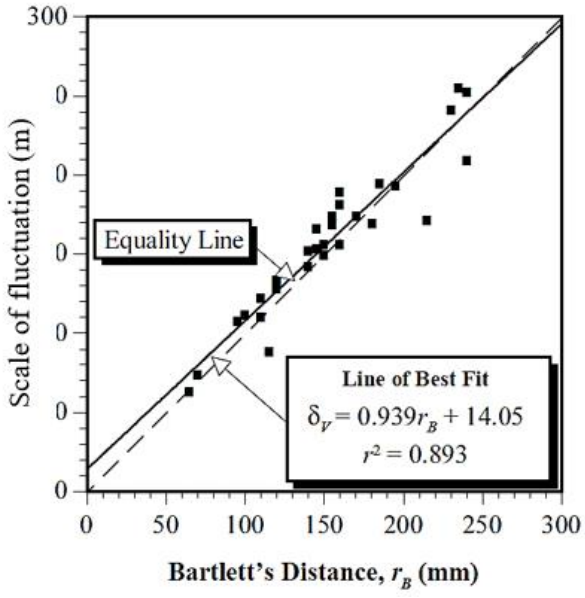

Figure 2. 8 Relation between two methods (Jaksa et al. 1999)

In the study of Jaksa et al. (1999), the evaluated vertical scale of fluctuations based on CPT tip resistance have a mean of 0.15 m (0.06-0.24) with a COV of 30% which is around lower limit of the reported scale of fluctuations in the literature. In addition, the scale of fluctuations in the horizontal direction is reported to be between 1 m and 2 m. However, the authors warn that reported scale of fluctuations and the real correlation structure of the soil may not be the same. The scale of fluctuation and correlation distance are reported to be equivalent where the soil shows strong correlation and beyond that point the parameters of soil become independent. Jaksa et al. (1999) draw attention to the point that the sampling distance should be less than the correlation distance of the soil and advise to consider the reported scale of fluctuations to decide on the spacing of the field test measurements.

Akkaya and Vanmarcke (2003) state that variability of parameters can be described by summation of trend and deviation from the trend. The way to describe the variability is evaluation of mean, standard deviation, and scale of fluctuation which is defined as the distance where the two points in that distance tend to be on the same side (above or below) of the trend. In the study of Akkaya and Vanmarcke (2003) the data from the Texas A&M University National Geotechnical Experimentation Sites (NGES) have been analyzed and variability of the data has been reported. Both first order statistics such as mean, standard deviation, skewness, kurtosis, and correlation structure (scale of fluctuations) of the data are provided. The soil profile at the site and presence of the trends have been determined by assumptions. The site consists of mostly clay and sand layers and their scale of fluctuations based on both CPT cone-tip resistance and CPT sleeve friction are reported. Two different methods which are calculating the area under the correlation function and fitting a model (exponential, i.e., Markov) have been utilized to calculate scale of fluctuations by Akkaya and Vanmarcke (2003). The vertical scale of fluctuations based on CPT cone tip resistance are reported as 0.61-3.72 m and 0.26-3.14 m for sand and clay sites, respectively. Likewise, the values based on CPT sleeve friction are reported as 0.36-3.53 m and 0.30-3.62 m for sand and clay sites, respectively. Although the data in the horizontal direction are limited, the analyses have been performed and the corresponding scale of fluctuations in the horizontal direction for cone resistance were reported as 2-25 m and

2.5-30 m for sand and clay sites, respectively. Likewise, the values for sleeve friction were reported as 7-19 m and 2-14 m. The horizontal scale of fluctuation is found to be much greater than the vertical scale of fluctuation. Akkaya and Vanmarcke (2003) also indicate that removing trend (detrending) eliminates the longer fluctuations.

Lloret-Cabot et al. (2014) also indicate that estimation of the scale of fluctuation, i.e. spatial correlation length, is crucial in the reliability-based designs and therefore it should be estimated accurately. The degree of soil heterogeneity can be obtained using SCL which affects the overall response of the structures, piles, soil masses such as slopes. Lloret-Cabot et al. (2014) investigated a classical approach (function fitting) and a new approach which combines the classical approach with conditional random field to calculate scale of fluctuation of the soil by utilizing CPT measurements. A new approach is described and compared with the conventional method which is fitting a correlation model to the measurements.

Firouzianbandpey et al. (2014) studied the scale of fluctuation in both vertical and horizontal directions for sand, silty sand layers based on CPTu measurements at the site situated in the North of Denmark. The soil site is characterized according to the data of CPTu by using Robertson classification chart and homogenous sublayers are determined and correlation structure of these homogenous sublayers are evaluated. Firouzianbandpey et al. (2014) state that the variability of soil has significant importance in geotechnical engineering. Mean, standard deviation and recently scale of fluctuation are used to describe the variability of the soil parameters. There are several different methods to include the heterogeneity of the soil like local average subdivision method (Fenton and Vanmarcke 1990) which requires mean, standard deviation and scale of fluctuation. Instead of maximum likelihood method, fitting exponential correlation function has been used to evaluate the scale of fluctuation due to limited data. The data is normalized (detrended) where the deviations from the trend are divided by standard deviation to obtain a stationary data through distance. The Markov (exponential) correlation function has been utilized to fit the correlation coefficients based on normalized tip resistance and sleeve friction with increasing lag distance. The results of the study indicate that the investigated soil site have quite different correlation structure in the vertical and horizontal directions (anisotropy), and

the scale of fluctuations in the vertical direction and in the horizontal direction are reported as 0.2-0.5 m and 1.2-2.0 m, respectively. In addition, it is reported that the scale of fluctuation in the horizontal direction is 2-7 times greater than the vertical direction due to soil deposition processes. This means that the soil parameters are correlated over a large distance in the horizontal direction (more homogenous) than that in the vertical direction.

In Table 2. 3, the summary of spatial correlation lengths in the vertical direction gathered from the literature are provided. It is seen that the SCL values may change according to the soil type and measurement type. Even for the same soil type, the reported SCL values may have different values.

Table 2. 3 Summary of spatial correlation length in the vertical direction from the literature (number in parenthesis is the mean value)

Reference	**Vertical SCL (m)**	**Soil type**	**Remarks**
Alonso and Krizek (1975) and Lumb (1975), reported by Huber (2013)	0.3 – 4	Clean sand and sand fill	SPT-N value
Vanmarcke (1977)	2.4	Sandy	SPT-N value
Keaveny et al. (1990)	0.3 – 1.0	Offshore cohesive soils	Undrained shear strength, CU triaxial
Phoon et al. (1995)	0.1 – 2.2	Sandy silty	Cone tip resistance
	0.7 – 1.1	Clay	Cone tip resistance
	2.0 – 6.2	Clay	Undrained shear strength obtained by vane test,
	0.8 – 6.1	Clay	Undrained shear strength obtained by various lab tests
Chiasson et al. (1995)	2 m autocorrelation distance	Lightly overconsolidated and highly sensitive clay deposit	Piezocone cone resistance and in-situ vane

Phoon and Kulhawy (1999a, 1999b)	0.8-6.1 (2.5)	Clay	Undrained shear strength
	0.1-2.2 (0.9)	Sand, clay	Cone tip resistance
	0.2-0.5 (0.3)	Clay	Corrected cone tip resistance
	2.0-6.2	Clay	Undrained shear strength from vane shear test
	1.6-12.7 (5.7)	Clay, loam	Natural water content
	2.4	Sand	SPT-N
	2.4-7.9 (5.2)	Clay, loam	Unit weight
Jaska et al. (1999)	0.63-2.55	Relatively homogeneous, stiff, overconsolidated clay known as Keswich Clay	Detrended residuals of cone tip resistance measurements
Cafaro and Cherubini (2002)	0.19-0.72	Clay	Cone tip resistance
Valdez-Llamas et al. (2003)	0.8–2.0	Superficial soft clay	Natural water content
	21	Deep deposits with alternating clayey and sandy soils	Natural water content
Akkaya and Vanmarcke (2003)	0.61-3.72	Sand	Cone tip resistance
	0.36-3.53	Sand	CPT sleeve friction
	0.26-3.l4	Clay	Cone tip resistance
	0.30-3.62	Clay	CPT sleeve friction
Phoon et al. (2003)	0.38-0.8	Offshore sediments	CPT data, lab-measured shear strength (UC etc) data
Uzielli et al. (2005)	0.13-1.11 (0.70)	Sand, Clay, Silt (Mixture)	Cone tip resistance
	0.12-0.60 (0.36)	Sand, Clay, Silt (Mixture)	CPT friction ratio
Schweiger et al. (2007)	1.0 – 10.0	for “materials such as keuper and middle trias formations”	Reports literature values

Liu and Chen (2010)	1.86 0.82	onshore alluvial deposits (loose sandy soils, cohesive soils, medium dense to dense sands and clay layers)	CPT cone tip resistance CPT sleeve friction
Akbas and Kulhawy (2010)	4.0-6.2	Ankara Clay	Liquid limit, w_L
	2.5-5.5	Ankara Clay	Natural water content, w_n
	1.0-3.0	Ankara Clay	Undrained shear strength, s_u
	3.0-3.8	Ankara Clay	SPT-N value
Zhang and Chen (2012)	1.36-3.01	Sandy	SPT-N value
Lloret-Cabot et al. (2014)	0.40–0.44	Filled sand in artificial island	Cone tip resistance
Firouzianbandpey et al. (2014)	0.45-0.50	Clayey silty sand	Normalized cone resistance
	0.2	Clayey silty sand	Normalized friction ratio
Liu et al. (2015)	0.1-0.5 0.05-1.0	Offshore sands Offshore clays	CPTU cone tip resistance
Nadim (2015)	0.18 – 0.39	Different soil units	Cone tip resistance
Overgard (2015)	0.4 – 3.0	Offshore sand and clay sublayers	CPT cone tip resistance
Shuwang and Linping (2015)	0.16—0.32 (0.23)	Very soft clay (sand inclusion)	Static cone penetration test
	0.14—1.00 (0.37)	Mud and very soft clay	
	0.16—0.57 (0.37)	Very soft clay and clay	
	0.13—0.32 (0.24)	Clay	
	0.10—0.43 (0.23)	Silty clay	
Bouayad (2017)	0.32-1.32 (0.78)	Onshore sandy soils (loose to medium dense sands, dense fine sands and silty sands)	CPT cone tip resistance
Pantelidis and Christodoulou (2017)	0.11-0.29	Onshore two clay sites	UC tests and light dynamic probing (DPL) in-situ tests

2.3 Effects of SCL on Reliability-Based Design in Geotechnical Engineering

The effects of spatial correlation length on settlement (Griffiths and Fenton 2009), bearing capacity (Fenton and Griffiths 2000, Jha 2016), slope stability (Sarma et al. 2014), drilled shafts (Luo et al. 2014), buried pipes (Elachachi et al. 2012), driven piles (Zhang and Chen 2012) and monopile offshore wind turbine (Carswell et al. 2013) have been investigated by various researchers. In this section, some of these studies are summarized.

Fenton and Griffiths (2000) studied the effect of spatial variability of soil parameters on bearing capacity of a shallow foundation. Elasto-plastic soil model has been utilized in the random finite element method based program. The effect of SCL (values of 0.5 m, 1 m, 2 m, 4 m, 8 m, 50 m) and COV (values of 0.1, 0.2, 0.5, 1.0, 2.0, 5.0) of soil parameters have been investigated. The results (Figure 2. 9) indicate that COV and SCL of soil parameters have a significant influence on the evaluated bearing capacity and the probability of failure. In Figure 2. 9, it is seen that increasing COV of soil parameters decreases the mean bearing capacity factor and increases the COV of bearing capacity factor. In addition, increasing the SCL from 0.5 m to 50 m increases both the mean and COV of bearing capacity. The decrease of mean bearing capacity factor is less for larger SCL because the initiation of bearing capacity failure is more likely for shorter SCL values.

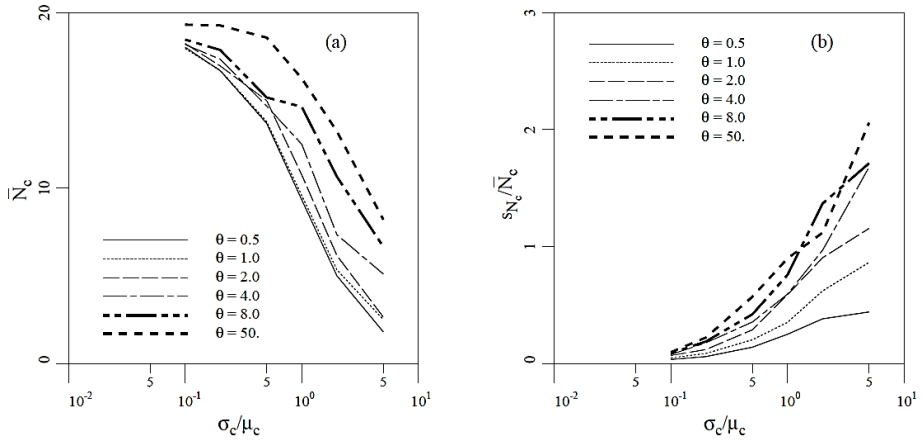

Figure 2. 9 The mean (a) and variation (b) of bearing capacity factor, N_c with varying soil variability and SCL, θ (Fenton and Griffiths 2000)

The results of the study (Fenton and Griffiths 2000) indicate that COV of soil parameters primarily affects the probability of failure while SCL has secondary effects (Figure 2. 10). It is seen that increasing the SCL value increases the probability at the left side of the turning point (COV of the bearing capacity) and decreases the probability at the other side.

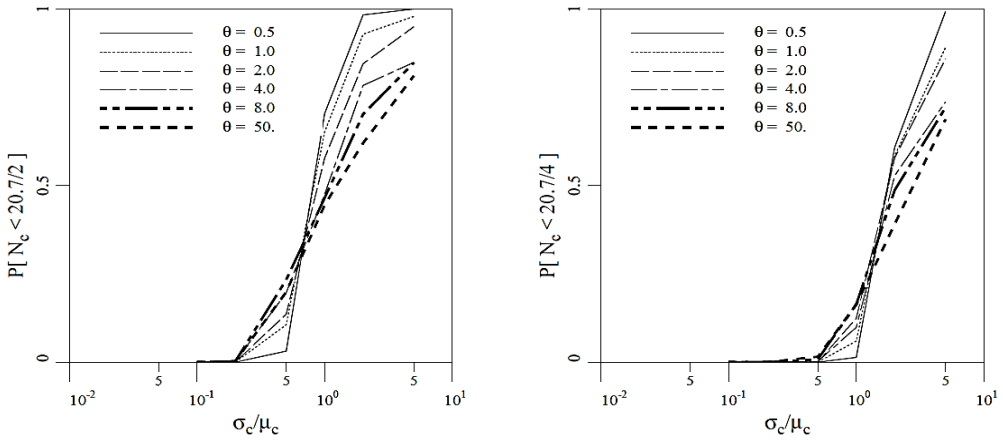

Figure 2. 10 Effect of factor of safety, F, SCL, θ, and COV of soil parameters for (a) F=2 and (b) F=4 (Fenton and Griffiths 2000)

Cho and Park (2009) state that statistical parameters like mean and variance are only a point parameter and cannot represent the spatial variability, i.e. the variability of the soil parameters through the distance. In the study, the bearing capacity of spatially variable soil, having cross-correlated shear strength parameters, under a strip foundation has been investigated probabilistically. The probabilistic analysis includes finite difference method and random field theory where Monte Carlo simulation is utilized to calculate the probability of failure. The random field is generated as being anisotropic non-Gaussian by KL expansion where different SCL in the vertical and horizontal directions are used for soil strength parameters. Then, the bearing capacity of c-φ soil is analyzed by assigning controlled displacement to the nodes of strip footing. The results (Figure 2. 11) show that the mean bearing capacity calculated by simulations is always less than the deterministic bearing capacity where single values are used for soil parameters. In addition, the results indicate that the mean bearing capacity calculated in the simulations increases with the increase in horizontal and vertical SCL's because the random field starts to become smooth (i.e. more similar values of soil properties with distance) as the SCL increases. The effects of SCL in the

horizontal direction is seen to be less effective comparing to that effect of the SCL in the vertical direction.

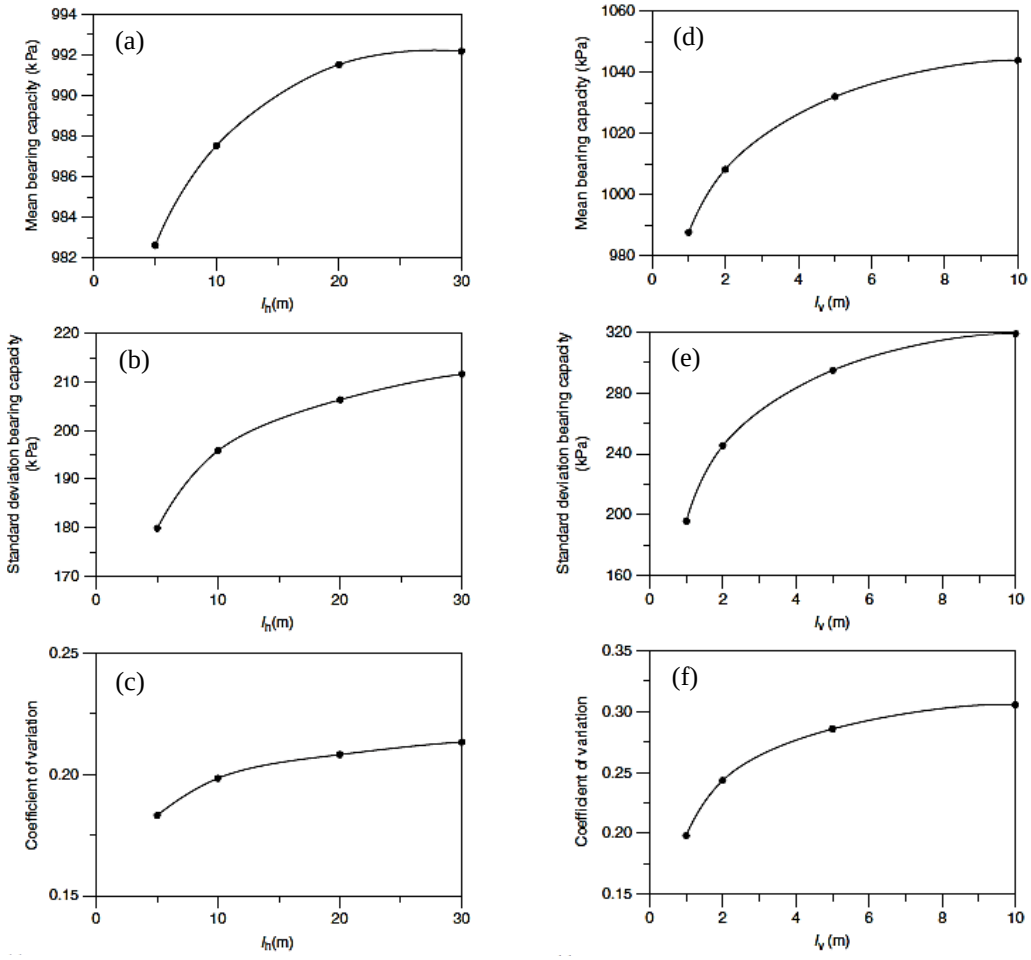

Figure 2. 11 Effect of horizontal SCL, l_h, on (a) mean, (b) standard deviation, and (c) coefficient of variation of bearing capacity; similarly effect of vertical SCL, l_v (d-e-f) (Cho and Park 2009)

Jha (2016) investigates the effects of anisotropic SCL of undrained shear strength on the reliability analysis of bearing capacity of strip footing. Random finite element method and Monte Carlo simulations are utilized to create a random field and capture the variability of the soil parameter, undrained shear strength. The geometry and boundary conditions of the model is given in Figure 2. 12. The analyses are performed by using Abaqus where the soil is modelled as elastic, perfectly plastic constitutive model and with a Mohr-Coulomb failure criterion.

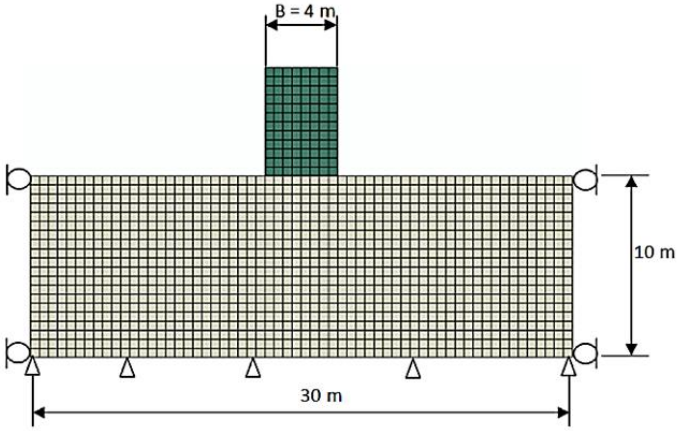

Figure 2. 12 The geometry and boundary conditions (Jha 2016)

The undrained shear strength, c_u, of the clay is defined as anisotropic random field where the mean, COV and SCL are used (Jha 2016). Lognormal distribution is assigned to the c_u due to non-negative nature of the parameter. For the correlation structure of the parameter, 2D exponential correlation model is utilized. The method of locally averaged random field using the Fourier series-based method is utilized. The scale of fluctuation of c_u in the vertical direction is taken as 0.5 m, 2.5 m, 5.0 m and horizontal scale of fluctuation is taken from 0.5 m to 100 m. The results of the study (Figure 2. 13) show that increasing scale of fluctuation of c_u leads to increase in COV of bearing capacity. In addition, normalized mean bearing capacity first decreases and reaches a minimum value and then increases with the increasing scale of fluctuation. Jha (2016) indicates that large scale of fluctuations overestimate the required factor of safety to achieve a specified reliability which means uneconomical, conservative results.

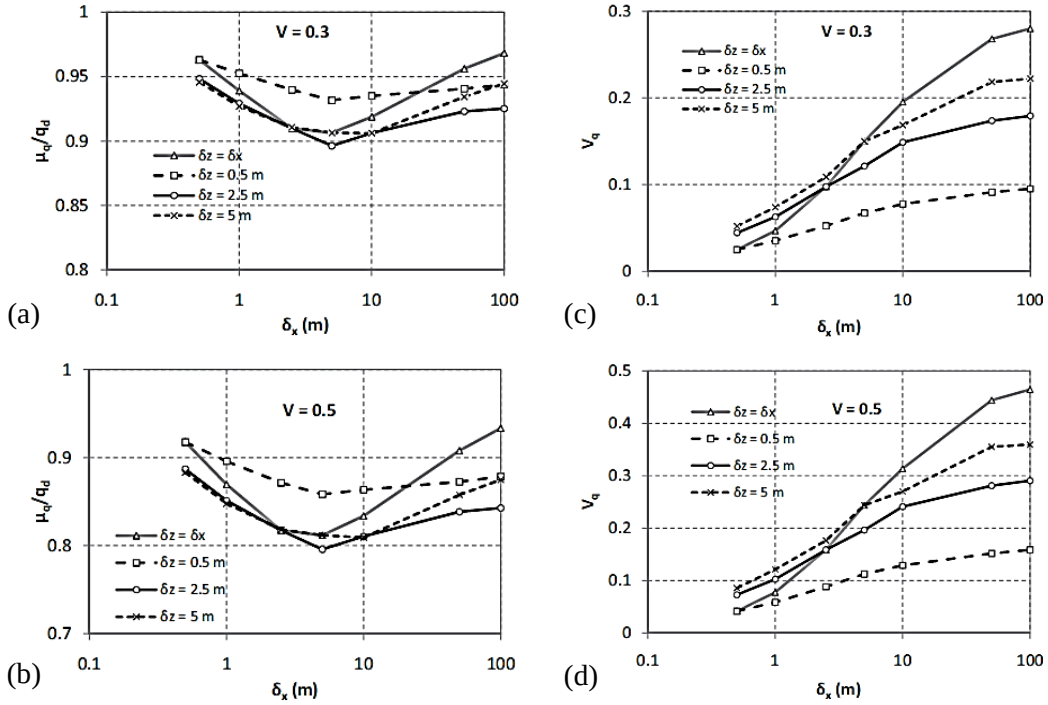

Figure 2. 13 Effect of SCL of c_u on normalized mean bearing capacity (a-b) and COV of bearing capacity (c-d) for parameters with a COV of 0.3 and 0.5, (Jha 2016)

Griffiths and Fenton (2009) investigated the settlement under a strip foundation on a spatially variable soil volume. The comparison between random finite element method and stochastic finite element method (SFEM) has been made. Young's modulus, E, is defined by lognormal distribution with a mean and standard deviation where the spatial variability is defined by Markov correlation function with a SCL equal in both horizontal and vertical directions (isotropic SCL for Young's modulus). The results indicate that increasing the SCL of E increases the mean settlement and variation of evaluated settlements of simulations for RFEM (Figure 2. 14). Griffiths and Fenton (2009) explained the increase of settlement due to the presence of weak regions in the soil model. When SFEM is utilized, the method underestimates the settlement and variation of the settlement. Therefore, it is stated that SFEM is not able to model spatial variability.

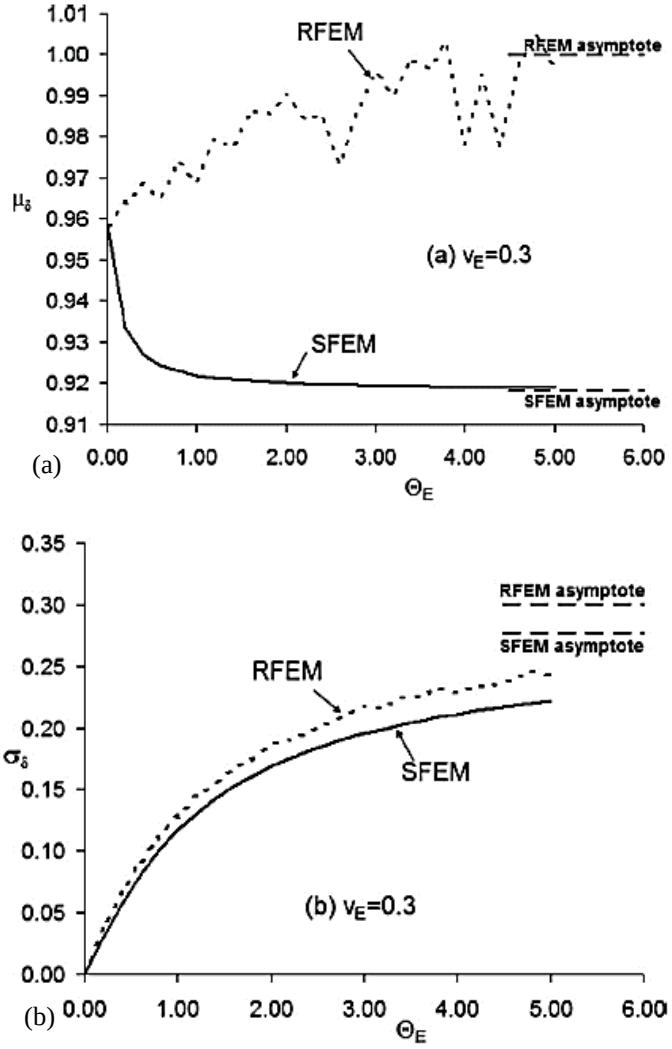

Figure 2. 14 The effects of SCL of E, θ_E, on (a) mean settlement and (b) standard deviation of calculated settlements, and comparison between RFEM and SDEM. (Griffiths and Fenton 2009)

Zhang and Chen (2012) investigate the SCL based on SPT-N blowcounts and effects on bearing capacity of driven piles in sand. In addition, spatial correlation between the SPT-N over the length of the pile and around the end of the pile is evaluated. The utilized formulation of the pile capacity is a direct method (Equation 2.15), where the field data is directly used to assign capacity.

$$Q_u = A_b f_b + A_s f_S \tag{2.15}$$

$$f_b = kN_b \tag{2.16}$$

$$f_s = \beta N_L \quad (2.17)$$

where A_b and A_s are the cross sectional area of pile end and the shaft area through the length of pile, respectively, and N_b and N_L are average SPT-N blowcounts at the end of pile and through the pile length.

In the study (Zhang and Chen 2012), the probability of failure is evaluated by employing the algorithm proposed by Smith (1986) where normalized data is used. The failure is defined as the case where the load on top of the pile is greater than the pile capacity. The mean (Equation 2.18) and variance (Equation 2.19) of the pile capacity are as follow:

$$E[Q_u] = A_b m_k m_{Nb} + ULm_\beta m_{NL} \quad (2.18)$$

$$var[Q_u] = A_b^2[m_k^2 var[N_b] + m_{Nb}^2 var[k]] + (UL)^2\left[m_B^2 var[N_L] + m_{NL}^2 var[\beta]\right] + A_b UL\rho_{(NL)(Nb)}\left[var[N_b]var[N_L]\right]^{1/2} \quad (2.19)$$

where the $\rho_{(NL)(Nb)}$ is the correlation coefficient between N_L and N_B. The formulation proposed by Vanmarcke (1977) which includes the variance reduction function is utilized to calculate the correlation coefficient where the correlation length has a great importance. In the probabilistic analyses, the correlation length is taken as between 0.5 m and 3.0 m and diameter of pile is taken as 0.3 m, 0.5 m, 0.8 m where the length of the pile is 20 m. Zhang and Chen (2012) analyzed three tested piles published in the literature. The correlation length of the cases is found by fitting exponential (Markov) and squared exponential (Gaussian) models proposed by Vanmarcke (1977) to the autocorrelation coefficients. The reported correlation distances (by Markov correlation function) are between 1.36 m-3.01 m for three analyzed test piles. The results of the study indicate the following:

- The correlation coefficient, $\rho_{(NL)(Nb)}$, increases with increasing correlation length for the same L/B ratio.
- For the same correlation length and pile diameter, the correlation coefficient decreases with increasing L/B ratio.

- As the diameter of pile increases, the overlapping distance, which is the distance over which the SPT-N values are averaged for the end of the pile and through the shaft, increases and therefore correlation coefficient increases.

Zhang and Chen (2012) state that ignoring correlation structure leads to an unsafe design where the probability of failure increases by considering correlation structure. Likewise, the results of the analyses of three tested piles indicate that spatial correlation of the SPT-N blowcount has great importance in the evaluation of the probability of failure of driven piles in sand and ignoring the correlation lead to underestimated probability of failure.

In the study of Luo et al. (2014), the reliability of drilled shafts (Figure 2. 15) is evaluated by two different probabilistic approaches and corresponding results are compared. Two probabilistic approaches are random field theory with Monte Carlo simulation and variance reduction technique with first order reliability method. Luo et al. (2014) draws attention to the importance of the spatial variability of soil in the reliability analyses and states that ignoring spatial variability of the soil may increase or decrease the reliability of the design.

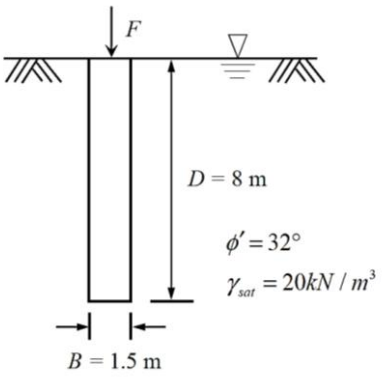

Figure 2. 15 Illustration of the design problem (Luo et al. 2014)

In the study (Luo et al. 2014), effective internal friction angle is modelled with a random field which is represented by mean, variance and scale of fluctuation. Different ranges of vertical scale of fluctuation are utilized and effects on the reliability of drilled shafts are studied where exponential correlation function and Cholesky decomposition

method are utilized. The results of random field theory (Figure 2. 16) indicate that the mean of ultimate limit state (ULS) compression capacity of drilled shaft is not affected by increasing scale of fluctuation. However, COV of the compression capacity and probability of serviceability failure are affected significantly by increasing scale of fluctuation. In addition, the probability of failure may increase or decrease according to the load on top of drilled shafts (Figure 2. 17). Increasing SCL of friction angle for a given load less than the mean capacity increases the probability of SLS failure, while for load greater than the mean decreases the probability.

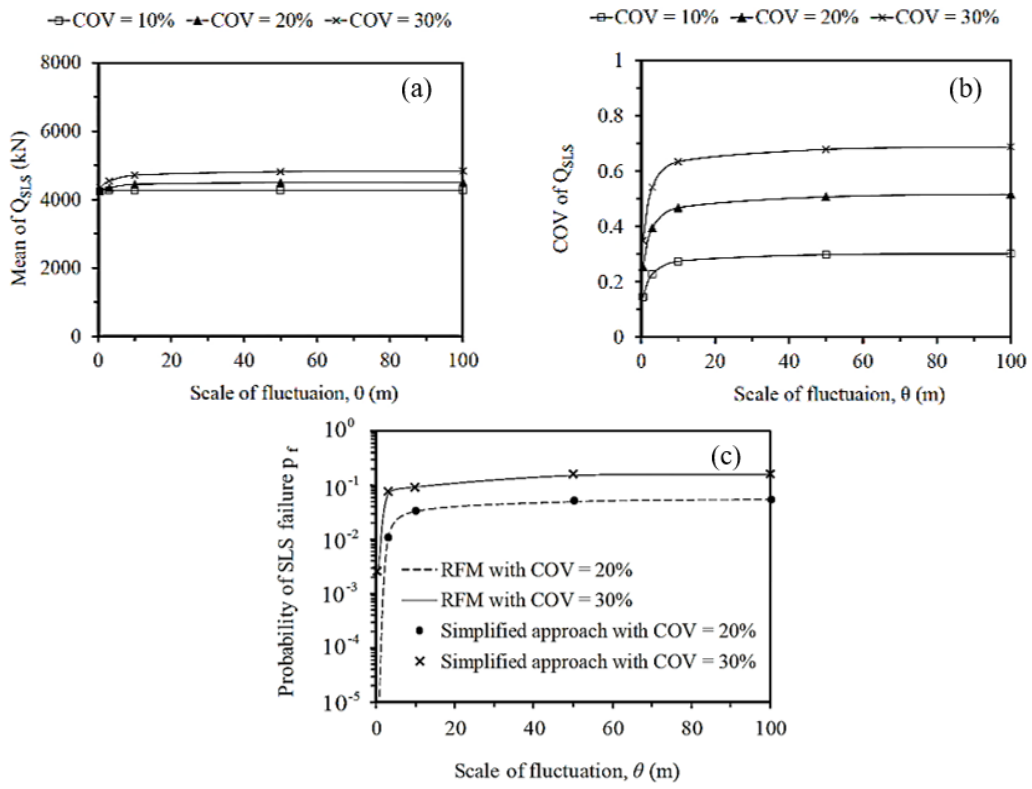

Figure 2. 16 The effect of SCL of friction angle on (a) mean compression capacity, (b) coefficient of variation of compression capacity and (c) probability of SLS failure (Luo et al. 2014)

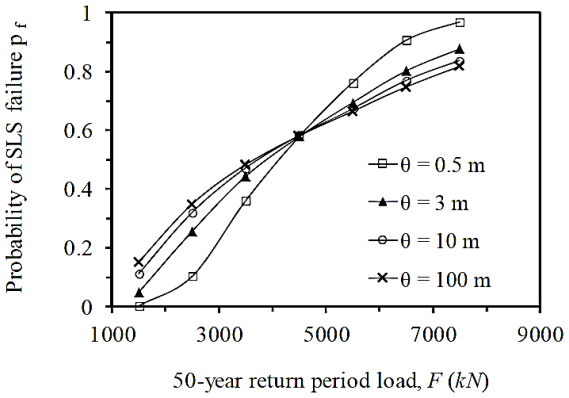

Figure 2. 17 Effect of spatial correlation length for different 50-year return period load (Luo et al. 2014)

Sarma et al. (2014) investigated the effects of the SCL of soil strength parameters on the response of the soil masses, i.e. slopes where the probability of failure is evaluated. Traditional methods generally do not include the variability of the soil parameters and correlation structures, instead, the methods use deterministic (single) values. In deterministic case, the soil cannot be modelled realistically and evaluated FS based on deterministic approach cannot represent the real response of the soil mass and cannot be used in risk assessments. Although there are simple, limit equilibrium-type, methods to analyze the slope stability, finite element and finite difference methods are mostly preferred due to stress-strain behavior of the soil to be taken into account. The FLAC^{2D} (finite difference model) and MATLAB have been utilized where covariance matrix decomposition method for random field and local averaging theory for controlling are employed.

Sarma et al. (2014) divides the variability of the parameters into two; trend and waviness about the trend, and the soil parameters are assumed to be statistically homogeneous. Covariance function (Equation 2.20-2.21) is utilized to calculate the correlation coefficient (Equation 2.22) of the data.

$$C[x_1, x_2] = Var[X(x_1), X(x_2)] \tag{2.20}$$

$$C[x_1, x_2] = E[X(x_1), X(x_2)] - \mu_x(x_1)\mu_x(x_2) \tag{2.21}$$

where x_1 and x_2 are position vectors and X is radom variable.

$$\rho[x_1, x_2] = \frac{c[x_1,x_2]}{\sigma_x(x_1)\sigma_x(x_2)} \quad (2.22)$$

The large covariance matrixes, C, are decomposed by using Cholesky's decomposition method (Equation 2.23). Then, the field is generated by Equation 2.24.

$$LL^T=[C] \quad (2.23)$$

$$X(x) = LU \quad (2.24)$$

where U is n size, number of element or zones, column vector.

In the study of Sarma et al. (2014), the analyzed case (Figure 2. 18) is taken from Chen (2007) that investigates the safety of the slope. All geometry of the slope and properties of the soil are kept constant and only the effects of the correlation structure of the soil is investigated where internal friction angle and cohesion is considered as a random field with a cross-correlation coefficient of -0.7. The normal distribution is assigned to the strength parameters. SCL values of 1 m, 2 m, 3 m, 5 m, 7 m, 10 m for soil strength parameters have been used in the random field for the isotropic case, and the combination of them is used for the anisotropic case.

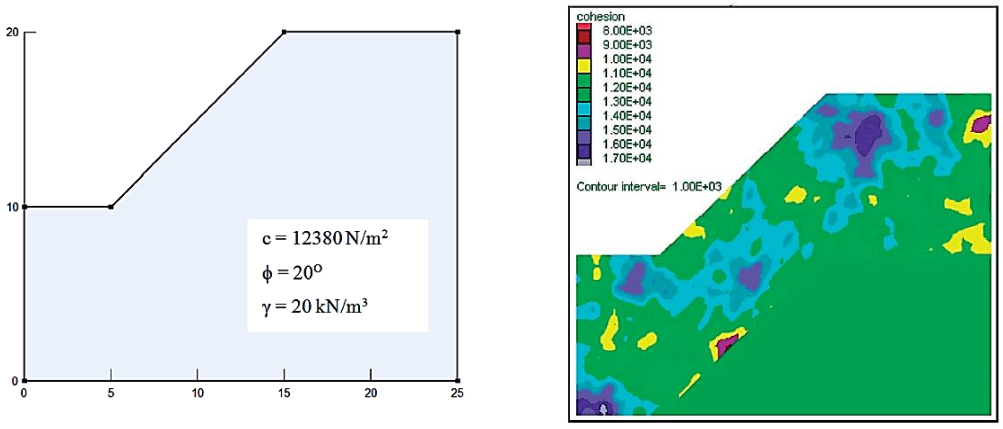

Figure 2. 18 (a) Model geometry, (b) generated random field for cohesion, where SCL of strength parameters is 5 m in both directions (Sarma et al. 2014)

The results of Sarma et al. (2014) show that the probability of failure increases with the increase of SCL of soil strength parameters and then does not change significantly beyond a point, for isotropic case (Figure 2. 19). The study also indicates that the increase of probability of failure is greater for the anisotropic case than that for the

isotropic. In Table 2. 4, it is seen that increasing the horizontal SCL of strength parameters increases the probability of failure.

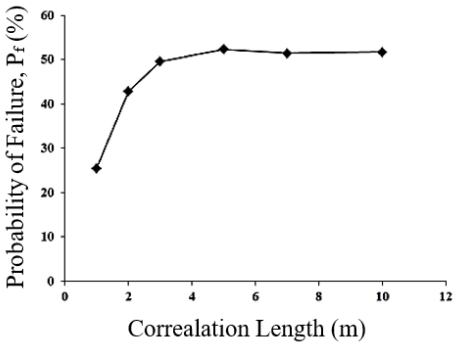

Figure 2. 19 Effect of SCL of strength parameters on probability of failure (Sarma et al. 2014)

Table 2. 4 Effect of anisotropy on probability of failure (Sarma et al. 2014)

SCL_v (m)	SCL_h (m)	P_f (%)
1	5	43.2
1	10	45.1
1	20	46.3
2	10	45.7
2	20	48.5
3	15	47.5
3	30	53.1

Elachachi et al. (2012) studied the failures such as concrete cracking state, having counter slope and excessive joint opening of buried structures. A model which includes the soil variability has been developed and serviceability limit state of the structures are considered. The key parameter for the variability of the soil is the SCL of soil modulus and Poisson's ratio which effects the soil-structure interaction. Soil parameters, soil modulus, E_s, and Poisson's ratio, υ_s, are defined as random field which is described by mean, variance and SCL's. The effects of the SCL of E_s and υ_s are investigated by considering four different cases, where the ratio between SCL and the length of the pipe are 0.01, 1, 10, 100 where small values represent a rough field, rapid fluctuations, and large numbers represent a more smooth field. The results (Figure 2. 20) indicate that the ratio of 0.01 causes more uniform bending stresses under the

buried pipe (Elachachi et al. 2012). The reason is that the soil volume shows rapid fluctuations, the case of 0.01 ratio does not lead to change of bending stresses due to the rigidity of the pipe.

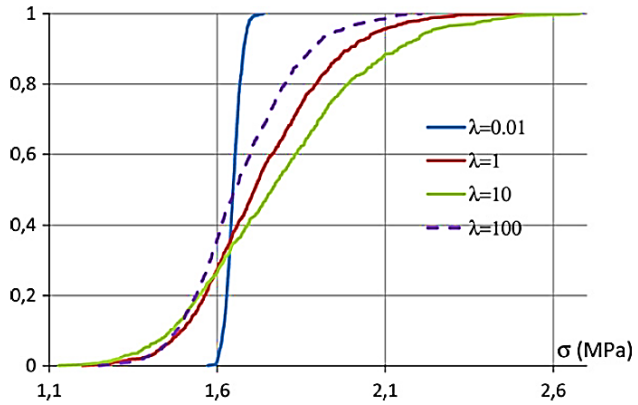

Figure 2. 20 The cumulative density function for bending stress for different fluctuation ratio (Elachachi et al. 2012)

The reliability index results show that the index increases as the SCL of E_s and υ_s goes towards zero and infinity. The increase of the reliability index means the decrease of probability of failure. Then, it is seen that the structure is safer when the SCL is infinite or zero because the pipe tolerates the rapid fluctuations, lower SCL, by its rigidity and the soil becomes homogeneous when the SCL is infinite. The study of Elachachi et al. (2012) shows the importance of considering SCL of soil parameter which greatly effects differential settlements, bending stresses and cracking of the pipes. Therefore, more realistic reliability-based design can be achieved by considering the inherent soil variability where the correlation length is the key parameter.

CHAPTER 3

METHODOLOGY

In this study, the variability of sea bottom soils in Turkish waters and the effect of the spatial variability of soil properties on foundation design are investigated. The variability is studied by using field data and some limited number of laboratory experiments such as sieve analysis, Atterberg limits, unconfined compression, triaxial tests, etc. as much as available. The SCL, the parameter representing the heterogeneous structure (correlation structure) of the soil medium, is evaluated based on site investigation data which are collected from several private geotechnical companies. Collected data include the data from both nearshore and offshore sites at different water depths. Two different field test data sets are collected; SPT data at nearshore sites and CPTu data at offshore/nearshore site. The data sampling intervals of SPT and CPTu are 1.5 m and 0.02 m respectively. The process of the evaluation of data can be summarized as follows:

i. The depth versus SPT-N, or depth versus CPT cone tip resistance and friction ratio etc. data are first digitized.
ii. The soil layers are classified according to both field measurements and laboratory tests (where available) and related soil profiles with depth are obtained.
iii. According to soil classification, the soils are grouped into broader groups such as “clays” and “sandy mixtures” etc, for which SCL values based on SPT-N, CPT-tip resistance, sleeve friction and friction ratio will be calculated layer by layer.
iv. The statistical evaluation for different soil groups is performed where statistical parameters; mean, μ, standard deviation, σ and SCL based on test data are obtained. The data are analyzed in two methods: (1) having a constant mean of

soil properties with depth and (2) an increasing mean value of soil properties with depth, and the SCL are obtained for each method, for each broad soil group, using four different autocorrelation functions for each layer separately.

The SCL's are evaluated by a MATLAB code (Appendix A) developed in this study, which analyzes the data, and fits different autocorrelation functions and reports the SCL values. Vanmarcke (1977) states that the initial steps of the spatial variability analysis should be the determination of the existence of a trend (i.e. stationarity or nonstationarity) and standardizing the data. This check can be done by calculation of mean first order increment (Equation 3.1) of the data in the vertical direction (Chiasson et al. 1995). If there is an increase or decrease in values with increasing depth, the data should be treated nonstationary ("trend approach"):

$$\bar{d}(\tau) = \frac{1}{n} \cdot [N(z_i + \tau) - N(z_i)] \tag{3.1}$$

where $\bar{d}(\tau)$ is the mean first order increment, $N(z_i)$ is the data, e.g. SPT-N blowcount, at depth z_i and τ is the spacing.

In this study, the calculated SCL's for both "constant" and "trend" approaches are compared. Treating the data as having constant mean and depth-dependent mean are illustrated in Figure 3. 1. It is clear that these two approaches will result in different SCL's and it is reported that removing the trend (detrending) eliminates the longer fluctuations (Akkaya and Vanmarcke, 2003). That is, the means should be subtracted from the measurements and then this deviation should be divided by standard deviation at each depth (Equation 3.2).

$$N_C(z) = \frac{N(z) - \bar{N}(z)}{\sigma_{N(z)}} \tag{3.2}$$

where the $N(z)$ and $\bar{N}(z)$ are the real measurement and trend at depth z, and $\sigma_{N(z)}$ is the standard deviation of the measurement. By doing this, the data can be treated as statistically homogeneous which means that the mean ($\mu = 0$) and standard deviation ($\sigma = 1$) are constant with depth. The similar procedure is called as "detrending" in the literature (DeGroot and Baecher 1993, Phoon and Kulhawy 1999a, b, Firouzianbandpey et al. 2014). The only difference between standardizing and detrending is that standardizing provides unit standard deviation. In this study, in the

"constant mean" approach, the average of the measurements is taken as the mean of the data and kept constant with depth. In the "trend approach", a linear function is employed as the trend of measurements, and the fluctuations about that trend is evaluated. Although further sophisticated depth-dependency functions can be fitted to the data, to use the same type of function for all data and for ease of interpretation, a linear trend equation with depth in SPT-N and CPT data is found to be sufficient to represent the depth-dependency.

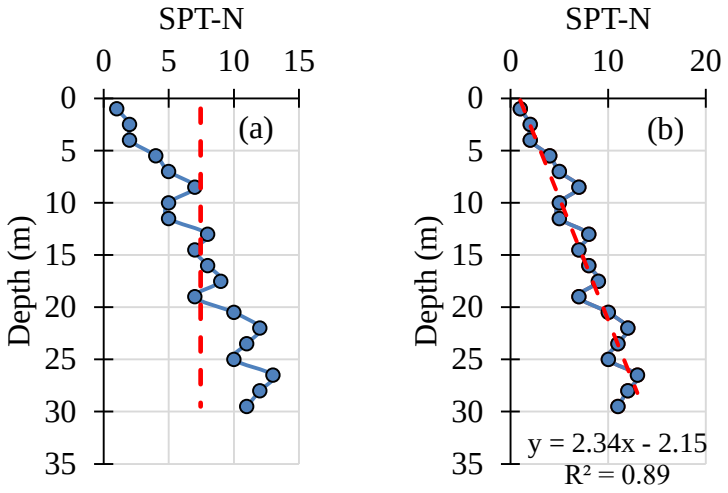

Figure 3. 1 (a) Constant mean and (b) depth-dependent mean approaches

The developed MATLAB code calculates the autocorrelation coefficients (Equation 3.3) of the data and plots these coefficients versus lag distances which is the distance between two points of concern (sampling interval). It should be noted that the data sampling interval between observation points has to be constant (Vanmarcke 1977, Fenton and Griffiths 2008, Liu and Chen 2010, Firouzianbandpey et al. 2014, Lloret-Cabot et al. 2014, Shuwang 2015, Zhang and Chen 2012). The SCL of test data is calculated by utilizing autocorrelation functions provided by Vanmarcke (1977) (Table 2. 1).

Autocorrelation coefficient is:

$$\rho_k = \frac{\sum_{i=1}^{n-k}(N_i-\bar{N}_i)(N_{i+k}-\bar{N}_{i+k})}{\sum_{i=1}^{n-k}(N_i-\bar{N}_i)^2} \quad k = 0, 1, 2, \dots, (\mathrm{n}-1) \qquad (3.3)$$

where the N_i and $\bar{N}_i$ are the real measurement and trend at depth i and N_{i+k} is the measurement at depth i+k. The autocorrelation coefficient is constrained by [-1.0, 1.0].

If the coefficient is positive, both variables tend to be higher and lower together. However, if the coefficient is negative, high value of one variable tends to be associated with a low value of the other variable (Kottegoda and Rosso, 2008). In the literature, the same autocorrelation function is also defined in terms of autocovariance function. The autocovariance of the data may be calculated by the method of moments (Equation 3.4) and the autocorrelation coefficients may be calculated by normalizing with the data variation (Equation 3.5). It is seen that combining Equation 3.4 and Equation 3.5 results in Equation 3.3.

Autocovariance function:

$$c_k = Cov(X_i, X_{i+k}) = E[(X_i - \bar{\bar{X}})(X_{i+k} - \bar{\bar{X}})] \quad (3.4)$$

Autocorrelation function:

$$\rho_k = \frac{c_k}{c_0} \quad (3.5)$$

where k is the lag distance, X_i is the value of parameter X at tha location of i and E is the expectation operator.

The four autocorrelation functions are utilized to fit the data and the SCL value of data can be obtained by using best-fit parameters (Table 2. 1). In Figure 3. 2, an illustration of the four autocorrelation functions is provided where SCL value is 1 m.

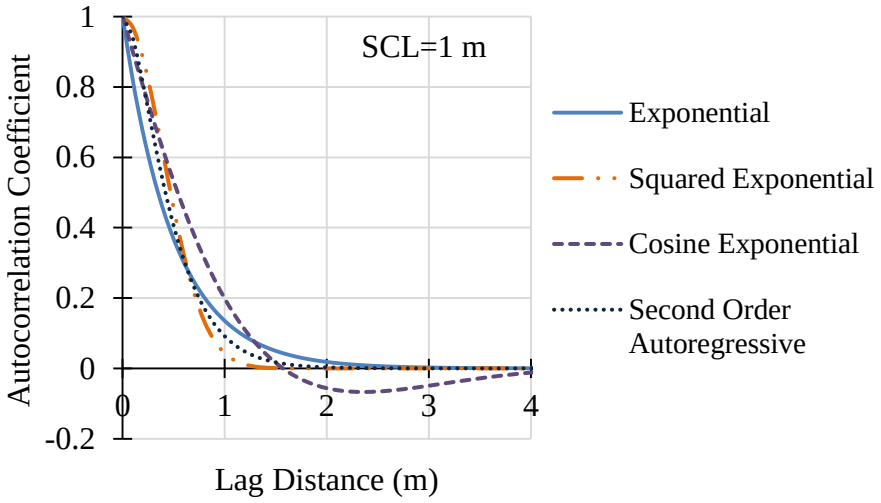

Figure 3. 2 Illustration of four autocorrelation functions for SCL=1 m

The best fit of the function can be obtained by using some basic functions in Matlab or minimizing the error in Equation 3.6.

$$E = \sum_{i=1}^{n}\left(\rho_s(\tau_i) - \rho(\tau_i)\right)^2 \qquad (3.6)$$

where $\rho_s(\tau_i)$ is the estimated autocorrelation coefficient by using the data (Eq. 3.3), $\rho(\tau_i)$ is the autocorrelation coefficient obtained by an autocorrelation function and n is the number of data point. If exponential correlation function is utilized, the SCL of data can be found by finding the root of the derivative of Equation 3.6 which can be written as (Eq 3.7):

$$\frac{\partial E}{\partial \theta} = -\sum 2 * \frac{\tau_i}{\theta^2} * (\rho_s(\tau_i) - \exp\{-2 * |\tau_i|/\theta\}) * \exp\{-2 * |\tau_i|/\theta\}) \qquad (3.7)$$

In this study, it is seen that if the mean of the measurement, $\overline{N}$, is taken as the trend value in Equation 3.3, there is no need to standardize or detrend the measurements. That is, the computed SCL for normal data, detrended data (zero mean) and standardized data (zero mean and unit standard deviation) become the same in case of taking mean as trend value.

In order to examine the CPT data, two additional functions are added into the MATLAB code. The purpose of these functions is to classify the soil type and to divide the data by soil type (boundaries of different layers) and discontinuity with depth. First of all, Robertson (2010) soil behaviour types chart (Figure 3. 4) is digitized and functions of each border of soil types are formulated. Then, the CPT with depth data is classified according to the Robertson's soil behavior types. That is, the CPT tip resistance and friction ratio data at each depth are compared with the borders and the corresponding soil behavior types are assigned to each data point (data is available at 2 cm vertical intervals). Afterwards, the data is divided into segments of continuous data with depth (discontinuities in the data are determined by comparing the difference between depth data with the frequency of data acquisition). Each data segment is divided into different soil layers according to Robertson's soil behavior type. The Robertson's soil behavior type zones 3 and 4, "Clay - silty clay to clay" and "Silt mixtures – clayey silt to silty clay", are evaluated together and named as a broad group

of “Clays”. Likewise, zones 5, 6 and 7, “Sand mixtures - silty sand to sandy silt”, “Sands - clean to silty sand” and “Gravelly sand to dense sand”, are evaluated together and grouped into a broad group of sandy mixtures and named as “Sands”. The thickness criterion is selected as 0.5 m (24 data with 0.02 m spacing) and greater thicknesses are considered as individual soil layers, i.e. SCL value of data is not calculated for a segment of soil that is less than 0.5 m thick. The classification of each data point, which is exemplified in Figure 3. 3, are converted into four major soil behavior types. That is, the zones in Robertson's soil behavior types chart, 1-2, 3-4, 5-6-7 and 8-9 are converted to (or grouped into) 2, 4, 6, 9, respectively and named as “modified classification”. The purpose of converting the classification is to simplify the procedure for the decision of soil layers and to calculate SCL of those broad groups of soils. The MATLAB code evaluates the modified classification and divides the segments into different soil layers.

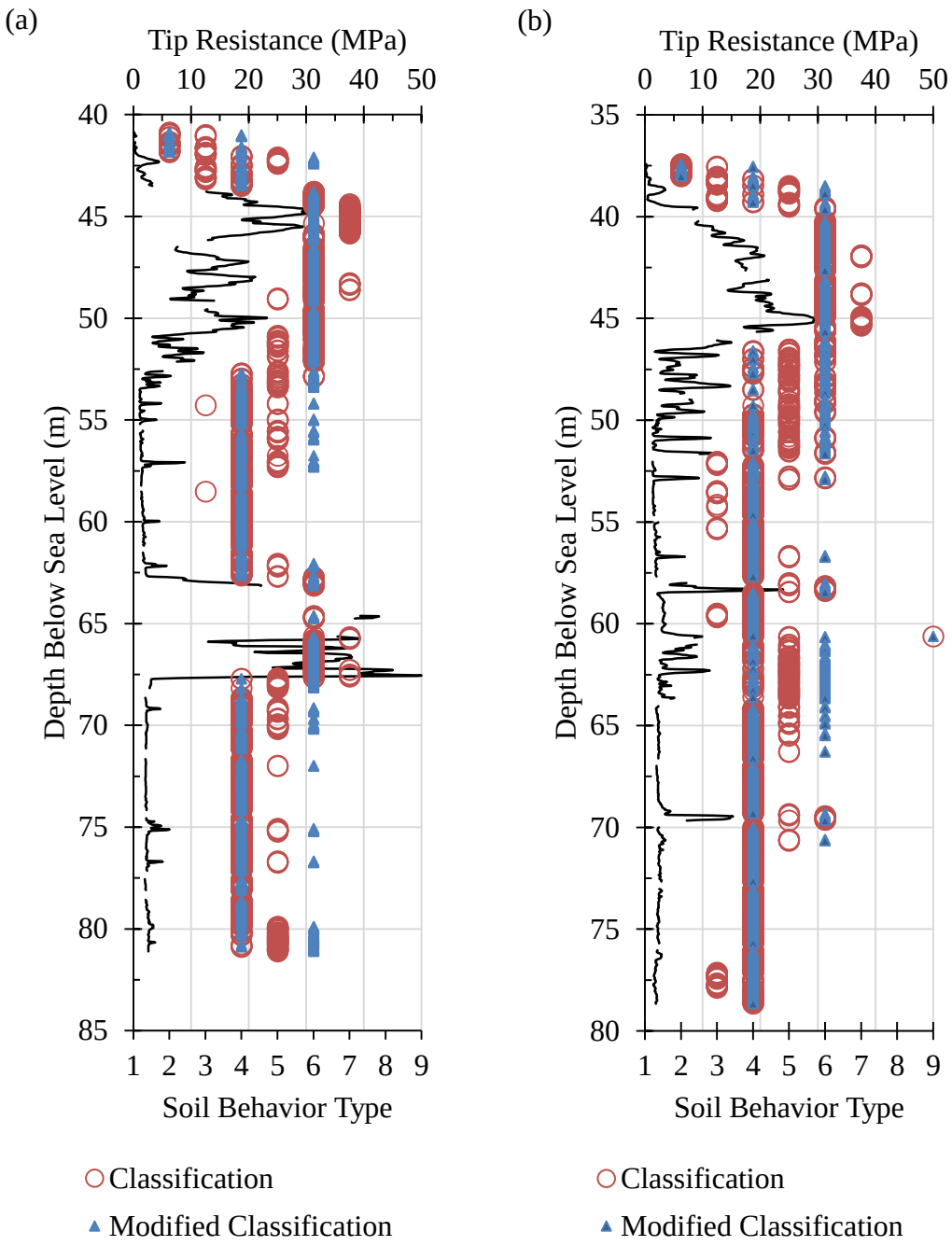

Figure 3. 3 Robertson (2010)'s soil behaviour classification and modified classification used in this study, as an example, for (a) sounding-1 and (b) sounding-2

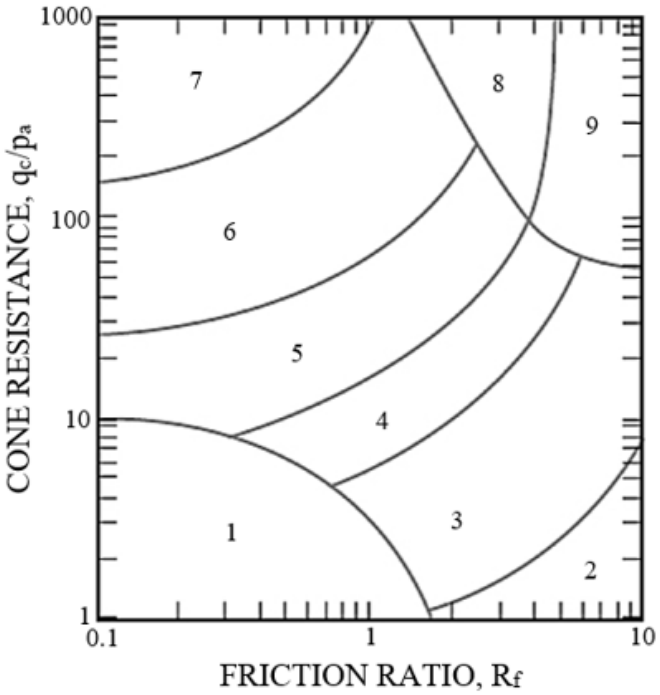

Zone	Soil Behavior Type
1	Sensitive, fine grained
2	Organic soils - clay
3	Clay - silty clay to clay
4	Silt mixtures - clayey silt to silty clay
5	Sand mixtures - silty sand to sandy silt
6	Sands - clean to silty sand
7	Gravelly sand to dense sand
8	Very stiff sand to clayey sand*
9	Very stiff fine grained*

* Heavily overconsolidated or cemented

Pa = atmospheric pressure = 100 kPa = 1 tsf

Figure 3. 4 Classification of soil behavior type chart (Robertson et al., 1986, updated by Robertson, 2010).

CHAPTER 4

CASE STUDIES

Statistical evaluation of soil properties based on nearshore/offshore site investigation data is rare in Turkey but has significant potential benefits for reliability based design of nearshore/offshore structures. In this chapter, site investigation data of two near-shore sites in the southern coast of Turkey and one large area of offshore/nearshore site on the northwestern part of Turkey are gathered; properties of these see bottom soils are presented. The data is analyzed, firstly, to understand what types of soils exist in the seabed, and whether the consistency of clays is soft or stiff, and whether the sandy soils are in loose or dense state etc. The variability of soil properties in terms of the mean and standard deviation values of estimated undrained shear strength for clays or estimated relative density for sands with depth is obtained. The SPT and CPT data are analyzed, secondly, to obtain the vertical SCL of SPT-N and CPT-cone tip resistance, side friction and friction ratio using four different autocovariance functions for each broad soil group. The results of the present study add to the database of SCL's based on real data and could be useful for future studies on reliability assessment of offshore foundations using advanced tools such as the random finite element method.

4.1 Iskenderun and Yumurtalık Sites (Nearshore-SPT data)

4.1.1. Site Description

Site investigation data at two sites obtained from nearshore soils in the Mediterranean Sea of the southern coasts of Turkey (Figure 4. 1) are used in this study. Summary of the available data used in this study is presented in Table 4. 1. Both sites are located at

the intersection of Arabian, African and Anatolian Plates and their geological formation are similar, which is mainly composed of the weathered Mesozoic Limestone, Ophiolitic Rocks and Eocene-aged limestones of Amanos Mountain and sediments transported by alluvial rivers, consisting of gravel, sand and clay that settled in the Holocene Epoch (Derinsu Site Investigation Reports 2011a-b, 2014 and 2015).

Table 4. 1 Information about the data at two nearshore sites

	Number of boreholes	Water depth (m)	Depth of boreholes from seabed (m)
Site 1 (Iskenderun)	27	2.8 to 18.2 m (average 8.9 m)	16 to 50.5 (average 30.5 m)
Site 2 (Yumurtalık)	14	5.2 to 25.7 m (average 16.1 m)	13.8 to 35.4 (average 25.2 m)

Figure 4. 1 Locations of Site 1 and Site 2 in the southern coast of Turkey and the location of boreholes

At two nearshore sites, SPT was performed by rotary drilling machine which is mounted on a catamaran barge (Derinsu Site Investigation Reports 2011a-b, 2014 and 2015). During the drilling process, both undisturbed and disturbed soil samples and rock core samples were obtained. In the laboratory, sieve analysis, hydrometer, Atterberg limits, in-situ water content, consolidation, triaxial (UU), unconfined compression, direct shear and point load index tests were performed, although shear strength tests are limited in number. The results of both laboratory tests, SPT-N values and field observations are utilized to identify the soil layers and profiles.

All soil units in the coastal regions are mixtures of various materials transported and accumulated. The majority of the sea-bottom sediments at both sites are composed of "mixture soils", that is silty, clayey and sandy materials with different proportions, which are classified as CL, CH, ML, MH, SM, SC, SW, SP according to Unified Soil Classification System (USCS). Only in some boreholes uniform clay layers (CL) of varying thicknesses are identified. Therefore, to determine the vertical SCL_{SPT-N}, the soil layers are grouped into two broad groups: (1) clay layers (Figure 4. 2b) and (2) mixture layers, composed of silty, clayey and sandy materials with different proportions (Figure 4. 2a), gravelly parts are not included in the SCL evaluation in this study. Results of Atterberg limits tests and sieve analyses at both sites are illustrated in Figure 4. 2.

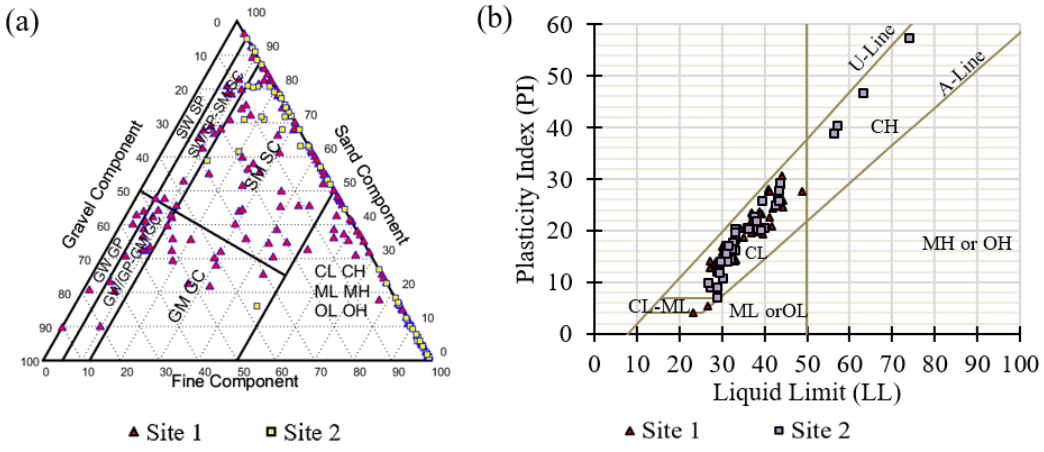

Figure 4. 2 Classification of soils at both sites, (a) sieve analyses, (b) Atterberg limits test results.

4.1.2. Evaluation of Spatial Variability

The SPT-N data, site description of the soils in borehole logs and laboratory classification tests (sieve analysis, hydrometer data, fines content, USCS classification and Atterberg limits), are used to identify sublayers that can be described as a relatively homogeneous soil layer. At both sites, the SPT is conducted at 1.5 m vertical spacing. The data in the same sublayer are counted and presented in Table 4. 2, which also provides the mean and coefficient of variation of the SPT-N data from two sites. Identification of relatively homogeneous sublayers and the need for studying the vertical SCL of each sublayer within itself are also noted by Phoon and Kulhawy (1999a, b), Uzielli et al. (2007), Overgard (2015) and Firouzianbandpey et al. (2014), among others. After identifying the layers which tend to be sufficiently homogeneous, these measured data are analyzed to estimate the mean value and standard deviation of vertical SCL based on SPT data. If the measured data shows a trend, trend analyses can be conducted by separating the random process into a deterministic trend and a residual variability around the trend (Overgard, 2015).

Table 4. 2 Variability of SPT-N data for two sites

	Sublayer identification	Number of Data	Mean SPT-N	COV (%)
Site 1	Mixture Soil (clayey, silty, sandy)	330	17	71
	Clay	100	10	80
Site 2	Mixture Soil (clayey, silty, sandy)	89	22	77
	Clay	73	8	88

By first eliminating the measurement error in SPT-N, Phoon et al. (1995) report that COV values of SPT-N are in the range of 25-49% in sandy and silty soils, whereas this value is 37-57% in clayey soils. Phoon and Kulhawy (1999) indicate that the values of COV which include both inherent variability and measurement errors are greater than the COV of inherent variability. In this study, COV of SPT-N data varies between 71 and 88% which is greater than the COV of inherent variability because data includes the measurement errors.

A very limited number of laboratory shear strength (UU triaxial) tests are available on undisturbed samples in cohesive soils. Therefore undrained shear strength (c_u) is determined by utilizing the relationship between SPT-N blowcount and c_u (Equation 4.1) depending on plasticity index (Stroud, 1974), acknowledging the limitations of the method. Figure 4. 3 shows that the c_u of clay layers at different boreholes increases linearly with depth below mudline and Table 4. 3 shows that the rate of increase of c_u with depth at site 1 and site 2 are within reported values in the literature.

$$c_u = f_1 * N_{60} \tag{4.1}$$

where N_{60} is the SPT-N value corrected for 60% energy efficiency and field procedures, and f_1 is a coefficient depending on the plasticity index of clay.

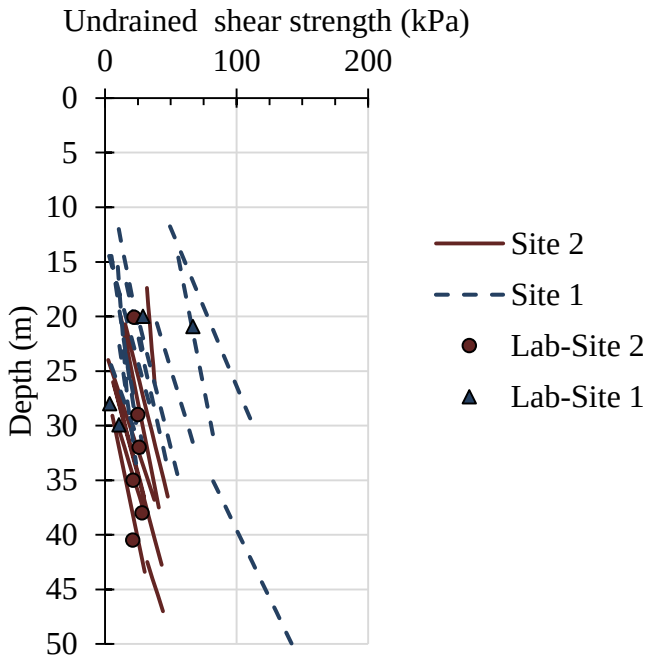

Figure 4. 3 Undrained shear strength profile at site 1 and site 2 by utilizing empirical equation of Stroud (1974) and SPT-N data from many boreholes with a few laboratory test data

Table 4. 3 Rate of increase of undrained shear strength with depth

Reference	Rate of increase of c_u with depth (kPa/m)	Remarks
This study	2.1 (range: 0.6-4.0, std.dev.: 1.0) at site 1 2.2 (range: 1.7-2.8, std.dev.: 0.4) at site 2	clays nearshore Turkey
Basack and Purkayastha (2009)	2.5	-
Cao and Wang (2014)	1.6	marine clays
Hossain et al. (2014)	1.02-2.55	clays at 14 sites, Gulf of Mexico
Wei et al. (2010), Kamei and Iwasaki (1995), Li-Zhong et al. (2008), Terzaghi et al. (1996)	0.8-3.5 for $(c_u/\sigma'_v) = 0.12 - 0.35$ *	-

* Using buoyant unit weight of 7 to 10 kN/m^3

By using empirical equations (Equation 4.2 and 4.3) based on the SPT-N blowcounts, effective friction angle (Kulhawy and Mayne 1990, Schmertmann 1975) and relative density (Gibbs and Holtz 1957) are estimated for all borehole soundings where mixture layers are identified.

$$D_r \approx \left(\frac{N}{12*\sigma'_{v0}+17}\right)^{0.5} \quad (4.2)$$

$$\emptyset' = \tan^{-1}\left[\frac{N}{12.2+20.3*\left(\frac{\sigma'_{v0}}{Pa}\right)}\right]^{0.34} \quad (4.3)$$

where N is the SPT-N blowcount and σ'_{v0} is in-situ vertical effective stress (saturated unit weight is taken as17.5 kN/m^3). Additionally, friction angle is obtained by using the NC (normally consolidated) curve in Figure 4. 4 provided by Stroud (1988).

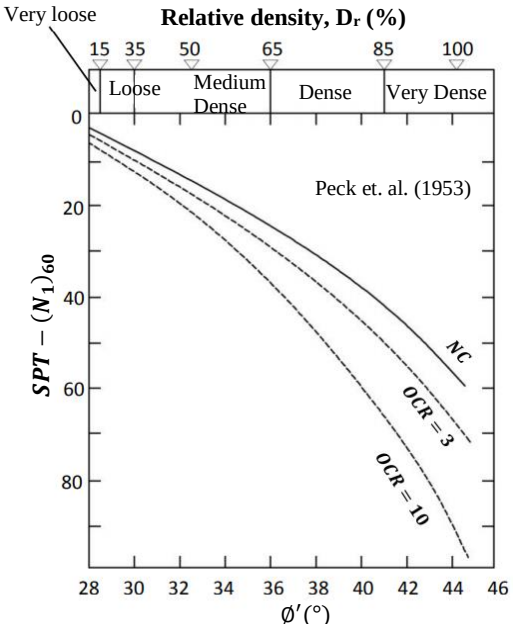

Figure 4. 4 $(\mathbf{N_1})_{\mathbf{60}} - \emptyset' - \mathbf{OCR}$ (overconsolidation ratio) relation (Stroud 1988)

The estimated effective friction angle and relative density are provided in Figure 4. 5 and the results are tabulated in Table 4. 4.The relative density results shows that the upper parts of the soil profile have greater D_r than deeper layers which are not realistic. Therefore, it is concluded that the empirical relative density equation (Gibbs and Holtz 1957) is not proper for the shallow sea bottom sands and it overestimates the D_r values at the shallow depths because it uses overburden corrected SPT-N, $N_{1,60}$ (in-situ effective stresses are normalized by 100 kPa). The weighted average relative density of the mixture layers at both sites is 29% (it is 28% for site 1 and 40% for site 2) and the mixture marine soils of this region can be classified as loose to medium dense.

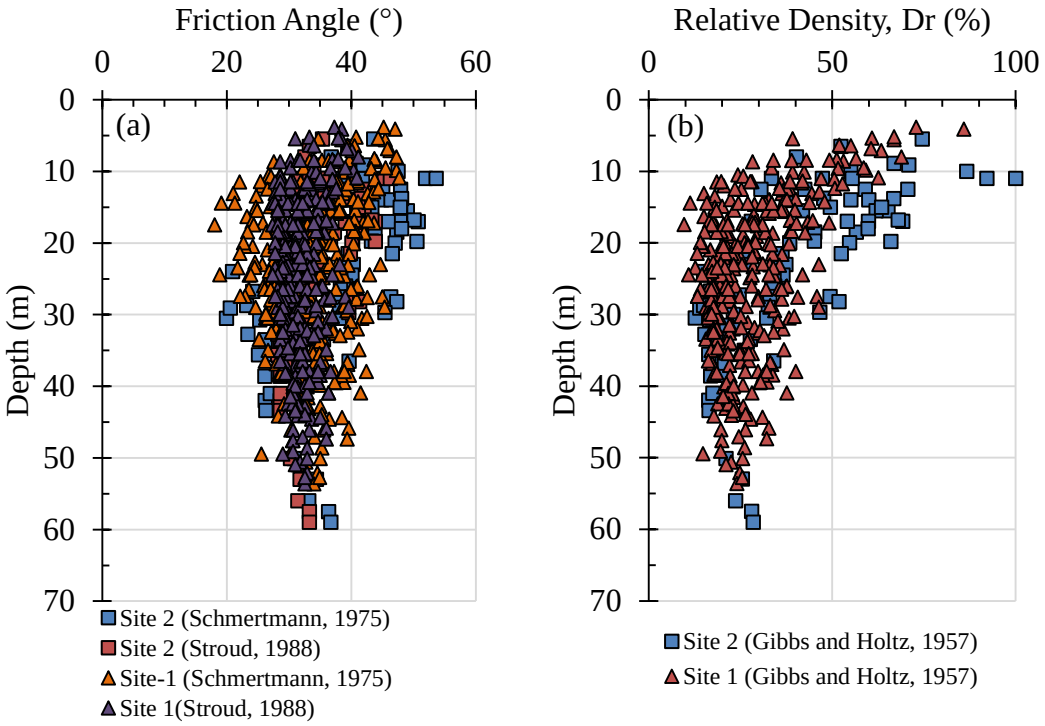

Figure 4. 5 Estimated (a) effective friction angle, (b) relative density, with depth

Table 4. 4 Friction angle and relative density obtained through SPT-N correlations

	Friction angle (°)				Dr (%)	
	Schmertmann, 1975		Stroud, 1988		Gibbs and Holtz, 1957	
	Site 1	Site 2	Site 1	Site 2	Site 1	Site 2
Average	33.6	37.6	31.7	34.2	28.3	39.6
Range	18.0-47.7	20.0-53.6	27.3-41.1	27.8-46.3	9.6-85.9	12.1-100
Stan. Dev.	6.1	8.5	2.9	4.9	11.7	20.1
COV (%)	18.0	22.7	9.0	14.4	41.2	50.7

During standard penetration testing (SPT), disturbed soil samples are obtained from the field at each SPT depth. In this study, the soils at each borehole (e.g. Figure 4. 6) are first classified according to the Unified Soil Classification System by using laboratory test results (sieve analyses, hydrometer test, Atterberg limits) and observations from the field as reported in borehole logs are interpreted. The layers are then grouped into two broad groups: (1) mixture layers and (2) clay layers to calculate corresponding vertical SCL_{SPT-N}. The soil layers that are classified as sandy gravel,

gravelly sand or fill are eliminated (not included in the analyses) because of the SPT-N refusal data within these layers. The same type soil layers at the same boreholes are not lumped together to obtain a single vertical SCL_{SPT-N}. Instead, they are considered separately and each clay layer has its own vertical SCL_{SPT-N}. In this study, vertical SCL_{SPT-N} is not calculated for layers that are less than 7.5 m thickness, because it would be questionable with a limited number of SPT-N data points within that layer. 26 boreholes at site 1 (average borehole depth of 30.5 m from seabed) and 14 boreholes at site 2 (average borehole depth of 25.2 m from seabed) are investigated and vertical SCL's based on SPT-N blowcounts are reported. It is known that SPT is prone to measurement errors (equipment-related and operator effects etc.), however this has not been considered in the current work. Therefore, evaluated vertical spatial correlation lengths represent not only the inherent variability of soils but also the effect of measurement errors.

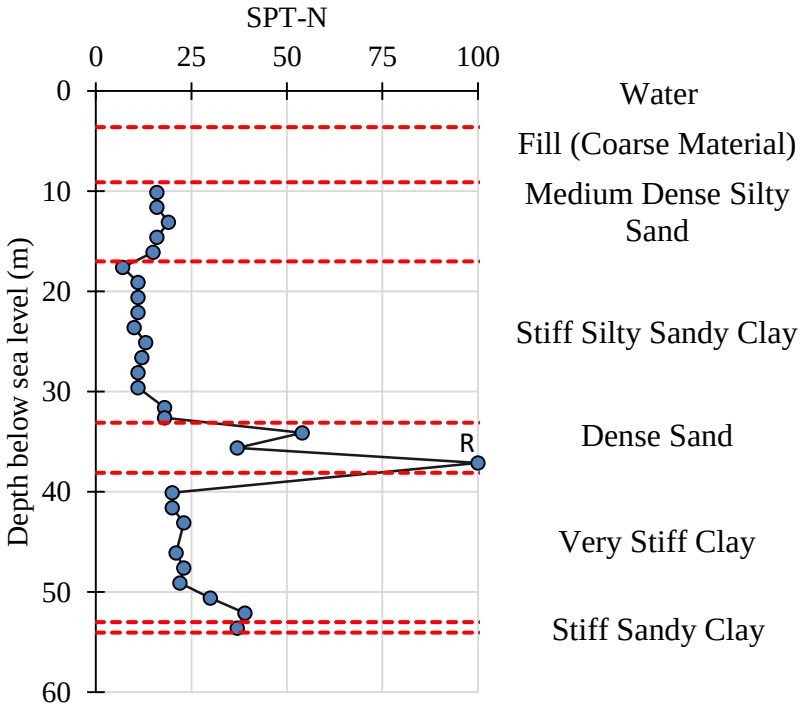

Figure 4. 6 YDSK-1 borehole at site 1

Exponential and squared-exponential autocorrelation functions are widely used to calculate SCL in the literature (DeGroot 1996, Akkaya and Vanmarcke 2003, Zhang and Chen 2012, Huber 2013, Lloret-Cabot et al. 2014, Firouzianbandpey et al. 2014, Zhang et al. 2016, Peng et al. 2017). In this study, four autocorrelation functions

proposed by Vanmarcke (1977) (Table 2. 1) have been utilized to see the effects of the autocorrelation functions on SCL and their corresponding goodness of fit (R-squared) values.

Figure 4. 7 shows an example plot of autocorrelation coefficients versus lag distance, the distance between the observation points for borehole YDSK-16 at site 1. The four autocorrelation functions in Table 2. 1 are utilized to fit the data and corresponding SCL_{SPT-N}'s and coefficient of determinations of fit are provided in Table 4. 5. The results indicate that although the coefficient of determination does not change significantly for "trend" and "constant" approaches, evaluated SCL values based on SPT-N in the vertical direction do.

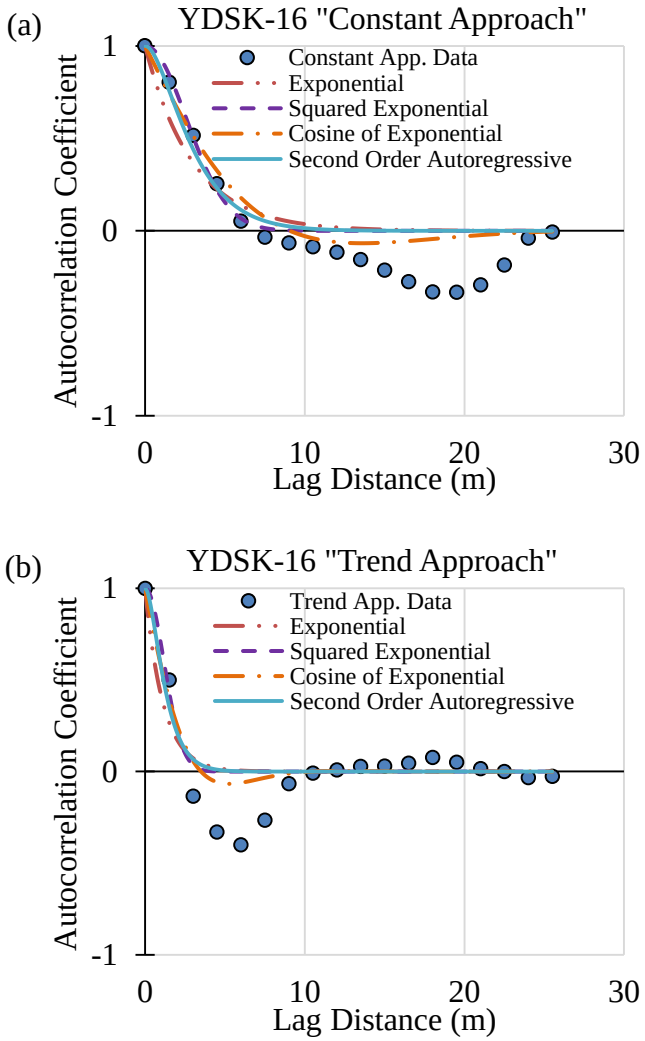

Figure 4. 7 Autocorrelation coefficient vs lag distance for borehole YDSK-16 and utilized autocorrelation functions (a) "constant approach" (b) "trend approach"

Table 4. 5 The spatial correlation lengths, SCL based on SPT-N data (both "constant" and "trend" approaches) for four autocorrelation functions for borehole YDSK-16

	"Constant mean with depth" approach		"Trend" approach	
Correlation Function	SCL (m)	R^2	SCL (m)	R^2
Exponential	6.05	0.75	2.30	0.71
Squared-Exponential	6.49	0.79	2.93	0.76
Cosine-Exponential	5.77	0.84	2.23	0.81
2nd Order Autoregressive	6.43	0.78	2.75	0.74

The SPT-N data at both sites are statistically evaluated. Autocorrelation coefficients and the vertical SCL_{SPT-N}'s are calculated by utilizing four different autocorrelation functions. The mean values, ranges and the standard deviations of the SCL_{SPT-N}'s with "trend approach" are tabulated in Table 4. 6, Figure 4. 8a and Figure 4. 8b. In Table 4. 6, the results are reported, for all boreholes, as the mean vertical SCL_{SPT-N} obtained by exponential autocovariance function and by all four autocorrelation functions. Figure 4. 8a shows the SCL_{SPT-N} of mixture soils and Figure 4. 8b shows that of clay layers, with four autocorrelation functions, for both sites 1 and 2.

Table 4. 6 The mean, and standard deviation of SCL based on SPT-N data (with "trend approach") for clays and mixtures.

		Site 1		Site 2	
		Mixtures	Clays	Mixtures	Clays
Four Functions	Mean (m)	2.19	1.75	1.52	1.67
	Range	0.07-5.20	0.06-3.19	0.08-4.55	0.06-3.13
	Standard Deviation (m)	1.26	0.91	1.28	0.91
Exponential Function only	Mean (m)	1.94	1.45	1.23	1.36
	Range	0.07-5.03	0.06-2.66	0.08-4.17	0.06-2.53
	Standard Deviation (m)	1.34	0.94	1.30	0.93

The mean vertical SCL_{SPT-N} of both sites using all four autocovariance functions and using the "trend approach", is 1.71 m (±0.86 m standard deviation) for clay layers, whereas it is 2.02 m (±1.26 m standard deviation) for mixture layers. For mixture layers, both the mean SCL_{SPT-N} and the standard deviation are slightly larger as compared to clay layers which are in agreement with literature. The vertical SCL values based on SPT-N data are within typical ranges reported in the literature for similar soil groups, both onshore and offshore (Table 2. 3).

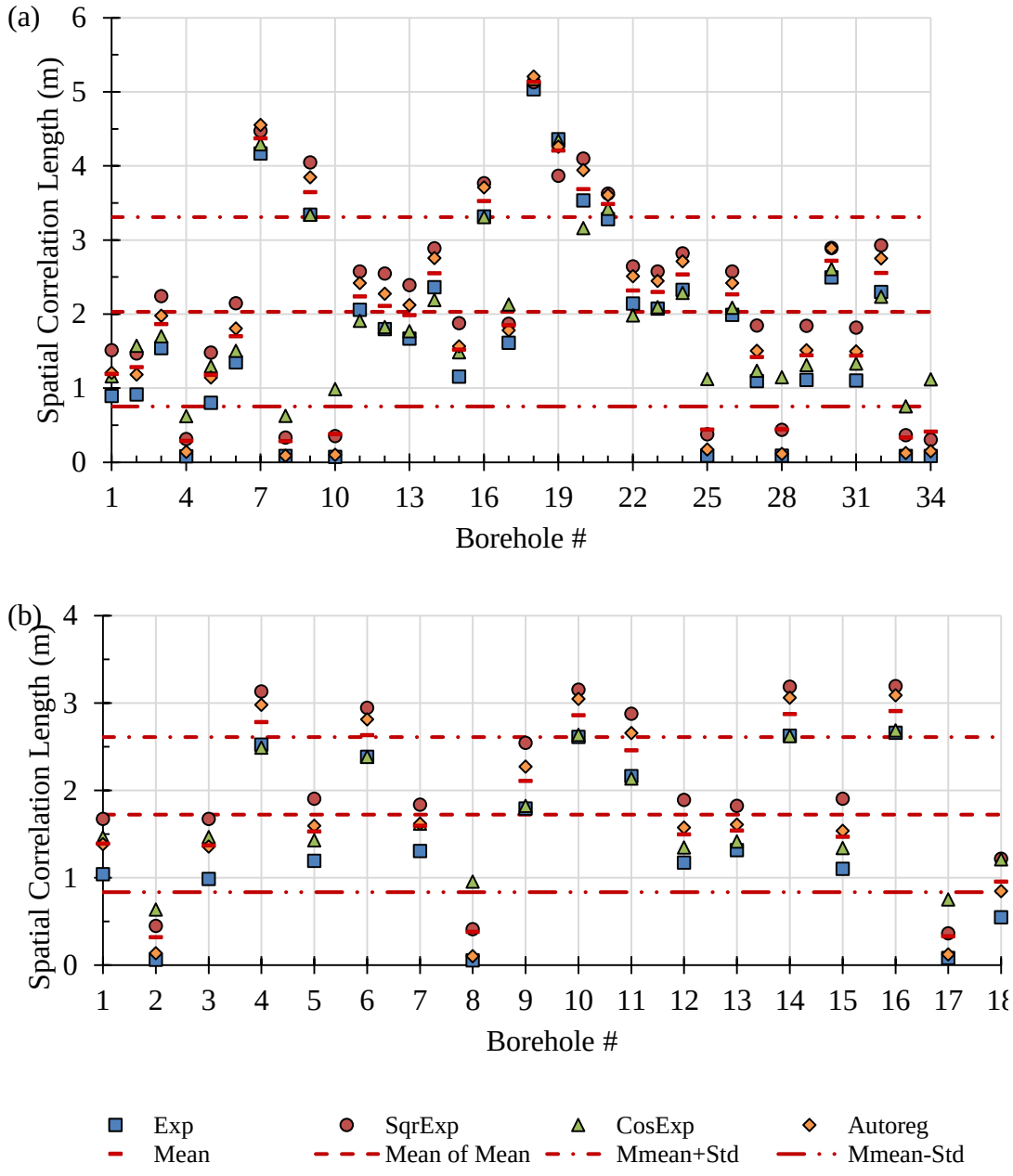

Figure 4. 8 Spatial correlation length based on SPT-N data of (a) all mixture soils, (b) all clay layers, for both Site 1 and Site 2, using "trend approach"

In Table 4. 7, the SCL values based on SPT-N data for both "constant and trend approaches" have been tabulated. It is clearly seen that assuming constant mean with depth results in larger SCL_{SPT-N} values compared with "trend approach". The same result that detrending eliminates the larger SCL has been reported in the study of Akkaya and Vanmarcke (2003).

Table 4. 7 The mean, and standard deviation of SCL based on SPT-N data (with both "constant approach" and "trend approach") for clays and mixtures.

		Constant Approach		Trend Approach	
		Mixtures	Clays	Mixtures	Clays
Four Functions	Mean (m)	4.20	3.85	2.03	1.71
	Range	0.09-9.59	0.27-6.74	0.07-5.20	0.06-3.19
	Standard Deviation (m)	2.14	1.41	1.29	0.89
Exponential Function only	Mean (m)	4.04	3.69	1.78	1.41
	Range	0.09-8.75	1.03-5.53	0.07-5.03	0.06-3.19
	Standard Deviation (m)	2.05	1.33	1.34	0.89

It is observed that, when calculating the autocorrelation coefficient, the $\bar{N}$ should be taken as the trend value at each point. In that case, there is no need to de-trending or standardizing the data because they all result in the same spatial correlation length. In the analyses, two different approaches, constant and trend, have been used and as stated in the study of Akkaya and Vanmarcke (2003), the "trend approach", where the fluctuations about the trend are considered, results in shorter fluctuation (shorter SCL). While the average of SCL_{SPT-N}'s with the "trend approach" for clays and mixtures are 1.71 m and 2.02 m, respectively, the SCL_{SPT-N}'s with "constant-mean with depth" approach are 3.85 m and 4.20 m, for clays and mixtures, respectively. This indicates that the SCL_{SPT-N} with "constant-mean" approach is at least two times the SCL_{SPT-N} with "trend approach". In addition to these, it should be noted that, the order of the trend function is important, as the order of the polynomial increases the scale of fluctuation decreases (Phoon 2008). The variation of the residuals about trend line and calculated spatial correlation lengths are directly related to the flexibility of the trend

line (degree of polynomial). In this study only a linear, i.e. a first order polynomial, equation is used for trend calculations.

When all four utilized autocorrelation functions are compared, the results show that squared exponential (Gaussian) autocorrelation function gives the highest SCL (in 72% of all evaluations) compared to the others; while the exponential (Markov) autocorrelation function results in the lowest SCL (in 78% of all evaluations). In addition, the autocorrelation functions, exponential and cosine-exponential mostly gives closer SCL's to each other (in 43% of all evaluations).

Cao and Wang (2014) state that selection of the most suitable correlation function is an important issue and the goodness of fit can be used to help select the most suitable functions. Table 4. 8 shows the goodness of fit in terms of R^2 values for all the SPT-N data reported in the manuscript with their means and ranges. All R^2 values are in the range of 0.55 and 0.86 with an average of 0.70. When the goodness of fit is low, the fitting of data to the autocovariance function has no statistical meaning, and the SCL obtained could be misleading. Therefore results with a coefficient of determination smaller than 0.50 are not considered. Considering all boreholes data for the mixture soils and for the clay soils, the Cosine Exponential Autocorrelation Function gives the highest R^2 values (greater than 0.64 with an average of 0.74), i.e. seems like the best fit among the four types of autocovariance functions.

Table 4. 8 Goodness of fit, represented by R^2 values, for four different autocorrelation functions (mean value and range in parenthesis)

	Exponential	Squared Exponential	Cosine Exponential	Second Order Autoregressive
Mixtures	0.68 (0.55 - 0.83)	0.70 (0.56 - 0.83)	0.74 (0.59 - 0.85)	0.69 (0.56 - 0.83)
Clays	0.68 (0.56 - 0.83)	0.70 (0.56 - 0.84)	0.74 (0.59 - 0.86)	0.69 (0.56 - 0.84)

4.1.1. Concluding Remarks

In this study, the vertical spatial correlation length of SPT-N data is determined using site investigation data from two sites in the southern coast of Turkey, based on SPT-N values at 1.5 m depth intervals, from 41 boreholes (depths of 23 m to 60 m from sea level) at average water depths of 8.9 m and 16.1 m for Site 1 and Site 2, respectively. At both sites, marine deposits exist where the soil profile generally consists of mixture layers (clayey, silty and sandy materials with different proportions) and low plasticity clay layers. At site 1, soft to stiff clay layers exists having the undrained shear strength (c_u) in the range of 5 to 100 kPa. At site 2, clays can be classified as soft to medium stiff clays with max c_u values of 50 kPa. The rate of increase in c_u with depth is found as 2.1-2.2 kPa/m (for both sites) by utilizing the relationship between SPT-N blowcount and undrained shear strength (Stroud 1974). The rate of increase of c_u with depth, at both sites in this study, are within reported values in the literature. For "mixture" layers at both sites, the mean friction angle is 34° and it is seen that the soils are mostly in loose to medium-dense state with a mean relative density of about 29%.

Both "constant approach" and "trend approach" are utilized in the evaluation of SCL based on SPT-N data. It is seen that "constant approach" overestimates the SCL_{SPT-N} values in cases where there exist a trend with depth. Therefore, it is better to perform "trend approach" and detrend the data in all cases. Vertical SCL of SPT-N data with "trend approach" is calculated using four autocovariance functions; namely, exponential (Markov), squared-exponential (Gaussian), cosine exponential and second-order autoregressive. Using four autocovariance functions, the mean vertical SCL_{SPT-N} values are calculated as 1.72 m (± 0.89 m standard deviation) for clay layers, whereas it is 2.03 m (± 1.28 m standard deviation) for mixture layers. For mixture layers both the mean SCL_{SPT-N} and the standard deviation are slightly larger compared to clay layers in "trend approach". When the SCL_{SPT-N} values are evaluated for clays and mixtures with "constant approach", the values becomes 3.85 m (± 1.42 m standard deviation) and 4.20 m (± 2.14 m standard deviation) respectively. Similar to "trend approach", mixtures have greater mean and standard deviation compared to clays. In addition, the treating the data results in shorter SCL values which is also stated by

Akkaya and Vanmarcke (2003). The vertical SCL_{SPT-N} values are within typical ranges reported in the literature for similar soil groups, both onshore and offshore (Table 2. 3). It is also better to note that the widely-used exponential function almost always gives the lowest value of spatial correlation length, whereas squared-exponential (Gaussian) autocorrelation function gives the highest SCL as compared to the other functions.

Estimation of SCL remains as a significant challenge due to a lack of high-resolution measurement data in geotechnical practice. Among the in-situ tests, the cone penetration test data has the highest resolution (typically on the order of a few cm's). However, other properties of soil such as water content, unit weight, undrained shear strength (from laboratory tests), and SPT-N data from the field can also be used to calculate the SCL, even though they have larger spacing between observation points (lower resolution) (Table 2. 3). Using the conventional statistical method described in the thesis, vertical SCL values found based on SPT-N in the literature are 2.4 m (Vanmarcke, 1977), 0-4 m (Alonso and Krizek 1975 reported in Huber 2013), 0.3 m (Lumb 1975 reported in Huber 2013), 1.36-1.63 m (Zhang and Chen, 2012), which are in agreement with the results in this study.

4.2 Yalova Region (CPT Data)

4.2.1. Site Description

The project site is located in Gulf of Izmit in the Sea of Marmara, on the northwestern part of Turkey (Figure 4. 9). There exists 65 cone penetration test (CPT) soundings where water depths are varying from 1.5 m to 64.2 m. The soundings are grouped into two; shallow water CPT (water depth < 10 m) and deep water CPT (water depth > 10 m). Total of 65 CPT soundings consisting of 45 deep water CPT and 20 shallow water CPT are analyzed. The average length of the CPT soundings and average water depths are provided in Table 4. 9. The cone tip resistance and sleeve friction measurements are taken at each sounding with a 0.02 m vertical spacing (resolution of the measurement).

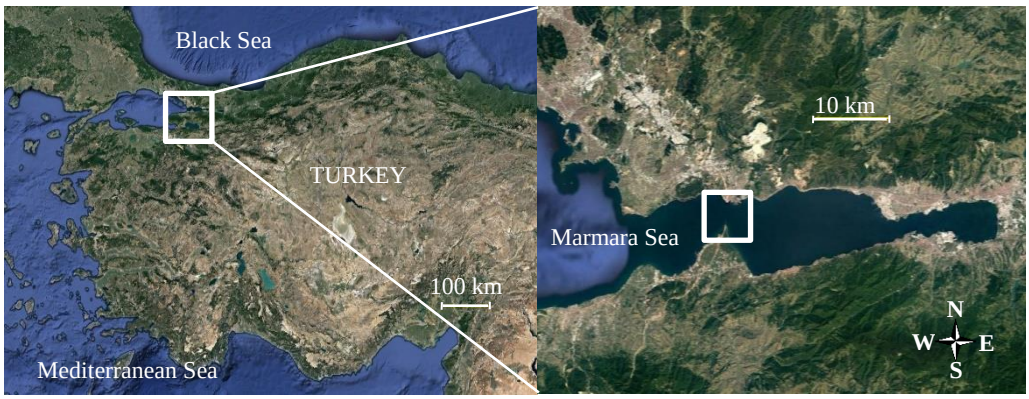

Figure 4. 9 Location of the CPT soundings

Table 4. 9 Length of CPT soundings and water depths

	Deep water CPT	Shallow water CPT
Total number	45	20
Length (m)	60.7 (20.4-200)	60.8 (9.5-200.6)
Water depth (m)	38.8 (16.7-64.2)	3.5 (1.4-9.5)

The classification of the soil profile is made by Robertson (2010)'s soil behavior types (Figure 3. 4): the soil profile at the CPT soundings includes clays/clay-silt mixtures and sands/silty sands according to the soil behavior types. Therefore, soils types are grouped into two broad groups; “Clays” and “Sands”, and all statistical analyses and SCL calculations based on CPT data are conducted for these two types of soil groups separately. Two CPT profiles (tip resistance and friction ratio) are given as an example of the data, in Figure 4. 10 where the soil behavior type zones 3-4 and 5-6-7 are called as “Clays” and “Sands” respectively.

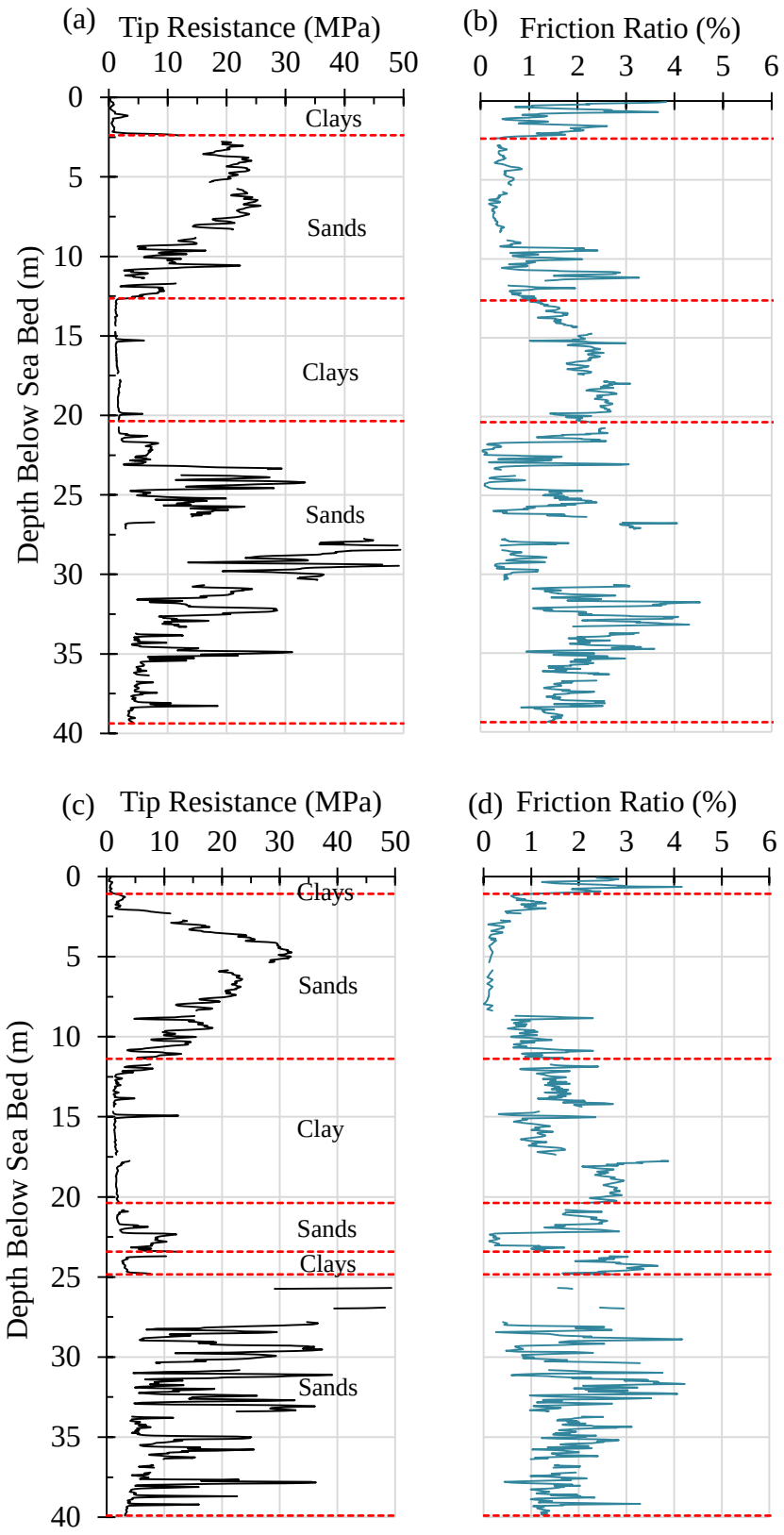

Figure 4. 10 Two representative CPT profiles and soil layers; (a)-(b) and (c)-(d) are tip resistance and friction ratio of soundings 1 and 2

4.2.2. Evaluation of Spatial Variability

The data at each CPT sounding are first divided into soil layers and then the data within these layers are utilized to evaluate the spatial variability. The resolution of gathered data is 0.02 m in the vertical direction which is very common interval for data acquisition for cone penetration test. Some examples of the CPT data (both cone tip resistance and friction ratio) can be seen in Appendix B. Soil properties like undrained shear strength, c_u, and relative density, D_r, are estimated by using empirical equations; Equation 4.4 and Equation 4.5. The following relationship is utilized to evaluate c_u:

$$c_u = \frac{q_t - \sigma_{v0}}{N_k} \tag{4.4}$$

where q_t is the measured cone tip resistance, σ_v is the total in situ vertical stress (saturated unit weight of all layers is taken as 20 kN/m^3) and N_k is the constant that can vary from 14 to 20 (Robertson, 2010). In addition, relative density, Dr, is found by the following relationship (Jamiolkowski et al. 2003):

$$D_r = \left(\frac{1}{0.0296}\right) \ln[q_t/[2.494 \left(\sigma'_{v0} \left(\frac{1+2K_0}{3*100}\right)\right)^{0.46}]] \tag{4.5}$$

where σ'_{v0} is the effective overburden pressure and K_0 is the at-rest earth pressure coefficient. In Figure 4. 11, undrained shear strength (N_k=17) and relative density (K_0=0.55) profiles are provided for two CPT soundings. The relative density of sands are mostly less than 50%, and undrained shear strength for clays are less than 100 kPa. Therefore, the sands are mostly in loose to medium dense state and clays are soft to medium stiff.

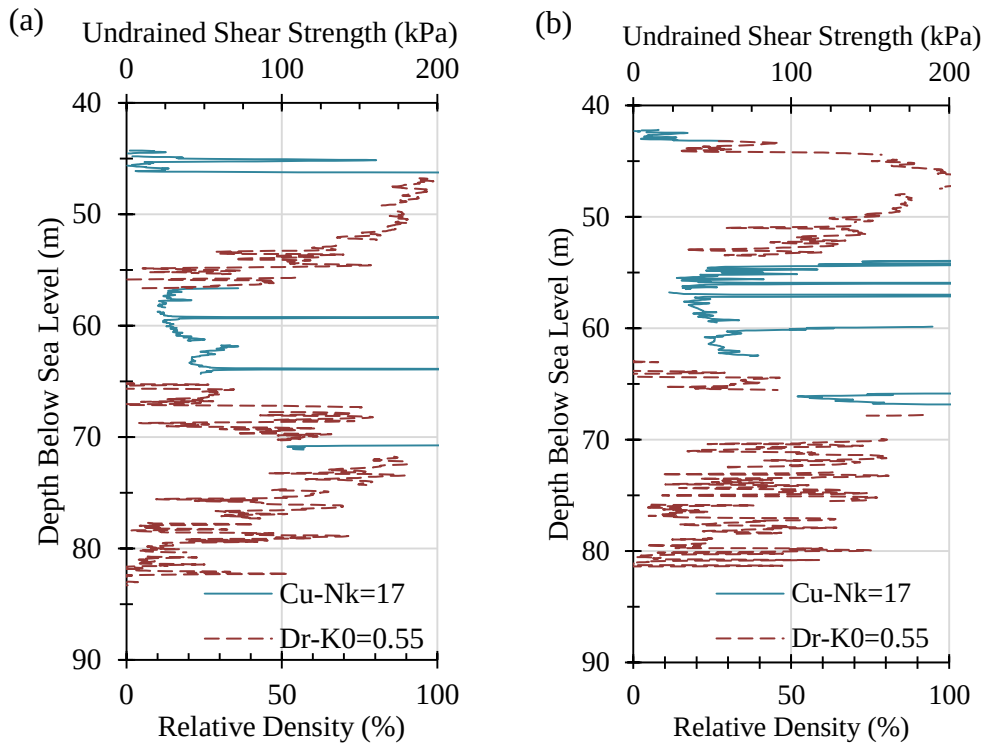

Figure 4. 11 Two representative undrained shear strength and relative density profiles; (a) Sounding-1 (b) Sounding-2, where N_k and K_0 are taken as 17 and 0.55.

The undrained shear strength, c_u, profiles for 9 CPT soundings having the highest water depths with an average of 51.3 m are provided in Figure 4. 12. The upper and lower limits (14 and 20) for constant N_k is utilized in Figure 4. 12a while average N_k value of 17 is employed in Figure 4. 12b. In addition, the summary of c_u for these 9 CPT soundings are also tabulated in Table 4. 10 for different N_k values. The results indicate that the employed N_k value has great importance on the undrained shear strength value obtained.

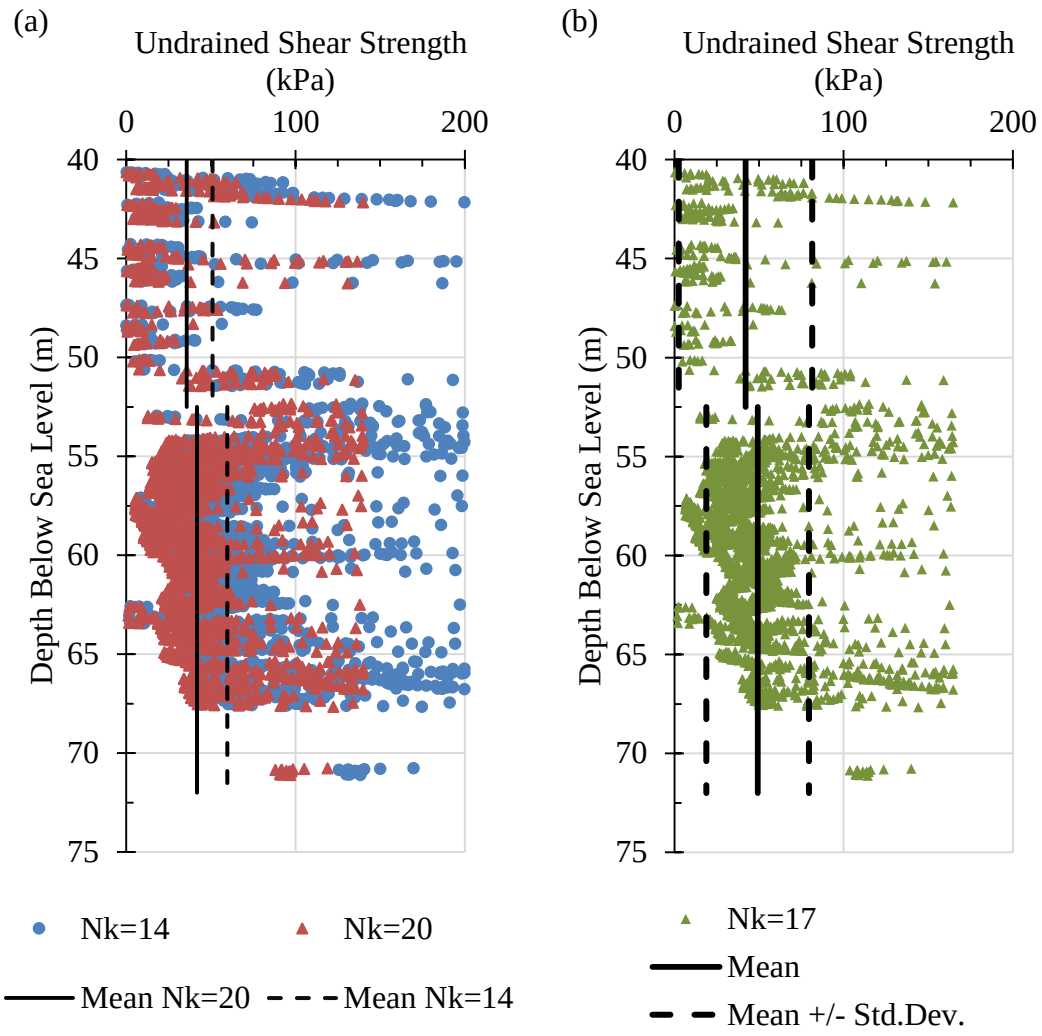

Figure 4. 12 Estimated undrained shear strength profile for nine CPT soundings with an average water depth of 51.3 m: (a) N_k=14 and 20, (b) N_k=17

Table 4. 10 Summary of undrained shear strength for 9 CPT soundings (average water depth of 51.3 m)

Undrained Shear Strength (kPa)			
Depth From Sea Level (m)=40-52.5			
N_k →	20	17	14
Mean	35.68	41.97	50.97
Standard Deviation	33.51	39.43	47.88
COV	93.94	93.94	93.94
Depth From Sea Level (m)=52.5-75			
N_k →	20	17	14
Mean	41.78	49.15	59.69
Standard Deviation	25.77	30.32	36.82
COV	61.69	61.69	61.69

In Table 4. 11, evaluated c_u for clays and D_r for sands are provided for all soundings. It is seen that clays at shallow watershave approximately two times greater undrained shear strength values and lower COV values than clays at deep waters. In addition, the relative density of sands does not differ at shallow and deep waters. D_r values are generally less than 50 % (medium-dense state) with a COV value of about 60 %. In the literature, the COV values of c_u and D_r are reported in the range of 6% to 80% and 11% to 74% respectively (Phoon and Kulhawy 1999a). Therefore the COV values of this study are within the range of values in the literature.

Table 4. 11 Summary of undrained shear strength and relative density for all shallow and deep water soundings

		Shallow Water Soundings			**Deep Water Soundings**		
	N_k→	**14**	**17**	**20**	**14**	**17**	**20**
c_u (kPa)	Mean	121.90	100.39	85.33	65.12	53.63	45.58
	Range	3-200	2-164	2-140	0-200	0-165	0-140
	Standard Dev.	43.21	35.58	30.24	38.42	31.64	26.90
	COV (%)	35.44	35.44	35.44	59.00	59.00	59.00
	K_0→	**0.4**	**0.55**	**0.7**	**0.4**	**0.55**	**0.7**
D_r (%)	Mean	46.33	43.94	41.86	50.24	47.85	45.77
	Range	5-100	2-98	0-95	5-100	2-98	0-96
	Standard Dev.	29.63	29.63	29.63	29.95	29.95	29.95
	COV (%)	63.95	67.44	70.78	59.61	62.60	65.43

Both “trend with depth approach” and “constant approach” are utilized in the evaluation of SCL based on CPT data. Cone tip resistance, friction ratio, and sleeve friction data have been utilized and corresponding SCL values with two approaches are provided in Table 4. 12 as averages. Detailed results can be seen in Table 4. 13, Table 4. 14, Table 4. 15 and Table 4. 16. The SCL based on CPT data of clays and sands for deep water CPT soundings are reported in Table 4. 13 and Table 4. 14 respectively. Likewise, results of shallow water CPT soundings are reported in Table 4. 15 and Table 4. 16 for clays and sands.

Table 4. 12 Summary of average vertical SCL values based on CPT data

			SCL (m)			
			Deep Water		Shallow Water	
			Clays	Sands	Clays	Sands
All four autocovariance functions	Cone tip resistance	Constant Approach, Mean	0.258	0.263	0.262	0.231
		Trend Approach, Mean	0.148	0.168	0.116	0.133
	Friction Ratio	Constant Approach, Mean	0.269	0.217	0.251	0.167
		Trend Approach, Mean	0.172	0.143	0.142	0.112
	Sleeve friction	Constant Approach, Mean	0.250	0.234	0.210	0.216
		Trend Approach, Mean	0.147	0.153	0.124	0.115

Based on the statistical evaluation, the following results are obtained:

- All average vertical SCL values based on CPT data, of clays and sands, in shallow and deep waters, using four different autocovariance functions are in the range of 0.11 m to 0.27 m (Table 4.12). The SCL values of CPT data based on "constant mean with depth approach" are always slightly larger than those based on "trend with depth approach".
- Sands and clays at deep water CPT soundings have slightly larger vertical SCL_{CPT} than sands and clays at shallow water soundings, in both constant and trend approach.
- Among four autocorrelation functions, squared exponential function gives the highest mean SCL_{CPT} values in 79% of all evaluations and 2^{nd} order autoregressive function gives the highest in 21% of all evaluations. In addition, cosine of exponential function always gives the smallest SCL_{CPT} values in both constant and trend approach.
- Sands have always greater SCL_{CPT}, although slightly, based on cone tip resistance compared to the values based on friction ratio and sleeve friction.
- In trend approach (where the fluctuations are evaluated about a linear trend line), friction ratio data gives the highest vertical SCL value than tip resistance and sleeve friction for clays.
- Based on cone tip resistance, sands have always larger vertical SCL than clays in trend approach.

- Clays have always (slightly) greater vertical SCL based on friction ratio than sands.

Table 4. 13 The mean, and standard deviation of the vertical SCL based on deep water CPT (with both “constant approach”and “trend approach”) for clays

Deep Water							
SCL CLAYS							
Correlation Function		Cone Tip Resistance		Friction Ratio		Sleeve Friction	
		“Constant mean with depth” approach	“Trend” approach	“Constant mean with depth” approach	“Trend” approach	“Constant mean with depth” approach	“Trend” approach
Exponential	Mean (m)	0.260	0.148	0.268	0.167	0.251	0.146
	Range (max/min)	0.749	0.441	0.732	0.469	0.755	0.380
		0.034	0.029	0.029	0.026	0.029	0.030
	Standard Deviation (m)	0.177	0.079	0.168	0.090	0.176	0.079
Squared-Exponential	Mean (m)	0.266	0.154	0.280	0.182	0.258	0.155
	Range (max/min)	0.906	0.542	0.868	0.569	0.926	0.450
		0.036	0.029	0.034	0.032	0.037	0.038
	Standard Deviation (m)	0.203	0.089	0.190	0.104	0.199	0.087
Cosine-Exponential	Mean (m)	0.238	0.137	0.249	0.158	0.231	0.136
	Range (max/min)	0.689	0.433	0.709	0.441	0.681	0.410
		0.027	0.024	0.021	0.020	0.023	0.023
	Standard Deviation (m)	0.178	0.082	0.168	0.093	0.178	0.084
2nd Order Autoregressive	Mean (m)	0.266	0.154	0.278	0.179	0.258	0.153
	Range (max/min)	0.845	0.502	0.810	0.533	0.857	0.425
		0.036	0.030	0.032	0.030	0.035	0.036
	Standard Deviation (m)	0.193	0.085	0.182	0.099	0.191	0.084

Table 4. 14 The mean, and standard deviation of the vertical SCL based on deep water CPT (with both “constant approach”and “trend approach”) for sands

Deep Water							
SCL SANDS							
		Cone Tip Resistance		Friction Ratio		Sleeve Friction	
		“Constant mean with depth” approach	“Trend” approach	“Constant mean with depth” approach	“Trend” approach	“Constant mean with depth” approach	“Trend” approach
Exponential	Mean (m)	0.2607	0.1636	0.2183	0.1411	0.2340	0.1496
		0.765	0.487	0.728	0.465	0.720	0.448
	Range	0.027	0.022	0.029	0.028	0.038	0.034
	Standard Deviation (m)	0.172	0.090	0.143	0.079	0.149	0.078
Squared-Exponential	Mean (m)	0.278	0.180	0.224	0.151	0.244	0.162
		0.926	0.579	0.880	0.581	0.874	0.550
	Range	0.026	0.027	0.034	0.031	0.042	0.036
	Standard Deviation (m)	0.201	0.104	0.159	0.091	0.169	0.088
Cosine-Exponential	Mean (m)	0.240	0.153	0.200	0.132	0.217	0.140
		0.715	0.455	0.692	0.437	0.668	0.428
	Range	0.016	0.020	0.020	0.018	0.031	0.024
	Standard Deviation (m)	0.169	0.092	0.146	0.082	0.151	0.081
2nd Order Autoregressive	Mean (m)	0.274	0.175	0.224	0.149	0.243	0.159
		0.863	0.535	0.817	0.534	0.813	0.511
	Range	0.026	0.025	0.034	0.030	0.042	0.038
	Standard Deviation (m)	0.190	0.099	0.153	0.087	0.162	0.085

Table 4. 15 The mean, and standard deviation of the vertical SCL based on shallow water CPT (with both “constant approach”and “trend approach”) for clays

Shallow Water							
SCL CLAYS							
		Cone Tip Resistance		Friction Ratio		Sleeve Friction	
Correlation Function		“Constant mean with depth” approach	“Trend” approach	“Constant mean with depth” approach	“Trend” approach	“Constant mean with depth” approach	“Trend” approach
Exponential	Mean (m)	0.259	0.115	0.245	0.141	0.210	0.120
		2.923	0.468	2.989	0.994	2.827	0.995
	Range	0.043	0.041	0.018	0.018	0.036	0.037
	Standard Deviation (m)	0.499	0.078	0.419	0.169	0.346	0.117
Squared-Exponential	Mean (m)	0.267	0.123	0.268	0.147	0.213	0.133
		2.961	0.404	3.292	0.999	2.333	1.155
	Range	0.050	0.048	0.027	0.027	0.044	0.043
	Standard Deviation (m)	0.477	0.069	0.453	0.149	0.301	0.130
Cosine-Exponential	Mean (m)	0.255	0.106	0.231	0.131	0.202	0.112
		3.248	0.468	3.014	0.883	3.131	0.960
	Range	0.037	0.036	0.019	0.019	0.033	0.030
	Standard Deviation (m)	0.535	0.070	0.417	0.148	0.381	0.110
2nd Order Autoregressive	Mean (m)	0.269	0.121	0.262	0.147	0.216	0.129
		2.857	0.444	3.212	0.965	2.640	1.095
	Range	0.048	0.047	0.023	0.023	0.042	0.042
	Standard Deviation (m)	0.497	0.072	0.444	0.156	0.330	0.125

Table 4. 16 The mean, and standard deviation of the vertical SCL based on shallow water CPT (with both “constant approach”and “trend approach”) for sands

Shallow Water							
SCL SANDS							
		Cone Tip Resistance		Friction Ratio		Sleeve Friction	
Correlation Function		“Constant mean with depth” approach	“Trend” approach	“Constant mean with depth” approach	“Trend” approach	“Constant mean with depth” approach	“Trend” approach
Exponential	Mean (m)	0.225	0.127	0.166	0.109	0.214	0.111
		3.328	2.110	2.336	1.117	4.138	0.915
	Range	0.039	0.030	0.015	0.013	0.016	0.016
	Standard Deviation (m)	0.388	0.158	0.187	0.104	0.400	0.078
Squared-Exponential	Mean (m)	0.247	0.145	0.178	0.121	0.222	0.126
		3.921	1.910	2.193	1.025	4.429	0.902
	Range	0.047	0.036	0.025	0.023	0.026	0.026
	Standard Deviation (m)	0.413	0.153	0.176	0.097	0.400	0.074
Cosine-Exponential	Mean (m)	0.213	0.121	0.148	0.101	0.206	0.103
		3.218	2.345	2.028	1.027	4.139	0.690
	Range	0.034	0.026	0.018	0.017	0.018	0.018
	Standard Deviation (m)	0.393	0.167	0.154	0.092	0.419	0.065
2nd Order Autoregressive	Mean (m)	0.240	0.140	0.175	0.118	0.222	0.121
		3.695	2.106	2.286	1.063	4.414	0.907
	Range	0.045	0.035	0.021	0.018	0.021	0.022
	Standard Deviation (m)	0.407	0.161	0.180	0.100	0.405	0.076

4.2.3. Concluding Remarks

In this part of the study, 65 CPT soundings; 45 deep water CPT and 20 shallow water CPT are analyzed. The average water depth of shallow and deep water CPT soundings are 3.5 m and 38.8 m respectively. The average length of the soundings is approximately 60 m below the seabed. The resolution of the data is 0.02 m with depth. All CPT data are first classified according to the Robertson (2010)'s soil behavior type and soil behavior type zones 3-4 and 5-6-7 are grouped together into broad groups of "clays" and "sands", respectively. All statistical analyses are conducted by the MATLAB code developed in this study, where soil profile is divided into same soil layers and the vertical SCL is evaluated by utilizing four autocovariance functions, using cone tip resistance, sleeve friction and friction ratio, separately.

Undrained shear strength, c_u, and relative density, D_r, values are calculated for clays and sands by using empirical equations. The average c_u is found as 100 kPa (σ=35.6 kPa) for shallow water soundings and 54 kPa (σ=31.6 kPa) for deep water soundings with a constant N_k value of 17. The results also show the importance of choosing the value of the N_k. The value varies from 14 to 20 and the change in the undrained shear strength can be as much as 40 kPa, depending on the N_k value. In addition, it is seen that D_r is mostly less than 50% meaning that sands are in loose to medium dense state.

Vertical SCL_{CPT} evaluations are conducted with both constant and trend approaches for deep and shallow CPT soundings separately. All measurements; cone tip resistance, friction ratio, and sleeve friction have been considered and corresponding vertical SCL values are reported in Table 4. 12. The results show that trend approach always results in smaller SCL values, although slightly. In addition, deep water clays and sands have greater vertical SCL_{CPT} values than shallow water clays, possibly because of more uniform deposition and formation processes in geological history. All average SCL_{CPT} values are found to be between 0.17 and 0.27 m for constant approach and between 0.11 and 0.17 m for trend approach. Detailed results are provided in Table 4. 13, Table 4. 14, Table 4. 15 and Table 4. 16.

The evaluation of CPT soundings indicates that data of shallow water soundings has less SCL_{CPT} values, meaning that the data fluctuate more frequently, i.e. a rough random field. The same result is reported in the study of Cheon and Gilbert (2014) and it is stated that deeper offshore marine soils have larger SCL_{CPT}'s compared to the shallower depths. In addition, Nadim (2015) states that although the soil types in the offshore and nearshore are similar, their spatial properties show significant differences, i.e. the correlation structures are different. Soil parameters may change more frequently from point to point in the nearshore while it is more stationary at deep waters.

CHAPTER 5

EFFECTS OF VARIABILITY ON BEARING CAPACITY AND SETTLEMENT

In this chapter, the variability of soil parameters and spatial correlation length are considered in the foundation design problems by using random finite element method tools. Both settlement and bearing capacity of shallow strip foundations are investigated and results are illustrated. The soil parameters can be defined by using statistical distributions, such as normal and lognormal distributions. Lumb (1966), Schultze (1971) and JCSS (2001) utilized normal distribution, while other researchers such as Jiang et al. (2014), Griffiths et al. (2002), Cho (2010) and Tabarroki et al. (2013) used lognormal distribution because of the non-negative values in soil parameters (cohesion, friction angle, undrained shear strength, unit weight etc.). It should be noted that the best and proper statistical distribution of soil parameters can be a separate study by using the real field and laboratory test data, and the best fitting distribution type probably depends on the soil property considered and the specific site. In this chapter, the only purpose is to study the effect of SCL, therefore one of the widely used statistical distribution types, lognormal distribution, is assigned to the soil parameters.

5.1 Effects on Initial (Elastic) Settlement

In the shallow and offshore sea, mostly pile foundation is preferred for structures. However, in this part of the study, only a shallow strip foundation is considered just to demonstrate the effect of variability and SCL of soil parameters on immediate (elastic)

settlement. In the finite element model, lower boundary is totally restricted to any movement (fixed boundary) and vertical deformation is allowed at the side boundaries. The width of shallow strip foundation, B, is 5 m under a 300 kN/m loading. The increase in vertical stress due to applied load decreases significantly at a depth of 4B below the base of foundation, therefore 20 m is taken as the vertical length of the model underneath the foundation. In addition, the lateral distance from the foundation to the side boundaries is investigated. It is a common practice to have at least about 3B horizontal distance between the foundation and the side boundary of the model to avoid boundary effects completely. After some preliminary runs about the dimensions of the model, it is seen that when the horizontal distance between the edge of the foundation and side boundary is as small as 1.5B, the change in the obtained settlement results is effected by less than 5%. Therefore, in order to decrease run time, the model size is selected as 20 m - 20 m (Figure 5. 1). The soil is modeled with an elastic model where the Poisson's ratio is taken as constant, 0.25, and the elasticity modulus is used as a random variable for analyses. This analyses only looks into immediate (elastic) settlement and does not include consolidation settlements. The modulus of elasticity is statistically represented by lognormal distribution and SCL of modulus of elasticity is taken as equal in the both vertical and horizontal direction (isotropic). This distribution is defined with an average of 10 MPa, and the analysis is performed with a coefficient of variation of 5%, 22.5%, and 40% to represent different degrees of variation. All parameters of the model can be seen in Table 5. 1. The RSETL2D software creates random field using the SCL (equal in the both horizontal and vertical directions; isotropic SCL) and exponential correlation function for the modulus of elasticity and maps them to the final elements. Monte Carlo sampling method is utilized and 2000 simulations are performed for settlement calculations to avoid the effect of insufficient number of simulations (Pieczynska et al. 2011). In Figure 5. 1, the random field (SCL_v=1 m and SCL_h=1 m) generated for the modulus of elasticity can be seen where the dark color shows high values.

Table 5. 1 Parameters used in the bearing capacity model

Soil parameter	Unit	Statistical distribution	Value
Elasticity modulus, E	MPa	Lognormal	10
Poisson ratio	-	-	0.25
Random field parameters			
Spatial correlation length (m) (isotropic) of elastic modulus	0.025 - 0.05 - 0.1 - 0.25 - 0.5 - 1 - 2 - 3 - 4 - 5 - 6 - 7 - 8 - 9 - 10 - 15 - 20		
COV (%)	5 - 22.5 - 40		

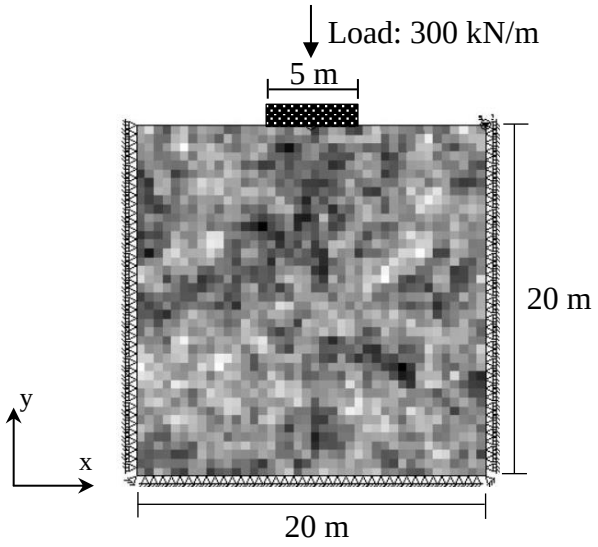

Figure 5. 1 Geometrical representation of model with random field of cohesion (SCL_v=1 m and SCL_h=1 m)

In each simulation of an analysis, a random field is created for the logarithm of elasticity modulus, E. In addition, the results obtained from each simulation is stored and a statistical distribution is used to represent the output data. In addition, E value in each simulation is also stored and at the end, the mean and standard deviation of E values in an analysis can be calculated. In Figure 5. 2, a random field created for elasticity modulus and magnified displaced mesh is provided where $\mu_E = 1 * 10^4, \sigma_E = 4 * 10^3$ and $n_{simulation} = 2000$. Also, probability density function of settlement results (with normal distribution parameters) and all utilized E values (with lognormal distribution parameters) in a single analysis are provided in Figure 5. 3.

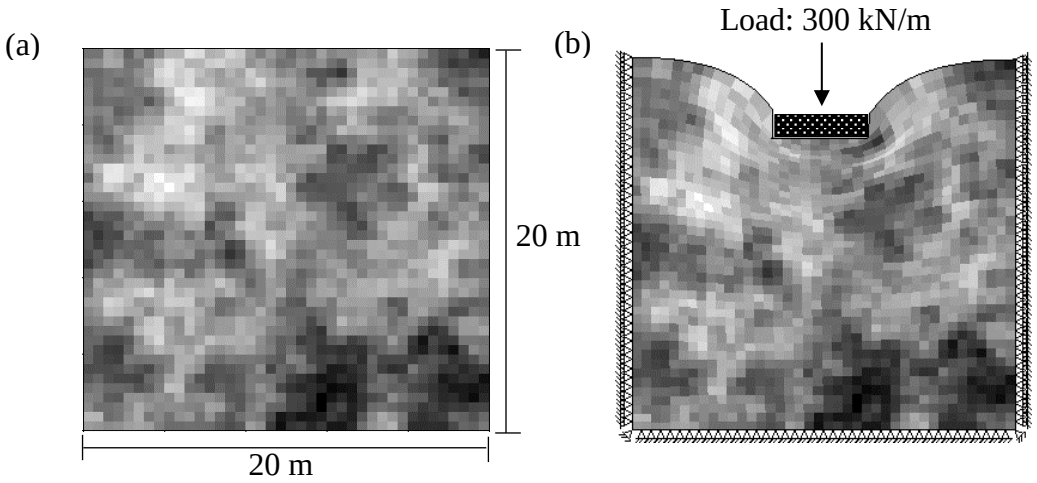

Figure 5. 2 (a) Generated random field for logarithm of E (SCL_E= 4 m) and (b) magnified displaced mesh

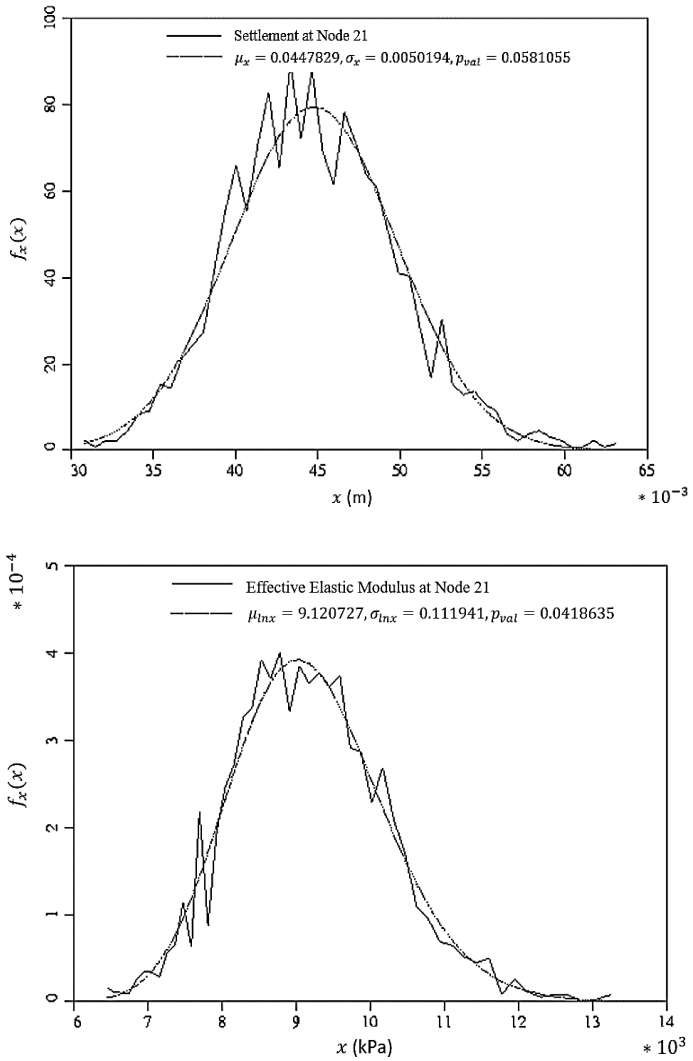

Figure 5. 3 Probability density function of (a) settlement and (b) effective elastic modulus with statistical parameters at the center point under the foundation

The effect of SCL and COV of soil parameters on the settlement is shown in Figure 5. 4. The average of the settlement of 2000 simulations is not affected significantly by increasing SCL of soil parameters. With the increase of SCL_E, relatively higher increase is observed for higher COV levels (Figure 5. 4a). It is also seen that increase of COV value of the elasticity modulus has greater effect on elastic settlement than SCL_E. Therefore, it may be concluded that the COV of the soil parameter has primary effect on the settlement, while SCL_E has secondary effects. In 2000 simulation results, COV of elastic settlement results increased significantly with the increase of SCL_E (Figure 5. 4b); the increase in the COV value of the elasticity modulus also increased the COV value of the settlement results.

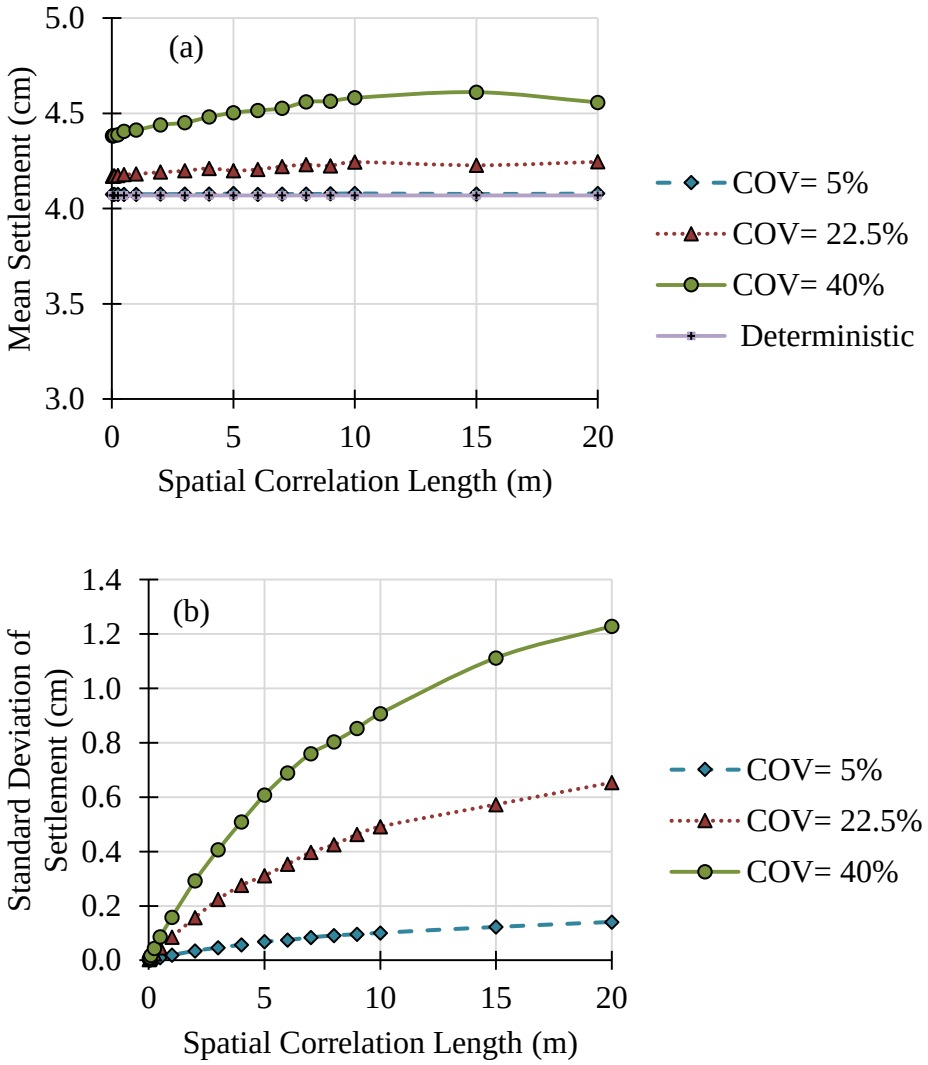

Figure 5. 4 The effect of COV of soil parameters and SCL_E on (a) mean settlement and (b) COV of settlement (2000 simulations)

By creating random field by using mean, standard deviation and SCL_E, the reliability of the foundation can be obtained for serviceability limit state (SLS), maximum allowable settlement. For this study, serviceability limit is taken as 4.5 cm, as an example for demonstration purposes, and the probability of exceeding SLS is obtained for different COV levels and SCL_E values (Figure 5. 5). Although deterministic results indicate that the limit is not exceeded, the probability of exceeding SLS can be as much as 50%. As the COV and SCL of elastic modulus increase, the range of initial settlement results widens and the area of probability density function over the values less than SLS increases. Figure 5. 5 shows that SCL_E and COV of soil can have significant effects on the probability of having greater settlement than the maximum defined limit.

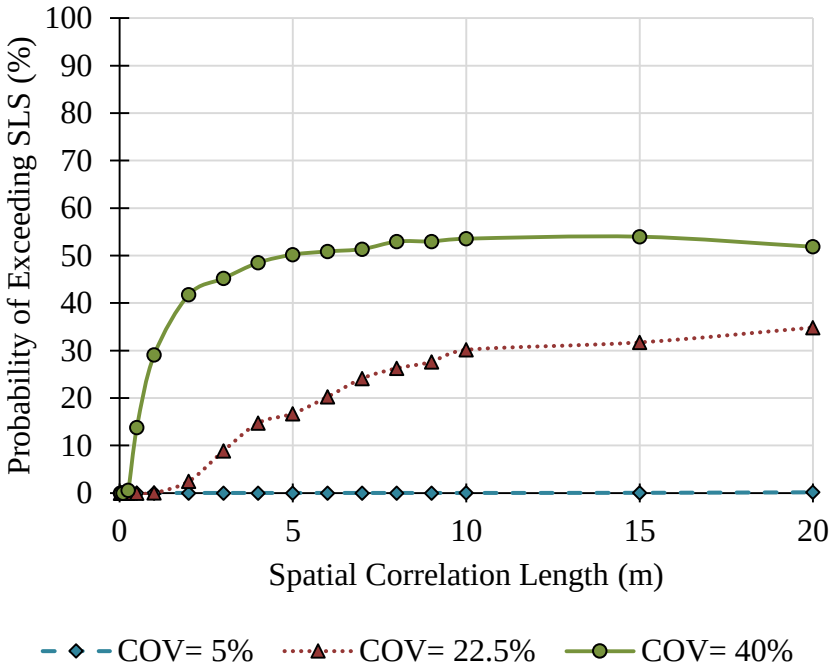

Figure 5. 5 Probability of exceeding SCL

5.2 Effects on Bearing Capacity

The effects of SCL and COV of soil parameters on bearing capacity of shallow foundation are investigated by using RBEAR2D software (Fenton and Griffiths 2008) using RFEM. A 4-m wide strip footing located on the ground surface (Figure 5. 6) and a general, c- ϕ soil is considered in the analyses. 5 levels of COV, between 5% and 40%, for the soil parameters are utilized in the analyses. The model parameters are given in Table 5. 2. In an analyses, same COV values are applied to all random variables. Both isotropic and anisotropic SCL analyses are performed where the ratio of horizontal SCL (δ_h) to the vertical (δ_v) is taken as 10 (Baecher and Christian 2003) in anisotropic case. Soil is modeled with elasto-plastic Von Mises constitutive soil model.

Table 5. 2 Parameters used in the bearing capacity model

Soil Parameters	Statistical Distribution	Mean Value
Cohesion (kPa)	Lognormal	10
Friction angle (deg.)	Lognormal	35
Dilation angle (kPa)	Lognormal	5
Elastic modulus (kPa)	Lognormal	20000
Poisson's Ratio	Deterministic	0.25
Random field parameters		
Spatial Correlation Length (m) of soil parameters	0.025 - 0.05 - 0.1 - 0.25 - 0.5 - 1 - 2 - 3 - 4 - 5 - 6 - 7 - 8 - 9 -10 - 15 - 20	
COV (%)	0 - 5 - 13.75 - 22.5 - 31.25 - 40	
Correlation coefficient (c-ϕ)	-0.5	

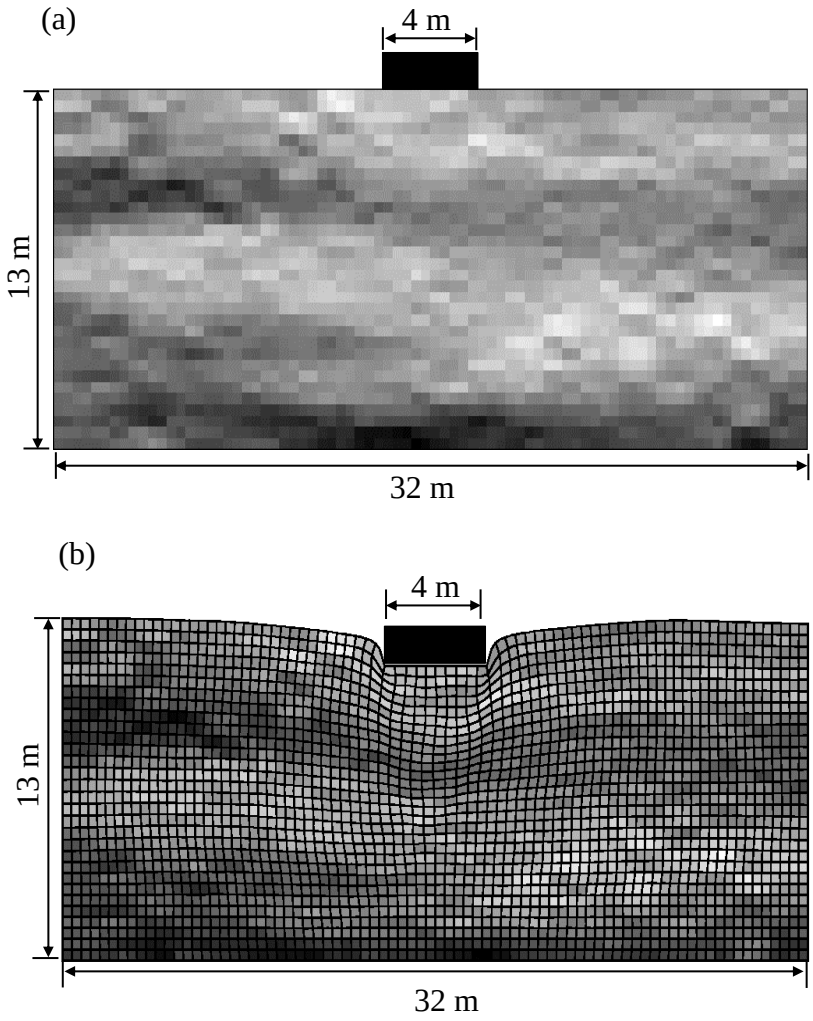

Figure 5. 6 Representation of model with random field of cohesion (SCL_v=10 m and SCL_h=100 m); (a) Geometry of the model, (b) deformed mesh

In the bearing capacity analysis, both anisotropic and isotropic spatial variability are considered. In Figure 5. 7, random fields for 1 m and 10 m SCL of cohesion in the vertical direction are provided for both isotropic and anisotropic cases.

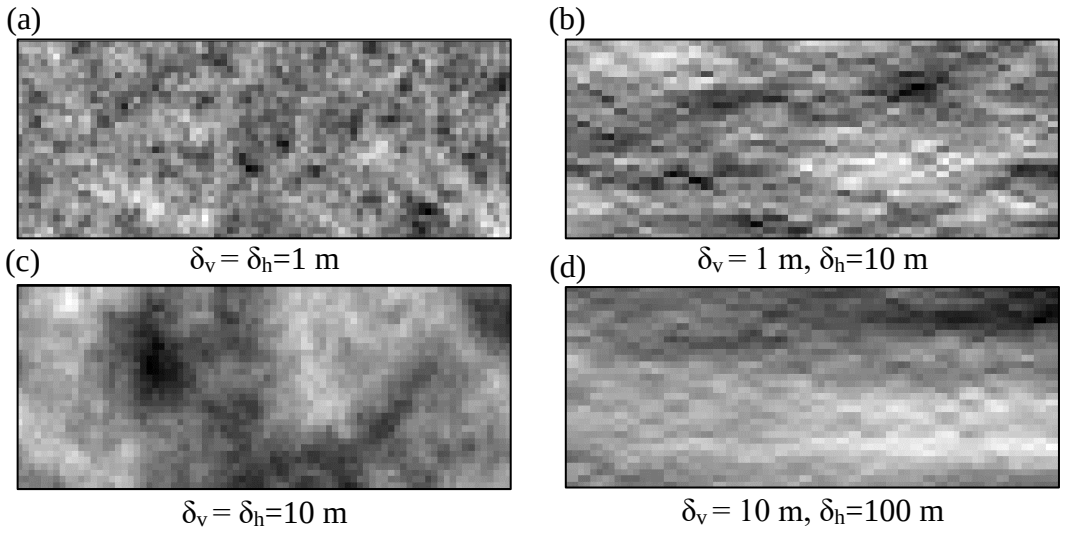

Figure 5. 7 Generated random field for isotropic (a-c) and anisotropic (b-d) cases (model geometry 13 m x 32 m)

Effect of the number of Monte-Carlo simulations is investigated by performing analyses with simulation numbers from 1 to 10000. The analyses are performed for COV of 22.5% and SCL of soil parameters are taken as 1, 2 and 3 m in both directions (isotropic). Figure 5. 8 indicates that the mean bearing capacity converges to a stable point at about 2000 simulation numbers regardless of the SCL value. Therefore, in all analyses, the number of simulations is taken as 2000.

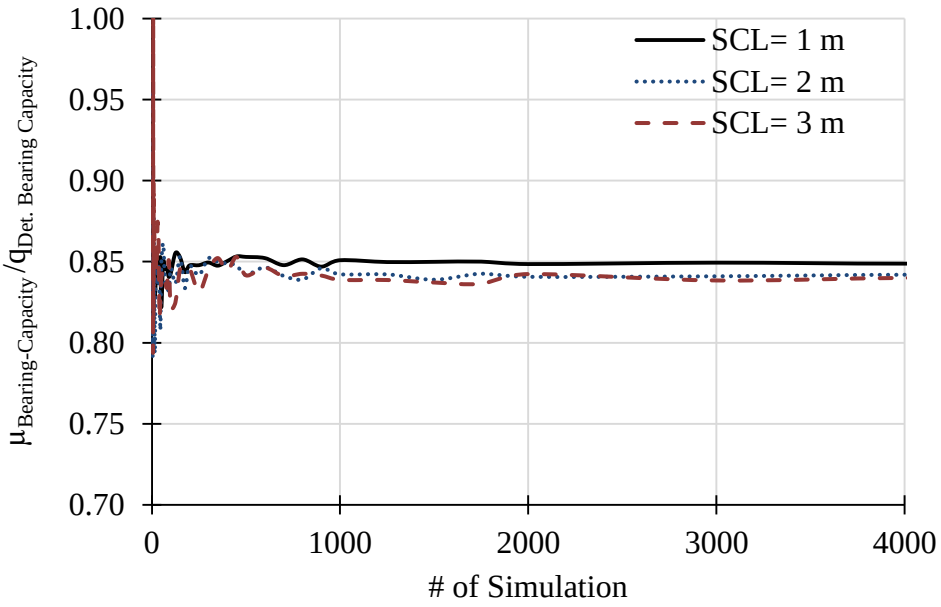

Figure 5. 8 Effect of number of Monte Carlo simulations on the mean bearing capacity for COV=22.5 % and $SCL_{v=h}$ 1 m, 2 m and 3 m cases.

The effects of SCL of soil parameters on bearing capacity of shallow strip foundation are analyzed for 5 level of COV of soil parameters. Both isotropic and anisotropic SCL cases are investigated and the results are provided in Figure 5. 9 and Figure 5. 10. The results indicate that, up to a value of SCL, as SCL increases normalized mean bearing capacity decreases (Figure 5. 9). After a specific value of SCL, as SCL increases normalized mean bearing capacity increases. The initial decrease may be explained by the relation between the values of SCL and the dimensions of bearing capacity failure zone, which depends on the width of the foundation, B. The affected zone is approximately 1.5B deep and 5B wide underneath the foundation. The bearing failure initiates due to having weaker zones in the bearing capacity failure zones which is more likely when SCL is small (i.e. random field is more rough) as compared to 1.5B. However, further increasing the SCL (relative to 1.5B) causes more smooth changes of soil parameters within the bearing capacity failure zone, i.e. soil volume starts to behave like a homogeneous volume. Therefore, it is less likely to have connected weak zones and greater mean bearing capacities are obtained. Likewise, Jha (2016) reported that normalized mean bearing capacity first decreases and reaches a minimum value and then increases with the increasing scale of fluctuation. In addition, the range of the results increases with increasing SCL of soil parameters because larger zones may be completely weak, or strong, together underneath the foundation. Therefore, much larger and much smaller results can be obtained which means COV of the results increases. Likewise, with the increase of COV of soil parameters, the value of strength parameters can take much larger and lower values and therefore variability of the results increases. The results of this study show that the COV of bearing capacity increases with the increase of SCL values and COV of soil parameters for both isotropic and anisotropic cases (Figure 5. 10). When isotropic and anisotropic cases are compared, it is seen that the decrease of mean bearing capacity is a little more in anisotropic case. In addition, COV of bearing capacity reaches greater amounts in anisotropic case.

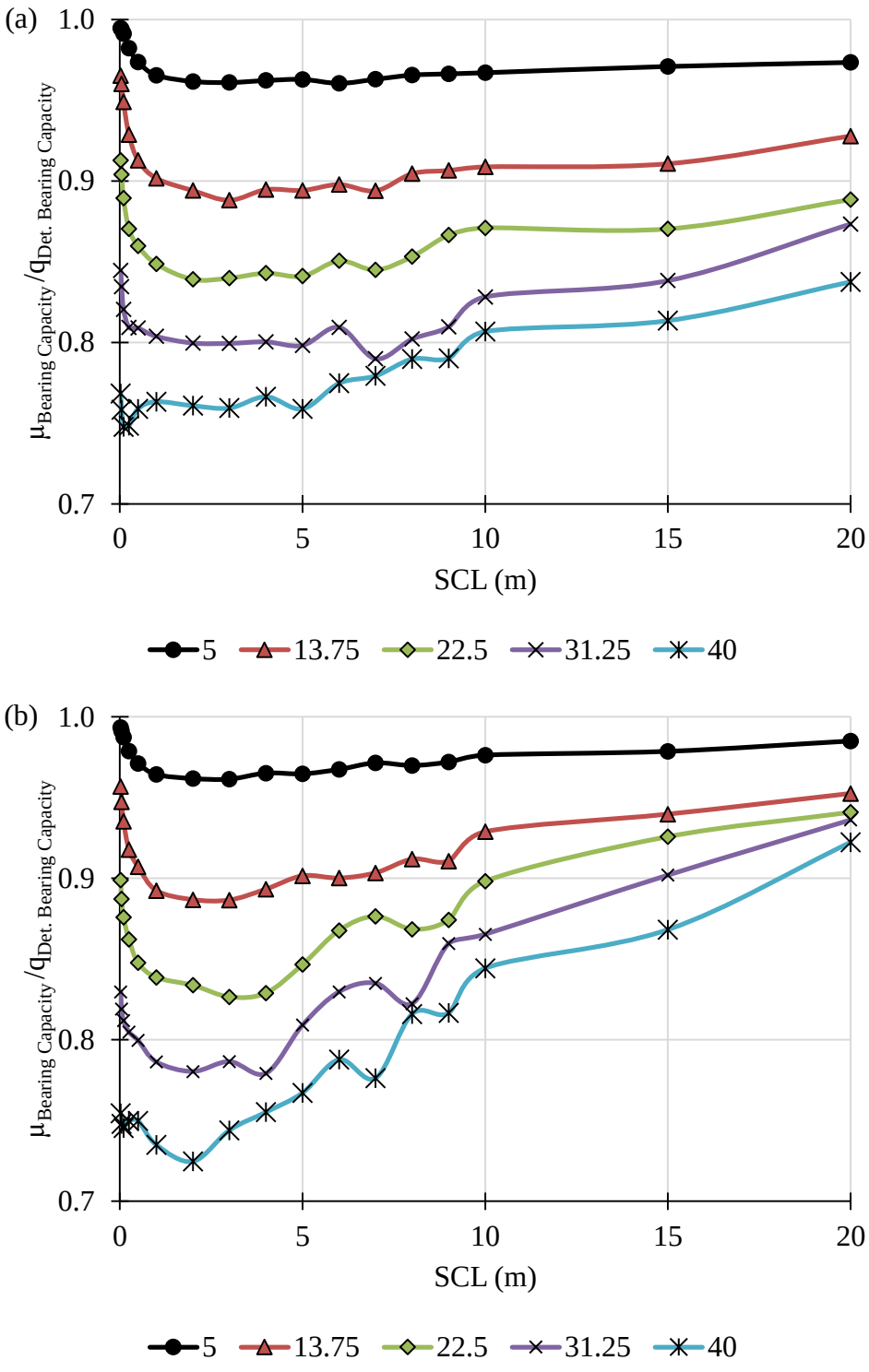

Figure 5. 9 Effect of SCL of soil parameters on mean bearing capacity for 5 levels of $COV_{soil\ parameters}$ for (a) isotropic case and (b) anisotropic case

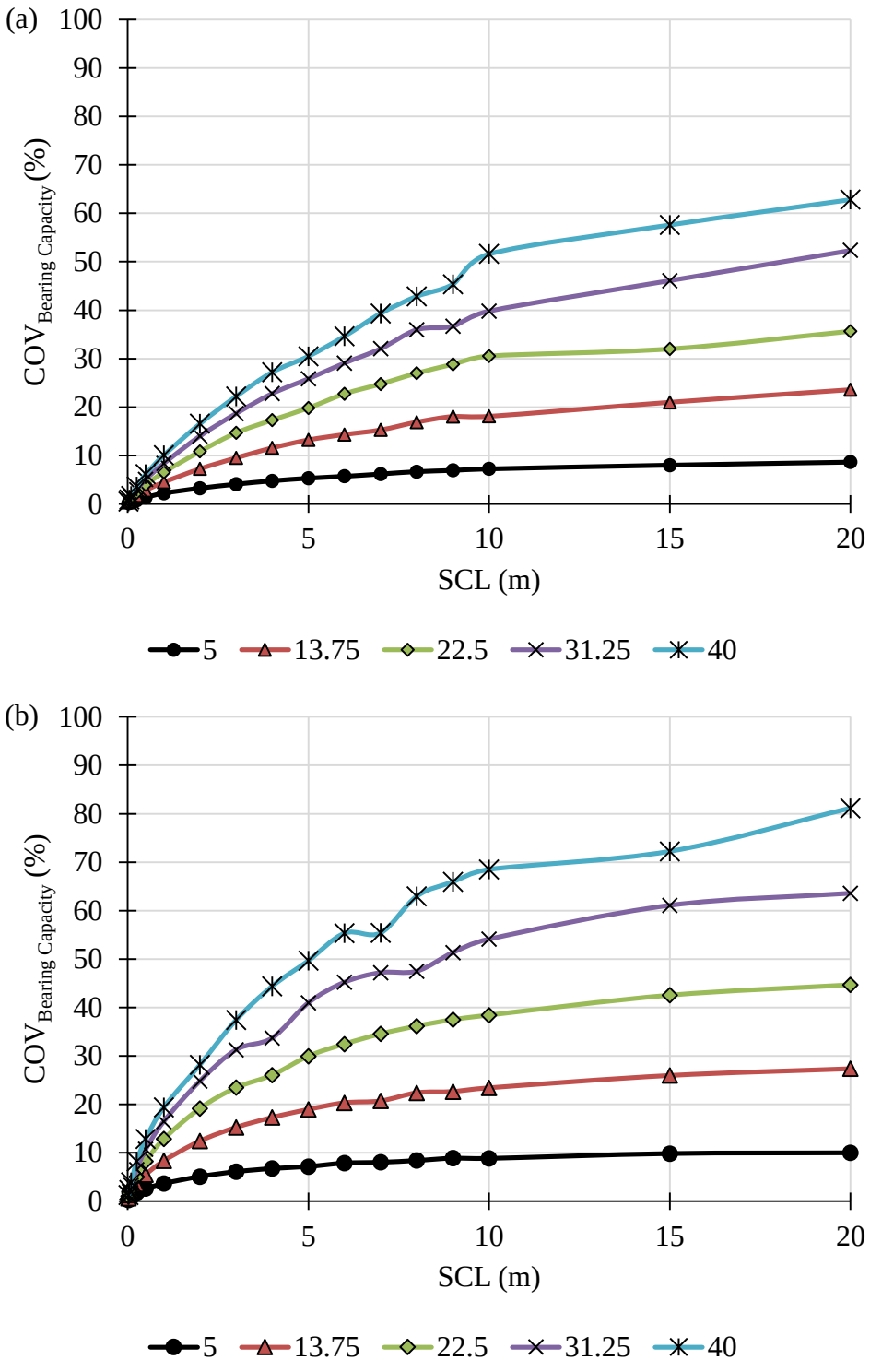

Figure 5. 10 Effect of SCL of soil parameters on $COV_{bearing\ capacity}$ for 5 levels of $COV_{soil\ parameters}$ for (a) isotropic case and (b) anisotropic case

The effect of SCL and COV of soil parameters on the probability of failure under a given loading is investigated and illustrated in Figure 5. 11. The foundation under a load that is greater and less than the deterministic bearing capacity of soil volume is called as “deterministically unsafe” and “deterministically safe” respectively. The effect of SCL on the probability of failure is found to be opposite for deterministically safe and unsafe cases. For deterministically safe case, increasing SCL increases the probability of failure because having larger weaker zones under the foundation becomes more possible with increasing SCL and larger weaker zones create more possibility to initiate the bearing failure. On the contrary, increasing SCL decreases the probability of failure for the deterministically unsafe case. The reason is that relatively stronger zones are formed by increasing SCL and larger loads can be carried by the foundation.

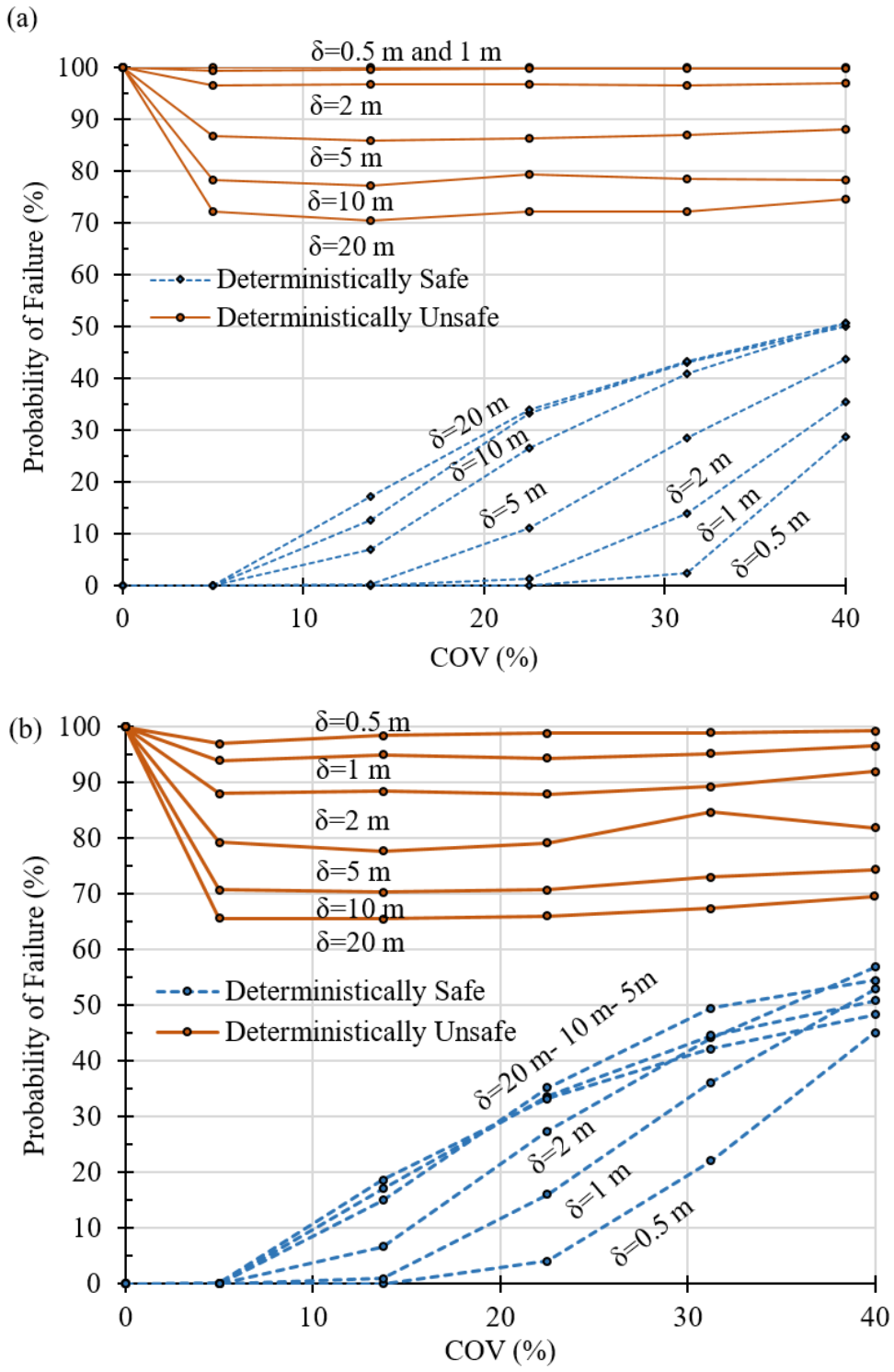

Figure 5. 11 Effect of SCL of soil parameters (δ) with different $COV_{\text{soil parameters}}$ levels on probability of failure at deterministically safe and unsafe conditions for (a) isotropic case and (b) anisotropic case

In addition, the mean bearing capacity of 2000 Monte Carlo simulations is found to be decreasing with increasing variability of soil parameters (Figure 5. 12). The average bearing capacity can decrease by about 25% of its deterministic value. The results show that for a given COV %, increasing SCL of soil parameters from 0.025 m to 3.0 m can decrease the mean bearing capacity as much as 11% of its deterministic bearing capacity.

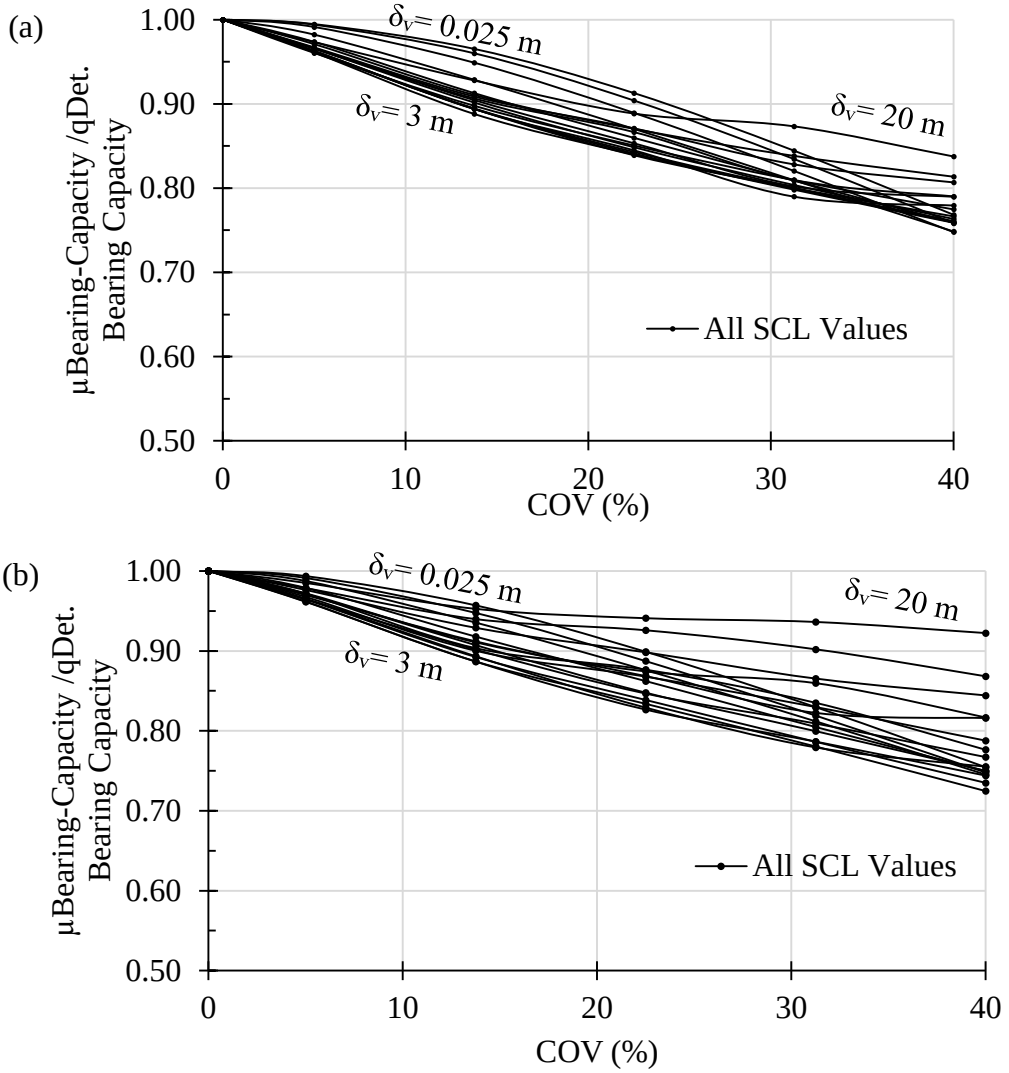

Figure 5. 12 Effect of SCL of soil parameters with different $COV_{soil\ parameters}$ levels on mean bearing capacity for (a) isotropic case and (b) anisotropic case

Increasing variability of obtained results given in Figure 5. 10 is also illustrated with the probability density functions of four cases. In Figure 5. 13, when SCL increases for the same $COV_{parameter}$, the standard deviation of evaluated bearing capacity

increases and wider range of results are obtained. That is, when SCL increases for the same $COV_{parameter}$, larger zones will be correlated to each other (i.e. will have similar values of soil parameters) underneath the foundation. If high strength values are assigned to much larger zones, much higher bearing capacity can be obtained. Similarly, much lower bearing capacity values can also be obtained if larger zones of low strength values exist. When SCL is kept constant and $COV_{parameter}$ increases from 5% to 40 %, the standard deviation increases. That is, either increasing SCL or $COV_{parameter}$ significantly increases the standard deviation of evaluated bearing capacity.

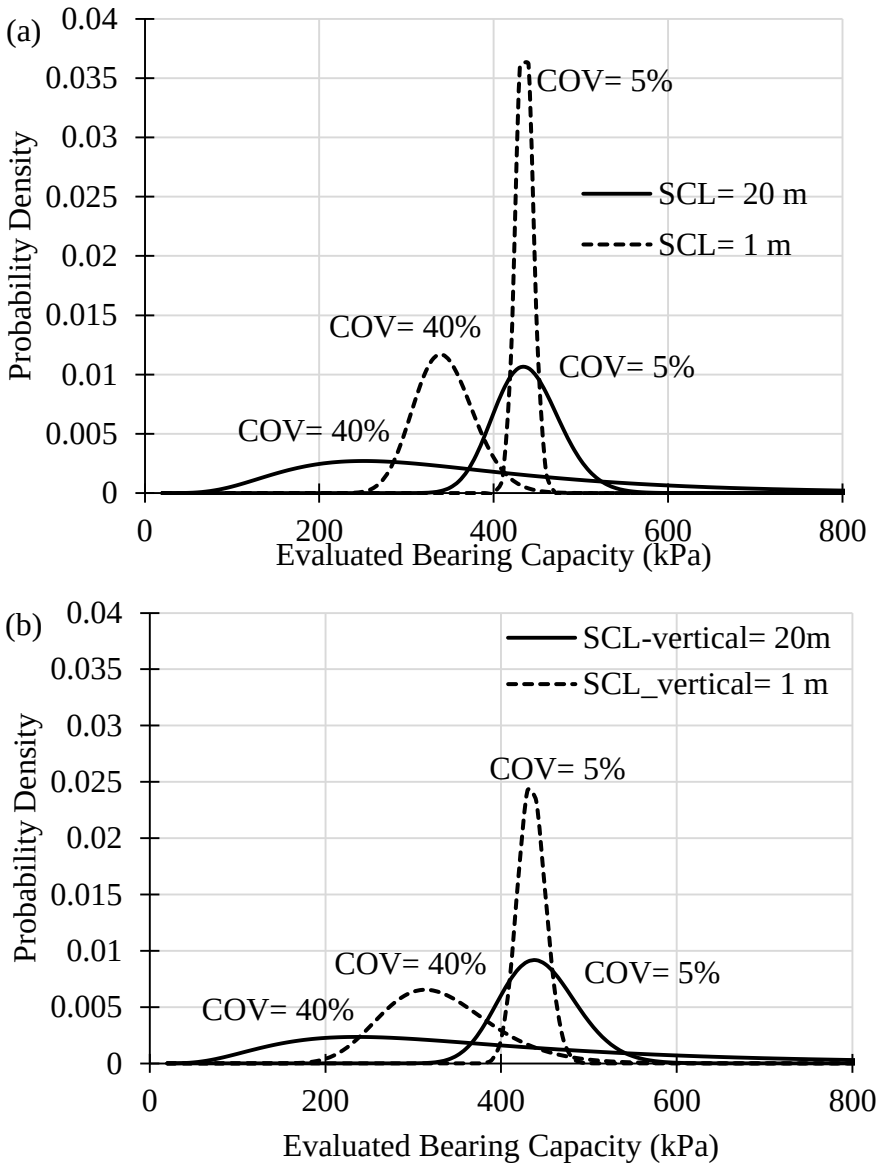

Figure 5. 13 Probability density function of δ=20 m & 1 m and $COV_{soil\ parameters}$ of 5% and 40% for (a) isotropic case and (b) anisotropic case

The effect of SCL and COV of soil parameters can be seen in Figure 5. 14. It is seen that for a given loading, the probability of failure increases as COV of soil parameters increases. For the same COV levels, increasing the SCL of soil parameters may increase or decrease the probability of failure according to the safety level which is also illustrated in Figure 5. 11.

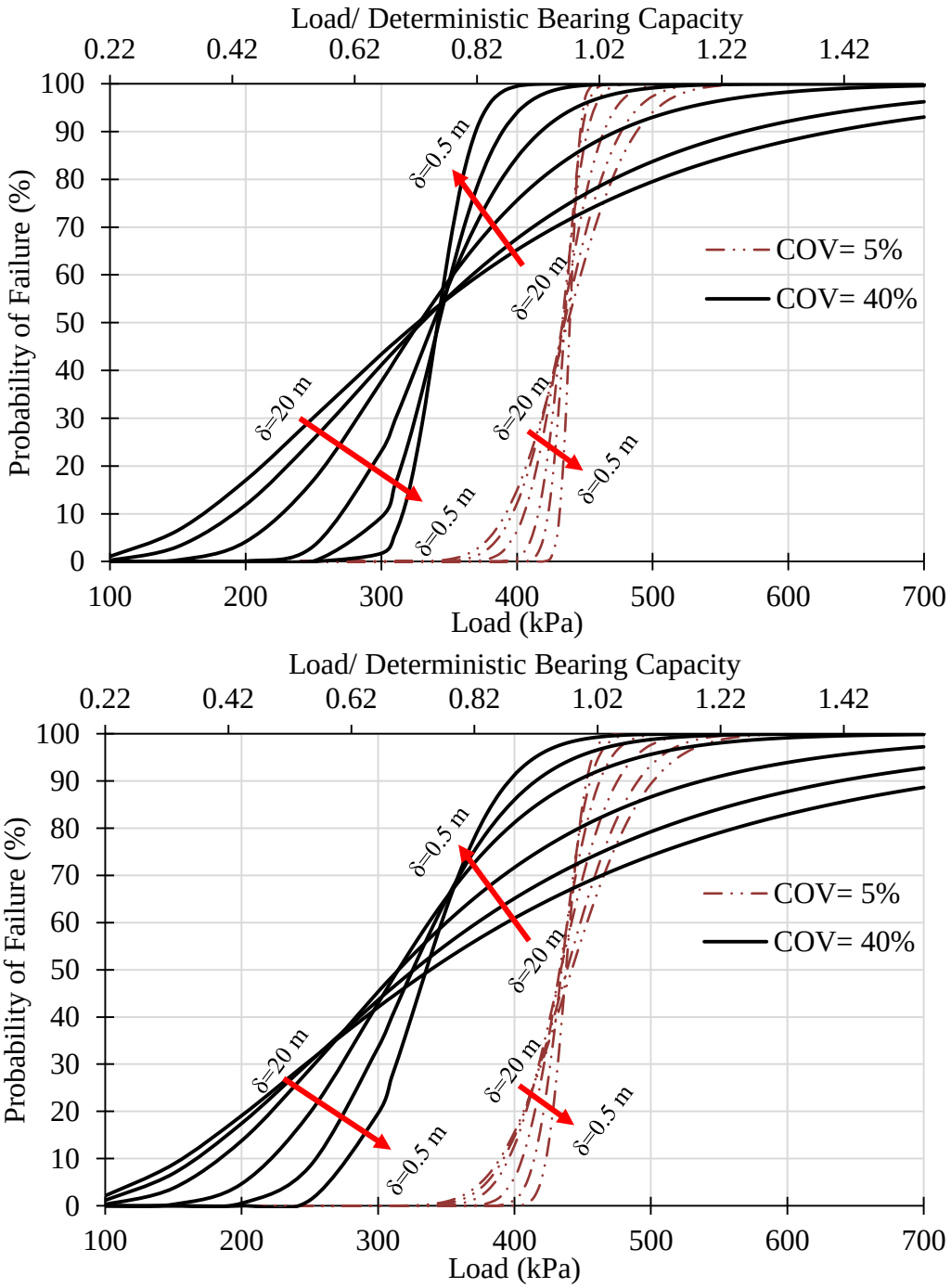

Figure 5. 14 Effect of spatial correlation length (δ) with different COV soil parameters levels on probability of failure under different load

The effect of SCL and coefficient of variation of soil parameters are investigated by using RBEAR2D, random finite element method. All analyses are conducted with 2000 Monte-Carlo simulations. The effect of SCL of soil parameters on the probability of failure, P_f, changes according to the safety level. Increasing SCL increases the P_f of deterministically safe cases, while it decreases the P_f of deterministically unsafe cases. Mean bearing capacity decreases with increasing COV of soil parameters. In addition, the mean bearing capacity may decrease by about 11% of its deterministic bearing capacity with the increase of SCL. Standard deviation of 2000 bearing capacity simulations increases by increasing SCL values and therefore probability of failure is effected significantly.

CHAPTER 6

CONCLUSIONS AND FUTURE STUDIES

6.1 Summary

Reliability-based design approach is a popular trend in geotechnical engineering field, especially in the recent decades. In this approach, the probability of failure, probability of exceeding any limit criteria, reliability index can be obtained as well as the results obtained in deterministic approaches such as deterministic factor of safety and bearing capacity etc. In the reliability-based design, variability of soil parameters is included in the analyses where the variability is represented by mean, standard deviation and spatial correlation length. In this study, the offshore and nearshore geotechnical site investigation data are used for 3 sites, and the following issues have been examined:

- The types and typical characteristics of sea bottom soils
- Ranges of values and statistical evaluation for engineering properties, such as effective friction angle, relative density, and undrained shear strength
- Spatial correlation length of soils in the vertical direction based on CPT and SPT data
- The effects of variability of both the coefficient of variability of soil parameters and SCL of soil parameters on settlement and bearing capacity of shallow strip foundations

One of the aims of this study is to emphasize the importance of variability of soil and to demonstrate the importance of probabilistic approach by providing the quantified

values of soil variability and specific values for settlement and/or bearing capacity influenced by this variability.

The variability of the soil is investigated by using SPT and CPT data from three different sites in Turkish waters. The soil profile at the SPT sites is obtained by evaluating laboratory test results, SPT-N data and field observations while Robertson (2010)'s soil behavior type chart is utilized for CPT sites. After digitizing the field data and identifying the soil layers, the statistical evaluation is carried out by a MATLAB code developed in this study, which finds engineering parameters of the soils at each data point and calculates SCL of field data in the vertical length by function fitting method. Four autocovariance functions; exponential, squared exponential, cosine exponential and second-order autoregressive, are utilized to calculate SCL for different soil groups.

The importance of variability of soil parameters is illustrated by extensive analysis where random finite element programs; RSETL2D and RBEAR2D are utilized. The programs are a combination of random field and finite element method which is developed by Fenton and Griffiths in 1992. In these programs, random fields of soil properties are generated by using statistical distribution parameters and the created random field is matched with finite element meshes. The settlement and bearing capacity results are obtained with a statistical distribution and related probabilistic studies are conducted for the probability of failure and exceeding any limit value. The results of the study emphasize the importance of the variability and probabilistic approach.

6.2 Conclusions

The results of this study can be summarized as follows:

i. Based on site investigation data for nearshore sea bottom soils at the Gulf of Hatay (SPT data): fines are mostly low plasticity clays (CL) and the coarse fraction is dominantly composed of sand-silt and sand-clay mixtures.

ii. Due to limited laboratory tests at SPT site, the engineering parameters are evaluated by using empirical equations. At site 1, soft to stiff clay layers exists having undrained shear strength (c_u) in the range of 5 to 100 kPa. At site 2, clays can be classified as soft to medium stiff clays with max c_u values of 50 kPa. The rate of increase of c_u with depth is found as 2.1-2.2 kPa/m which are in the range of reported values in the literature. The average relative density of the coarse fraction is found as 29-40 % and the coarse fraction is classified as loose to medium dense with an average effective friction angle of approximately 35°.

iii. The SCL in the vertical direction based on SPT data is evaluated for clays and mixture type of soils separately. When mean is assumed to be constant with depth, evaluated SCL_{SPT-N} for clays and mixtures are 3.85 m (±1.41 m standard deviation) and 4.20 m (±2.14 m standard deviation), respectively. In addition, if mean of the measurements is assumed to be linearly increasing with depth, the SCL_{SPT-N} values become 1.71 m (±0.86 m standard deviation) for clays and 2.02 (±1.26 m standard deviation) for mixtures, respectively. The second approach is recommended to represent true variability. It is known that SPT is prone to measurement errors (equipment-related and operator effects etc.), however this has not been considered in the current work. Therefore, evaluated vertical spatial correlation lengths represent not only the inherent variability of soils but also the effect of measurement errors.

iv. In the evaluation of SPT data with depth dependent (trend) approach, the squared exponential (Gaussian) autocorrelation function mostly gives the highest SCL_{SPT-N} results (in 72% of all evaluations) while exponential autocorrelation function (Markov) results in generally lowest values (in 78% of all evaluations).

v. The CPT soundings (both shallow and deep water soundings) mostly consist of clays and sands (Robertson (2010)'s soil behavior types 3-4 and 5-6-7, respectively). The average undrained shear strength of clays at shallow water soundings is found as 100 kPa (σ=35.6 kPa) and the average value of clays at deep water soundings is found as 54 kPa (σ=31.6 kPa). It can be concluded that clays at shallow water soundings are medium stiff to stiff and at deep

water soundings are soft to medium stiff. In addition, sands are mostly in the medium dense state in both shallow and deep waters.

vi. The vertical SCL based on CPT data is found to be between 0.210 m and 0.269 m for clays and between 0.167 m and 0.263 m for sands by constant approach, and between 0.116 m and 0.172 m for clays and between 0.112 m and 0.168 m for sands by trend approach for which group of soil.

vii. Sands and clays at deep water CPT soundings have slightly larger vertical SCL_{CPT} values than sands and clays at shallow water soundings, in both constant and trend approach. This can possibly be attributed to more uniform deposition and formation processes in geological history, in deep water seabeds as compared to shallow waters, for which deposition of more heterogeneous soils can be expected.

viii. The results indicate that assuming that there exists a trend with depth and detrending your data (in other words, evaluating the vertical SCL about the trend) results in smaller SCL values.

ix. When cosine exponential function is utilized to fit the autocorrelation coefficient data, it gives the highest goodness of fit value.

x. The importance of sampling interval on the vertical SCL is found to be crucial. The SCL values based on SPT is found to be always greater than the SCL of CPT data. Depending on the real correlation structure, the larger sampling intervals may overestimate the spatial correlation length. It is always better to have frequent observation points within the SCL.

xi. The effects of variability on settlement and bearing capacity of shallow strip foundation are investigated by using random finite element tools; RSETL2D and RBEAR2D. The Monte Carlo simulations are utilized in the analyses. The effect of simulation number has been investigated and after 2000 simulation numbers, results converge to a constant value, therefore 2000 simulations is found to be sufficient.

xii. The effect of COV and SCL of soil parameters has a significant influence in the settlement. The increase in COV of soil parameters significantly increases the mean and COV of the settlement results obtained from 2000 simulations. In addition, increasing SCL has significant effects on settlement results. The

effect of SCL increases with increasing COV value of soil parameters. For a given serviceability limit state (SLS), increasing SCL may increase the probability of exceeding SLS settlement as much as 50%.

xiii. Bearing capacity analyses show that COV and SCL of soil parameters have significant influence on the results. The variability has inverse effects on for deterministically safe and unsafe cases. Increasing COV and SCL increase the probability of failure for a given loading for deterministically safe cases and decrease for deterministically unsafe cases.

xiv. Mean bearing capacity decrease, $\mu_{\text{Bearing Capacity}}$ with increasing COV value and SCL value of soil parameters. The COV may decrease the $\mu_{\text{Bearing Capacity}}$ as much as 25% of deterministic bearing capacity. In addition, SCL may cause a decrease by 11% of deterministic bearing capacity.

6.3 Future Work and Recommendation

The following topics can be studied in future studies:

- Evaluation of spatial correlation length of soil parameters in the horizontal direction and its effects on geotechnical design
- Evaluation of spatial correlation length based on not only field data but also laboratory tests performed on soil samples obtained with a high resolution (lower separation distance), and comparison of results
- The methods and techniques to handle inclined soil layers for evaluation spatial correlation length in the horizontal direction
- Developing more advanced software where the random field is generated for all separate soil parameters with different statistical parameters and can analyze any/all geotechnical problems.

REFERENCES

Akbas, S. O., & Kulhawy, F. H. 2010. Characterization and estimation of geotechnical variability in Ankara clay: a case history. Geotechnical and Geological Engineering, 28(5), 619-631.

Akkaya, A., and E. H. Vanmarcke. 2003. Estimation of Spatial Correlation of Soil Parameters Based on Data from the Texas A&M University NGES. Probabilistic Site Characterization at the National Geotechnical Experimentation Sites, 29–40. doi:10.1061/9780784406694.ch03.

Alonso, E. E., and R. J. Krizek. 1975. Stochastic formulation of soil properties. In Proc. 2nd Int. Conf. on Applications of Statistics and Probability in Soil and Structural Engineering 2:9–32.

Andersen, L.V., M.J. Vahdatirad and J.D. Sørensen. 2011. Reliability-Based Assessment of the Natural Frequency of an Offshore Wind Turbine Founded on a Monopile. Proc. Thirteenth Intern. Conf. on Civil, Structrl. and Environl. Engrg Compig, B.H.V. Topping and Y. Tsompanakis, Civil- Comp press, Stirlingshire, Scotland, paper 83.

Andersen, L.V., M.J. Vahdatirad, M.T. Sichani and J.D. Sørensen. 2012. Natural Frequencies of Wind Turbines on Monopile Foundations in Clayey Soils: a Probabilistic Approach, Comput. Geotech., No. 43, pp. 1-11.

Baecher, G. B., and J. T. Christian. 2003. Reliability and Statistics in Geotechnical Engineering. Reliability and Statistics in Geotechnical Engineering. John Wiley & Sons: London and New York. doi:10.1198/tech.2005.s838.

Basack, S., and R. D. Purkayastha. 2009. Engineering Properties of Marine Clays from the Eastern Coast of India."Journal of Engineering and Technology Research 1 (6): 109–14.

Bouayad, D. 2017. "ssessment of Sandy Soil Variability Based on CPT Data. Procedia Engineering, Proc. of the 1st International Conference on the Material Point Method, 175: 310 – 315.doi:10.1016/j.proeng.2017.01.033.

Cafaro, F., and C. Cherubini. 2002. Large Sample Spacing in Evaluation of Vertical Strength Variability of Clayey Soil. Journal of Geotechnical and Geoenvironmental Engineering 128 (7): 558–68. doi:10.1061/(ASCE)1090-0241(2002)128:7(558).

Cao, Z., Y. Wang, and M. Asce. 2014. Bayesian Model Comparison and Characterization of Undrained Shear Strength. Journal of Geotechnical and Geoenvironmental Engineering 140 (6): 4014018-1–9. doi:10.1061/(ASCE)GT.1943-5606.0001108.

Carswell, W., S. R. Arwade, A. T. Myers, and J. F. Hajjar. 2013. Reliability Analysis of Monopile Offshore Wind Turbine Support Structures. Safety, Reliability, Risk and Life-Cycle Performance of Structures and Infrastructures, 223.

Cassidy, M. J., M. Uzielli, and Y. Tian. 2013. Probabilistic Combined Loading Failure Envelopes of a Strip Footing on Spatially Variable Soil. Computers and Geotechnics 49: 191–205. doi:10.1016/j.compgeo.2012.10.008.

Cheon, J. Y., and R. B. Gilbert. 2014. Modeling Spatial Variability in Offshore Geotechnical Properties for Reliability-Based Foundation Design. Structural Safety 49. Elsevier Ltd: 18–26. doi:10.1016/j.strusafe.2013.07.008.

Cherubini, C. 2000. Reliability Evaluation of Shallow Foundation Bearing Capacity on c', f' soils. Canadian Geotechnical Journal 37: 264–269.

Chiasson, P., J. Lafleur, M. Soulié, and K. T. Law. 1995. Characterizing Spatial Variability of a Clay by Geostatistics. Canadian Geotechnical Journal 32 (1): 1–10. doi:10.1139/t95-001.

Cho, S. E. 2010. Probabilistic Assessment of Slope Stability That Considers the Spatial Variability of Soil Properties. Journal of Geotechnical and Geoenvironmental Engineering 136 (7): 975–84. doi:10.1061/(ASCE)GT.1943-5606.0000309.

Cho, S. E., and H. C. Park. 2009. Effect of Spatial Variability of Cross-Correlated Soil Properties on Bearing Capacity of Strip Footing. International Journal for Numerical and Analytical Methods in Geomechanics 34: 1–26. doi:10.1002/nag.791.

DeGroot, D.J. 1996. Analyzing spatial variability of in-situ soil properties. In C.D. Shackleford, P.P. Nelson and M.J.S. Roth (eds.), Uncertainty in the Geologic Environment: From Theory to Practice, Geotechnical Special Publication No. 58: 210-238. New York: ASCE.

DeGroot, D. J., and G. B. Baecher. 1993. Estimating Autocovariance of In-Situ Soil Properties. Journal of Geotechnical Engineering 119 (1): 147–66. doi:10.1061/(ASCE)0733-9410(1993)119:1(147).

Derinsu Geological and Geotechnical Soil Investigation Report, Iskenderun Harbor, February 2011a.

Derinsu Geological and Geotechnical Soil Investigation Report, Iskenderun Harbor, October 2011b.

Derinsu Geological and Geotechnical Soil Investigation Report, Yumurtalık Adana, March 2014.

Derinsu Geological and Geotechnical Soil Investigation Report, Yumurtalık Adana, November 2015.

Elachachi, S. M., Breysse, D., & Denis, A. 2012. The effects of soil spatial variability on the reliability of rigid buried pipes. Computers and Geotechnics, 43, 61-71.

Fenton, G, and D V Griffiths. 2000. Bearing Capacity of Spatially Random c - φ Soils. Proc. 10th Int. Conf. on Computer Methods and Advances in Geomechanics (IACMAG 01), 1411–15.

Fenton, G. A., & Griffiths, D. V. 2008. Risk Assessment In Geotechnical Engineering, Hoboken, NJ: John Wiley & Sons.

Fenton G. A. and Vanmarcke E. H. 1990. Simulation of random fields via local average subdivision. Journal of Engineering Mechanics, Vol. 116, Issue 8, pp. 1733-1749.

Firouzianbandpey, S., D. V. Griffiths, L. B. Ibsen, and L. V. Andersen. 2014. Spatial Correlation Length of Normalized Cone Data in Sand : Case Study in the North of Denmark. Canadian Geotechnical Journal 857 (July 2013): 844–57. doi:10.1139/cgj-2013-0294.

Gibbs, H. J. & Holtz W. G.. 1957. Research on Determining the Density of Sands by Spoon Penetration Testing, Proc. 4th.ICSMFE, London, 1: 35-39.

Griffiths, D V, and Gordon a Fenton. 1993. Seepage beneath Water Retaining Structures Founded on Spatially Random Soil. Géotechnique. doi:10.1680/geot.1993.43.4.577.

Griffiths, D. V., and G. A. Fenton. 2000. Bearing Capacity of Heterogeneous Soils by Finite Elements. Proc. of the 5th International Congress on Numerical Methods in Engineering and Scientific Applications, 27–37.

Griffiths D. V., and G. A. Fenton. 2001. Bearing Capacity of Spatially Random Soil: The Undrained Clay Prandtl Problem Revisited. Géotechnique 51 (4): 351–59. doi:10.1680/geot.2001.51.4.351.

Griffiths, D.V. and G.A. Fenton. 2007. Probabilistic methods in geotechnical engineering, CISM Courses and Lectures No. 491, Pub. Springer, Wien, New York.

Griffiths, D. V., and Gordon A. Fenton. 2009. Probabilistic Settlement Analysis by Stochastic and Random Finite-Element Methods. Journal of Geotechnical and Geoenvironmental Engineering 135 (11): 1629–37. doi:10.1061/(ASCE)GT.1943-5606.0000126.

Griffiths, D.V., G. A. Fenton and D. E. Tveten. 2002. Probabilistic geotechnical analysis: How difficult does it need to be? Proc. of an International Conference on, "Probabilistics in Geotechnics: Technical and Economic Risk Estimation", (eds. R. Poettler et al.), Pub. VGE, Essen, Germany, pp.3-20.

Griffiths, D. V., G. A. Fenton, and H.R. Ziemann. 2006. The Influence of Strength Variability in the Analysis of Slope Failure Risk. Geomechanics II Proceeding of the Second Japan-U.S. Workshop on Testing, Modeling and Simulation, P.V. Lade and T. Nakai, Eds., Kyoto, Japan, September, 2005. Also in Geotechnical Special Publication No. 156, ASCE, 113–23. doi:10.1061/40870(216)9.

Griffiths, D. V., J. Huang, and G. A. Fenton. 2009. Influence of Spatial Variability on Slope Reliability Using 2-D Random Fields. J Geotech Geoenviron, 135 (10): 1367–78.

Hommels A., Huber M., Molenkamp F., and Vermeer P.A. 2010. Inverse modelling including spatial variability applied to the construction of a road embankment. In T. Benz, editor, Proceedings of the 7th European Conference on Numerical Methods in Geotechnical Engineering, Trondheim, NUMGE, pages 369–374, 2010.

Hossain, M. S., J. Zheng, D. Menzies, L. Meyer, and M. F. Randolph. 2014. Spudcan Penetration Analysis for Case Histories in Clay. Journal of Geotechnical and Geoenvironmental Engineering 140 (1): 4014034. doi:10.1061/(ASCE)GT.1943-5606.0001133.

Huber, M. 2013. Soil variability and its consequences in geotechnical engineering. PhD. Thesis in Institute of Geotechnical Engineering of Stuttgart University, Stuttgart, Germany.

Jaksa, M. B., W. S. Kaggwa, and P. I. Brooker. 1999. Experimental evaluation of the scale of fluctuation of a stiff clay, In Proc. 8th Int. Conf. on the Application of Statistics and Probability, 1:415-422, December 1999, Sydney, AA Balkema, Rotterdam.

Jamiolkowski, M., Lo Presti, D. C. F., & Manassero, M. 2003. Evaluation of relative density and shear strength of sands from CPT and DMT. In Soil behavior and soft ground construction (pp. 201-238).

JCSS Probabilistic Model Code (2001).

Jha, S. K. 2016. Reliability-Based Analysis of Bearing Capacity of Strip Footings Considering Anisotropic Correlation of Spatially Varying Undrained Shear Strength. International Journal of Geomechanics, 6016003. doi:10.1061/(ASCE)GM.1943-5622.0000638.

Jiang S. H., Li D. Q., Cao Z. J., Zhou C. B. and Phoon K. K. 2014. Efficient System Reliability Analysis of Slope Stability in Spatially Variable Soils Using Monte Carlo Simulation. Journal of Geotechnical and Geoenvironmental Engineering, Vol. 141, Issue 2, 04014096.

Kamei, T., and K. Iwasaki. 1995. Evaluation of Undrained Shar Strength of Cohesive Soils Uing a Flat Dilatometer. Soils and Doundations 35 (2): 111–16.

Keaveny, J. M., F. Nadim, and S. Lacasse. 1990. Autocorrelation functions for offshore geotechnical data. Proc. ICOSSAR 1990. International Conference on Structural Safety and Reliability. Perth, Australia, 263–270

Kottegoda, N. T., and R. Rosso. 2008. Applied Statistics for Civil and Environmental Engineers. Blackwell.

Kulhawy, F. H., B. Birgisson, and M. D. Grigoriu. 1992. Reliability based foundation design for transmission line structures: Transformation models for in-situ tests. Report EL-5507(4). Palo Alto, CA: Electric Power Research Institute.

Kulhawy, F. H., & Mayne, P. W. 1990. Manual on estimating soil properties for foundation design (No. EPRI-EL-6800). Electric Power Research Inst., Palo Alto, CA (USA); Cornell Univ., Ithaca, NY (USA). Geotechnical Engineering Group.

Lacasse, S. and F. Nadim. 1996. Uncertainties in characterizing soil properties. In Uncertainty in the Geologic Environment: From Theory to Practice. Geotechnical Special Publication No. 58, ASCE: Madison, WI, 49–75.

Lacasse, S. 2013. 8th Terzaghi Oration. Protecting Society from Landslides – the Role of the Geotechnical Engineer. 18th International Conference on Soil Mechanics and Geotechnical Engineering - Challenges and Innovations in Geotechnics, 15–34.

Li, K. S., and P. Lumb. 1987. Probabilistic design of slopes. Can. Geotech. J., 24, 520–531.

Liu, C.-N., and C.-H. Chen. 2010. Estimating Spatial Correlation Structures Based on CPT Data. Georisk: Assessment and Management of Risk for Engineered Systems and Geohazards 4 (2): 99–108. doi:10.1080/17499511003630504.

Liu, Z., S. Lacasse, F. Nadim, M. Vanneste, and G. Yetginer. 2015. Accounting for the Spatial Variability of Soil Properties in the Reliability-Based Design of Offshore Piles. In Frontiers in Offshore Geotechnics III, 978–1.

Lloret-Cabot, M., G. A. Fenton, and M. A. Hicks. 2014. On the Estimation of Scale of Fluctuation in Geostatistics. Georisk: Assessment and Management of Risk for Engineered Systems and Geohazards 8 (2): 129–40. doi:10.1080/17499518.2013.871189.

Luo, Z., Wang, L., Khoshnevisan S., Juang C. H. Effect of spatial variability on the reliability-based design of drilled shafts. Proceedings of the Geo-Congress 2014,GSP (Geotechnical Special Publication);234, 23-26 Feb 2014, Atlanta, Georgia, 3274-3282.

Lumb P. 1966. The variability of natural soils. Canadian Geotechnical Journal, Vol. 3, Issue 2, pp. 74-97.

Lumb, P.. 1975. Spatial variability of soil properties. In Proceedings of the 2nd International Conference on Application of Statistics and Probability to Soil and Structural Engineering, Aachen, 2:397–421.

Nadim, F.. 2015. Accounting for Uncertainty and Variability in Geotechnical Characterization of Offshore Sites. doi:10.3233/978-1-61499-580-7-23.

Oguz, E. A., Yagizer, Y., and Huvaj, N. 2017. Probabilistic Slope Stability Analyses : Effects of the Coefficient of Variation and the Cross-Correlation of Shear Strength Parameters. Geotechnical Frontiers 2017, 363–71. doi:10.1061/9780784480458.036.

Overgård, Ida Elise. Reliability-based Design of a Monopile Foundation for Offshore Wind Turbines based on CPT Data. Master's thesis, Norwegian University of Science and Technology, June 2015.

Paice, G. M., D. V. Griffiths, and G. A. Fenton. 1996. Finite Element Modeling of Settlements on Spatially Random Soil. Journal of Geotechnical Engineering 122 (9). doi:10.1061/(ASCE)0733-9410(1996)122.

Pantelidis, L., and P. Christodoulou. 2017. Spatial Correlation Length of Clay Soils in Practice and Its Influence in Probabilistic Bearing Capacity Analysis. Proc. Geo-Risk 2017, 487–96.

Peng, X. Y., L. L. Zhang, D. S. Jeng, L. H. Chen, C. C. Liao, and H. Q. Yang. 2017. Effects of Cross-Correlated Multiple Spatially Random Soil Properties on Wave-Induced Oscillatory Seabed Response. Applied Ocean Research 62. Elsevier B.V.: 57–69.

Phoon K-K. 2008. Reliability-based Design in Geotechnical Engineering: Computations and Applications. Taylor and Francis: New York, NY.

Phoon, K.-K., and F. H. Kulhawy. 1999a. Characterization of Geotechnical Variability. Canadian Geotechnical Journal 36 (4): 612–24. doi:10.1139/t99-038.

Phoon, K.-K., and F. H. Kulhawy. 1999b. Evaluation of Geotechnical Property Variability. Canadian Geotechnical Journal 36 (4): 625–39. doi:10.1139/t99-039.

Phoon, K.-K., F. H. Kulhawy, andM.D. Grigoriu.1995. Reliability-based design of foundations for transmission line structures. Electric Power Research Institute, Palo Alto, Calif., Report TR-105000.

Phoon, K.-K., S.-T. Quek, and P. An. 2003. Identification of Statistically Homogeneous Soil Layers Using Modified Bartlett Statistics. Journal of Geotechnical and Geoenvironmental Engineering 129 (7): 649–59. doi:10.1061/(ASCE)1090-0241(2003)129:7(649).

Pieczyńska, J, W Puła, D V Griffiths, and G a Fenton. 2011. Probabilistic Characteristics of Strip Footing Bearing Capacity Evaluated by Random Finite Element Method. Civil Engineering, 1673–82.

Popescu, R., G. Deodatis, and A. Nobahar. 2005. Effects of Random Heterogeneity of Soil Properties on Bearing Capacity. Probabilistic Engineering Mechanics 20 (4): 324–41. doi:10.1016/j.probengmech.2005.06.003.

Robertson, P.K., Campanella, R.G., Gillespie, D. and Greig, J. 1986. Use of piezometer cone data. Use of In-Situ Tests in Geotechnical Engineering (GSP 6), ASCE, Reston, VA: 1263-1280.

Sarma, C. P., A. M. Krishna, and A. Dey. 2014. Probabilistic Slope Stability Analysis Considering Spatial Variability of Soil Properties : Influence of Correlation Length. In Computer Methods and Recent Advances in Geomechanics, 1125–30.

Schmertmann, J. H.. 1975. Measurement of in situ shear strength. SOA Report, In Proc., ASCE Spec. Conf. on In Situ Measurement of Soil Properties, Raleigh, NC, 2: 57-138.

Schultze E. 1971. Frequency distributions and correlations of soil properties. First International Conference on Applications of Statistics and Probability to Soil and Structural Engineering Proceedings. Hong Kong University Press, pp. 372-387.

Schweiger, H. F., G. M. Peschl, and R. Pöttler. 2007. Application of the Random Set Finite Element Method for Analysing Tunnel Excavation. Georisk: Assessment and Management of Risk for Engineered Systems and Geohazards 1 (1): 43–56. doi:10.1080/17499510701204141.

Shuwang, Y., and G. Linping. 2015. Calculation of Scale of Fluctuation and Variance Reduction Function. Transactions of Tianjin University 21 (1): 41–49.

Shuwang, Y., and G. Linping. 2015. “Calculation of Scale of Fluctuation and Variance Reduction Function.” Transactions of Tianjin University 21 (1): 41–49.

Stroud M. A.. 1988. The standard penetration test – its implication and interpretation. Penetration Testing in the UK, Thomas Telford, London.

Stroud, M. A.. 1974. The standard penetration test in insensitive clays and soft rocks. In Proc. of the European Symposium on Pentration Testing ESOPT, Stockholm 1974. Stockholm, National Swedish Building Research, 367-375.

Tabarroki M., Ahmad F., Banaki R., Jha S. and Ching J. 2013. Determining the factors of safety of spatially variable slopes modeled by random fields. Journal of Geotechnical and Geoenvironmental Engineering. Vol. 139, Issue 12, pp. 2082-2095.

Terzaghi, K., R. B. Peck, and G. Mesri. 1996. Soil Mechanics in Engineering Practice, John Wiley & Sons.

Uzielli, M., G. Vannucchi, and K.-K. Phoon. 2005. Random Field Characterisation of Stress-Normalised Cone Penetration Testing Parameters. Géotechnique 55 (1): 3–20. doi:10.1680/geot.55.1.3.58591.

Uzielli, M., S. Lacasse, F. Nadim, and K.-K. Phoon. 2007. Soil Variability Analysis for Geotechnical Practice. Characterization and Engineering Properties of Natural Soils, no. December: 1653–1752. doi:10.1201/NOE0415426916.ch3.

Vahdatirad, M. J., L. V. Andersen, J. Clausen, and J. D. Sørensen. 2011. The dynamic stiffness of surface footings for offshore wind turbines: reliability based assessment. In Proceedings of 13th international conference on civil, structural and environmental engineering computing (eds B. H. V. Topping and Y. Tsompanakis), paper 82. Stirlingshire, Scotland, UK: Civil-Comp Press.

Vahdatirad, M. J., L. V. Andersen, L. B. Ibsen, J. Clausen, and J. D. Sørensen. 2013. Probabilistic Three-Dimensional Model of an Offshore Monopile Foundation: Reliability Based Approach. In International Conference on Case Histories in Geotechnical Engineering. 7.

Valdez-Llamas, Y. P., G. Auvinet, and J. Núñez. 2003. Spatial variability of the marine soil in the Gulf of Mexico. In: Proceedings of the Offshore Technology Conference, Houston, Texas, OTC 15266.

Vanmarcke, E. H. 1977. Probabilistic Modelling of Soil Profiles. Journal Of The Geotechnical Engineering Division, ASCE, 1227–46.

Wei, L., R.. Pant, and M. Tumay. 2010. A Case Study of Undrained Shear Strength Evaluation from In Situ Tests in Soft Louisiana Soils. Soil Behavior and Geo-Micromechanics, 35–42. doi:10.1061/41101(374)6.

Zhang, L., and J.-J. Chen. 2012. Effect of Spatial Correlation of Standard Penetration Test (SPT) Data on Bearing Capacity of Driven Piles in Sand. Canadian Geotechnical Journal 49 (4): 394–402. doi:10.1139/t2012-005.

Zhang, L. L., Y. Cheng, J. H. Li, X. L. Zhou, D. S. Jeng, and X. Y. Peng. 2016. Wave-Induced Oscillatory Response in a Randomly Heterogeneous Porous Seabed. Ocean Engineering 111: 116–27. doi:10.1016/j.oceaneng.2015.10.016.

APPENDICES

APPENDIX A

MATLAB CODE

A.1. Main Body of the Script

```
%The code analyses the data and evaluate spatial correlation length.
clear
clc
%The excel files in the current folder is found.
folder= pwd;
filetype='*.xlsx';  % or xls
f=fullfile(folder,filetype);
d=dir(f);
d=struct2cell(d);
names=d(1,:);
%Spacing of the CPT data should be defined.
Spacing=0.02;
%Defining the limit data number and tolerance for division of data.
DataLimit=24;
MeanTol=0.2;
%Read Water Depths from the same folder.
WaterDepthFileName = 'WaterDepth.txt';
A= importdata(WaterDepthFileName);
for NumFile=1:size(names,2)

    %The workspace is cleaned except some variables
    clearvars -except  names NumFile filetype Spacing DataLimit MeanTol A
    %The excel file is defined.
    fileName=char(names(NumFile));
    fileName=fileName(1:end-size(filetype,2)+1);
    [status,sheets] = xlsfinfo(fileName);

    for s = 1:numel(sheets)

        %Reading of excel sheet.
        ExcelData=xlsread(num2str(fileName),s);
        %Sleeve Friction is added.
        ExcelData(:,4)=[ExcelData(:,2).*ExcelData(:,3)./100];
        %Classification is made..
```

```
        [ExcelData]=Classification(ExcelData);

        %Dividing the Excel Data (both the whole into segments and segments
        %into different soil layers).
        [PiecewiseExcelData]=division_v3(ExcelData, Spacing, DataLimit, MeanTol);


        %Storing water depth of current sounding.
        for i=1:size(A.data,1)
        if size(fileName,2)==size(cell2mat(A.textdata(i)),2)
        if cell2mat(A.textdata(i))==fileName
        WaterDepth=A.data(i);
        end
        end
        end

        %Evaluation of Dr for sands and Cu for clays.
        [PiecewiseExcelDataDrCu]=DrCu(PiecewiseExcelData,WaterDepth,NumFile,fileName);

        %Calculating spatial correlation length.
        [SCL]=SCL_CPT_V2(PiecewiseExcelData, Spacing,DataLimit);

        %empty cells are deleted.
              Delete=[];
            for d=1:size(SCL,1)
               if size(SCL{d},1)==0
                   Delete(end+1)=d;
               end
            end
              SCL(Delete,:)=[];

        %Writing Excel File
        WriteExcel(SCL,NumFile,fileName);

    end
end
```

A.2. Functions of Main Script

```
function[AllData]=Classification(Data)

%cone resistance and friction ratio is defined.
c_res=Data(:,2)*10;
f_rat=Data(:,3);

%Borders of Robertson's soil behavior type chart is defined.
f1=-1.9602.*f_rat.^4+6.2054.*f_rat.^3 -2.9064.*f_rat.^2 -9.4567.*f_rat+11.229;
f2=0.0056.*f_rat.^3 - 0.0254.*f_rat.^2 + 0.3901.*f_rat + 0.5072;
f3=0.0855.*f_rat.^4 - 0.705.*f_rat.^3 + 2.9103.*f_rat.^2 - 0.6976.*f_rat + 3.9826;
f4=0.76514.*f_rat.^4-4.0449.*f_rat.^3+9.6011.*f_rat.^2+2.9771.*f_rat+6.7018;
f5=37689.*f_rat.^6 - 967763.*f_rat.^5 + 1E+07.*f_rat.^4 - 6E+07.*f_rat.^3 + 2E+08*f_rat.^2 -
3E+08.*f_rat + 2E+08;
f6=9.8386.*f_rat.^3 - 7.2942.*f_rat.^2 + 40.17.*f_rat+ 21.077;
f7=1071.9.*f_rat.^3 - 895.91.*f_rat.^2 + 610.49.*f_rat+ 87.311;
f8=91.297.*f_rat.^4 - 1091.3.*f_rat.^3 + 4902.5.*f_rat.^2 - 9934.1*f_rat + 7911.4;
f9=0.1325.*f_rat.^4 - 4.0772.*f_rat.^3 + 47.081.*f_rat.^2 - 243.98*f_rat + 541.81;
```

```
%The value of cone resistance is compared with the border values.
   for i = 1:size(f_rat)

if f_rat(i) < 0.323564
   if c_res(i) < f1(i)
      result(i,1) = 1;
   elseif (f1(i) < c_res(i)) && (c_res(i) < f6(i))
      result(i,1) = 5;
   elseif (f6(i) < c_res(i)) && (c_res(i) < f7(i))
      result(i,1) = 6;
   else result(i,1) = 7;
   end
end

if (0.323564 < f_rat(i)) && (f_rat(i) < 0.738356)
   if c_res(i) < f1(i)
      result(i,1) = 1;
   elseif (f1(i) < c_res(i)) && (c_res(i) < f4(i))
      result(i,1) = 4;
   elseif (f4(i) < c_res(i)) && (c_res(i) < f6(i))
      result(i,1) = 5;
   elseif (f6(i) < c_res(i)) && (c_res(i) < f7(i))
      result(i,1) = 6;
   else result(i,1) = 7;
   end
end

if (0.738356 < f_rat(i))&& (f_rat(i) < 1.03349)
   if c_res(i) < f1(i)
      result(i,1) = 1;
   elseif (f1(i) < c_res(i)) && (c_res(i) < f3(i))
      result(i,1) = 3;
   elseif (f3(i) < c_res(i)) && (c_res(i) < f4(i))
      result(i,1) = 4;
   elseif (f4(i) < c_res(i)) && (c_res(i) < f6(i))
      result(i,1) = 5;
   elseif (f6(i) < c_res(i)) && (c_res(i) < f7(i))
      result(i,1) = 6;
   else result(i,1) = 7;
   end
end

if (1.03349 < f_rat(i))&& (f_rat(i) < 1.41258)
   if c_res(i) < f1(i)
      result(i,1) = 1;
   elseif (f1(i) < c_res(i)) && (c_res(i) < f3(i))
      result(i,1) = 3;
   elseif (f3(i) < c_res(i)) && (c_res(i) < f4(i))
      result(i,1) = 4;
   elseif (f4(i) < c_res(i)) && (c_res(i) < f6(i))
      result(i,1) = 5;
   else result(i,1) = 6;
   end
end

if (1.41258 < f_rat(i)) && (f_rat(i) < 1.66491)
   if c_res(i) < f1(i)
```

```
        result(i,1) = 1;
    elseif (f1(i) < c_res(i)) && (c_res(i) < f3(i))
        result(i,1) = 3;
    elseif (f3(i) < c_res(i)) && (c_res(i) < f4(i))
        result(i,1) = 4;
    elseif (f4(i) < c_res(i)) && (c_res(i) < f6(i))
        result(i,1) = 5;
    elseif (f6(i) < c_res(i)) && (c_res(i) < f8(i))
        result(i,1) = 6;
    else result(i,1) = 8;
    end
end

if (1.66491 < f_rat(i)) && (f_rat(i) < 1.69284)
    if c_res(i) < f1(i)
        result(i,1) = 1;
    elseif (f1(i) < c_res(i)) && (c_res(i) < f2(i))
        result(i,1) = 2;
    elseif (f2(i) < c_res(i)) && (c_res(i) < f3(i))
        result(i,1) = 3;
    elseif (f3(i) < c_res(i)) && (c_res(i) < f4(i))
        result(i,1) = 4;
    elseif (f4(i) < c_res(i)) && (c_res(i) < f6(i))
        result(i,1) = 5;
    elseif (f6(i) < c_res(i)) && (c_res(i) < f8(i))
        result(i,1) = 6;
    else result(i,1) = 8;
    end
end

if (1.69284 < f_rat(i)) && (f_rat(i) < 2.48835)
    if c_res(i) < f2(i)
        result(i,1) = 2;
    elseif (f2(i) < c_res(i)) && (c_res(i) < f3(i))
        result(i,1) = 3;
    elseif (f3(i) < c_res(i)) && (c_res(i) < f4(i))
        result(i,1) = 4;
    elseif (f4(i) < c_res(i)) && (c_res(i) < f6(i))
        result(i,1) = 5;
    elseif (f6(i) < c_res(i)) && (c_res(i) < f8(i))
        result(i,1) = 6;
    else result(i,1) = 8;
    end
end

if (2.48835 < f_rat(i)) && (f_rat(i) < 3.8313)
    if c_res(i) < f2(i)
        result(i,1) = 2;
    elseif (f2(i) < c_res(i)) && (c_res(i) < f3(i))
        result(i,1) = 3;
    elseif (f3(i) < c_res(i)) && (c_res(i) < f4(i))
        result(i,1) = 4;
    elseif (f4(i) < c_res(i)) && (c_res(i) < f8(i))
        result(i,1) = 5;
    else result(i,1) = 8;
    end
end
```

```
if (3.8313 < f_rat(i)) && (f_rat(i) < 4.84993)
   if c_res(i) < f2(i)
      result(i,1) = 2;
   elseif (f2(i) < c_res(i)) && (c_res(i) < f3(i))
      result(i,1) = 3;
   elseif (f3(i) < c_res(i)) && (c_res(i) < f9(i))
      result(i,1) = 4;
   elseif (f9(i) < c_res(i)) && (c_res(i) < f5(i))
      result(i,1) = 9;
   else result(i,1) = 8;
   end
end

if (4.84993 < f_rat(i)) && (f_rat(i) < 5.98554)
   if c_res(i) < f2(i)
      result(i,1) = 2;
   elseif (f2(i) < c_res(i)) && (c_res(i) < f3(i))
      result(i,1) = 3;
   elseif (f3(i) < c_res(i)) && (c_res(i) < f9(i))
      result(i,1) = 4;
   else result(i,1) = 9;
   end
end

if (5.98554 < f_rat(i))&& ( f_rat(i) < 10)
   if c_res(i) < f2(i)
      result(i,1) = 2;
   elseif (f2(i) < c_res(i)) && (c_res(i) < f9(i))
      result(i,1) = 3;
   else result(i,1) = 9;
   end
end

% %This part is only for warning purpose (optional)
% if ( f_rat(i) > 10)
%     result(i,1) = 999999;
% end

i = i+1;
   end

AllData=[Data result];

end
```

```
function [PiecewiseExcelDataNew]=division_v3(ExcelData, Spacing, DataLimit, MeanTol)


      %Modified classification data is added.
      Classification=ExcelData(:,end);
      Classification(Classification==3)=4;
      Classification(Classification==5 | Classification==7)=6;
      Classification(Classification==1)=2;
      Classification(Classification==8)=9;
      ExcelData(:,end+1)=Classification;
```

```
%Definition of some parameters.
PiecewiseExcelData={};
PiecewiseExcelDataNew={};
NumOfMatrix=[];
LB=0;
LowerBound=0;
UpperBound=0;

%Dividing the data.
for i=1:size(ExcelData,1)-1
   if (ExcelData(i+1,1)- ExcelData(i,1))> Spacing+0.000000001

      %Boundaries of matrix is found.
      LB=i-UpperBound;
      UpperBound=Upper;
      LowerBound=Upper-LB+1;

      %The matrix is ddivided into pieces.
      %Overcoming the 1 row data problem.
      if size(PiecewiseExcelData,1)>0 && size(cell2mat(PiecewiseExcelData(end)),1)==1
         LowerBound=LowerBound+1;
      end

      if LowerBound==UpperBound
      PiecewiseExcelData(size(PiecewiseExcelData,1)+1,:)={ExcelData(LowerBound+1,:)};
      else

PiecewiseExcelData(size(PiecewiseExcelData,1)+1,:)={ExcelData(LowerBound:UpperBound,:)};
      end
   else
      Upper=i+1;
   end
end
     %The last piece is added.
      PiecewiseExcelData(end+1,:)={ExcelData(UpperBound+1:end,:)};

%Examining the matrix piece by piece.
for i=1:size(PiecewiseExcelData,1)
   Changes=[];
   Divide=cell2mat(PiecewiseExcelData(i));

  %Jump rows of classification data is stored.
   for j=1:size(Divide,1)-1
     if Divide(j,6)~=Divide(j+1,6)
       Changes(1:2,end+1)=[j;Divide(j,6)] ;
     end
   end

   ChangesNew=Changes;


   if size(Changes,2)==0

      %Overcoming the 1 row data problem.
      if size(Divide,1)>1
      PiecewiseExcelDataNew(size(PiecewiseExcelDataNew,1)+1,:)={Divide(2:end,:)};
      else
      PiecewiseExcelDataNew(size(PiecewiseExcelDataNew,1)+1,:)={Divide};
```

```
            end
            NumOfMatrix(end+1)=1;

        else

        %Erasing the jump rows, if the data limit is not satisfied.

        if size(Changes)>=2
        for j=2:size(Changes,2)
            if (Changes(1,j)-Changes(1,j-1))<DataLimit
                if j==2 && Changes(1,j-1)>DataLimit
                    ChangesNew(:,j)=zeros;
                    else
                        ChangesNew(:,j-1:j)=zeros;
                end
            end
        end
       end

        if size(Changes,2)==1 && ((ChangesNew(1,1)-Divide(1,1)<DataLimit) || Divide(1,end)-
ChangesNew(1,end)<DataLimit)
            ChangesNew=[];
        end

          if size(Changes,2)>2
            m=size(Changes,2);
                if Changes(1,m)-Changes(1,m-1)>DataLimit
                  ChangesNew(:,m-1)=Changes(:,m-1);
                end
          end

        if Changes(1,1)<DataLimit
           ChangesNew(:,1)=[0 0]';
        end

        if size(ChangesNew,2)>0
        if size(Divide,1)-Changes(1,end)<DataLimit
            ChangesNew(:,end)=[0 0]';
        end
        end

        % Erasing zero columns.

        if size(ChangesNew,2)>=1
        ChangesNew(:,ChangesNew(1,:)==0)= [];
        end

       % Missing last row is added.
       if size(ChangesNew,2)>0 && size(Changes,2)>2
       if Changes(1, end)-Changes(1, end-1)<DataLimit && size(Divide,1)-Changes(1,
end)>DataLimit
            if ChangesNew(2,end)~=Changes(2,end)
               ChangesNew(1:2,end+1)=Changes(1:2,end);
            end
       end
       end

        %Erasing the first row, if the conditions are not satisfied.
```

```
        if size(ChangesNew,2)==1 && ChangesNew(2,1)==Divide(end,end) && size(Divide,1)-
Changes(1,end)>DataLimit
        ChangesNew(:,1)= [];
        end

        % Erasing the last row, if the conditions are not satisfied.
        if size(ChangesNew,2)>0 && size(Changes,2)>2
        if ChangesNew(2,end)~=Changes(2,1) && Changes(1,end-1)-Changes(1,end-2)>DataLimit
        ChangesNew(:,end)=[];
        end
        end

        ChangesNew=[[1;Divide(1,6)] ChangesNew [size(Divide,1);Divide(end,6)]];


      %For 3 jump changes, the data is erased if left and rigth data
      %are same.
      if size(ChangesNew,2)==3
            if ChangesNew(2,2)==ChangesNew(2,1) && ChangesNew(2,2)==ChangesNew(2,3)
            ChangesNew(:,2)=[];
         end
      end

      %For 4 jump changes, if datalimit is not satisfied, middle 2 jump
      %is erased.
      if size(ChangesNew,2)==4
         if ChangesNew(1,3)-ChangesNew(1,2)<DataLimit
            ChangesNew(:,2:3)=[];
         end
      end

      %Some small adjustments by considering the mean of soil type
      %zones.
      Store=ones(size(ChangesNew));
      for n=2:size(ChangesNew,2)-1
        if abs(mean(Divide(ChangesNew(1,n-1):ChangesNew(1,n),6))-
mean(Divide(ChangesNew(1,n):ChangesNew(1,n+1),6)))<MeanTol
          Store(:,n)=[0 0]';
        end
      end

       ChangesNew=Store.*ChangesNew;

        % Erasing zero columns.
        if size(ChangesNew,2)>=1
        ChangesNew(:,ChangesNew(1,:)==0)= [];
        end



        NumOfMatrix(end+1)=(size(ChangesNew,2)-1);
        %Erasing the segments into soil layers according to the jumpes.
        for k=2:size(ChangesNew,2)

PiecewiseExcelDataNew(size(PiecewiseExcelDataNew,1)+1,:)={Divide((ChangesNew(1,k-
1)+1):ChangesNew(1,k),:)};
        end
       end
```

```
    end

        %The original data that is lost is being retrieved.
        Location=[1];
        for i=2:size(NumOfMatrix,2)
        Location(end+1)=sum(NumOfMatrix(1:i-1))+1;
        end
        m=0;
        for i=1:size(Location ,2)
        m=m+1;
        First=[cell2mat(PiecewiseExcelData(m)) ] ;
        First=First(1,:);
        PiecewiseExcelDataNew(Location(i))={[First ;
cell2mat(PiecewiseExcelDataNew(Location(i)))]};
        end

       %When 2 same row exist, one of them is erased.
       for i=1:size(PiecewiseExcelDataNew,1)
        control=cell2mat(PiecewiseExcelDataNew(i));
        if size(control,1)>1
         if control(1,1)==control(2,1)
           control(1,:)=[];
           PiecewiseExcelDataNew(i)={control};
         end
        end
       end

end
```

```
function[PiecewiseExcelDataDrCu]=DrCu(PiecewiseExcelData,WaterDepth,NumFile,fileName)

PiecewiseExcelDataDrCu={};
Row=3;

for i=1:size(PiecewiseExcelData,1)
Data=cell2mat(PiecewiseExcelData(i));
UWeightS=20;
UWeightW=10;
Nk1=14;
Nk2=20;
Nk3=17;
K01=0.4;
K02=0.7;
K03=0.55;
[M,F] = mode(Data(:,6));
Ratio=100*F/size(Data,1);

%Calculation of Cu for clays.
if M==4
Class=M*ones(size(Data,1),1);
TStress=Data(:,1).*UWeightS+(-WaterDepth)*UWeightW;
Cu1=((Data(:,2)*1000)-TStress)./Nk1;
Cu2=((Data(:,2)*1000)-TStress)./Nk2;
Cu3=((Data(:,2)*1000)-TStress)./Nk3;
PiecewiseExcelDataDrCu{i}=[Data Cu1 Cu2 Cu3 Class];
end
```

```
%Calculation of Dr for sands.
if M==6
Class=M*ones(size(Data,1),1);
EStress=Data(:,1).*(UWeightS-UWeightW);
Dr1=(1/0.0296)*log(Data(:,2)./(2.494*(EStress.*((1+2*K01)/300)).^0.46));
Dr2=(1/0.0296)*log(Data(:,2)./(2.494*(EStress.*((1+2*K02)/300)).^0.46));
Dr3=(1/0.0296)*log(Data(:,2)./(2.494*(EStress.*((1+2*K03)/300)).^0.46));
% Dr2=(1/2.93)*log((1000.*Data(:,2))./(205*(EStress.*((1+2*K0)/3)).^0.51));
PiecewiseExcelDataDrCu{i}=[Data Dr1 Dr2 Dr3 Class];
end

if M==2 || M==9
Class=M*ones(size(Data,1),1);
PiecewiseExcelDataDrCu{i}=[Data];
end


%Writing to excel file.
if i>1
Row=Row+size(PiecewiseExcelDataDrCu{i-1},1)+1;
end
RowAdd=num2str(Row);
StartColumn1='A';
Start= strcat(StartColumn1,RowAdd);
ResultsFileName='ResultsDrCu';
Sheet=NumFile;
Temp=PiecewiseExcelDataDrCu(i);
xlswrite(ResultsFileName,Temp{1},Sheet,Start)

end

%Writing headings to excel sheets.
fileName={fileName, 'WaterDepth', WaterDepth};
xlswrite(ResultsFileName,fileName,Sheet,'A1');
Heading={'Depth (m)','Tip Resistance (MPa)','FR (%)','Sleeve Friction
(MPa)','Classification','Arranged Classification','Dr1(0.4) or Cu1 (14)','Dr2(0.7) or
Cu2(20)','Dr3(0.55) or Cu3(17)','Layer Name'};
xlswrite(ResultsFileName,Heading,Sheet,'A2');
warning('off','MATLAB:xlswrite:AddSheet')

end
```

```
function[SCL]=SCL_CPT_V2(PiecewiseExcelData, Spacing, DataLimit)


z=Spacing;
SCL={};

for i=1:size(PiecewiseExcelData,1)

B=cell2mat(PiecewiseExcelData(i));

if size(B,1)>DataLimit

%The name of soil layer is obtained.
[M,F] = mode(B(:,6));
```

```
Ratio=100*F/size(B,1);


for Focus=2:size(B,2)-2

%Workspace is cleared except some parameters.
clearvars -except B Focus i PiecewiseExcelData SCL Spacing z DataLimit M F Ratio

x=B(:,Focus);
y=B(:,1);
A=[x y];

%First Part-"constant approach". Mean of data is assumed to be constant
%through depth.

meanCPT=mean(A(:,1));
dif1=(A(:,1)-meanCPT);
for k=0:size(A,1)-1  ;
    dif12=zeros((size(A,1)-k),1);
for m=1:size(A,1)-k
  dif2(m,:)=(A((m+k),1)-meanCPT);
  dif12(m,:)=dif1(m).*dif2(m);
end
autoCor(k+1,:)=sum(dif12,1)/sum((dif1.^2),1);
lagDis(k+1,:)=k*z;
end
% figure
% scatter(lagDis,autoCor);
% str=sprintf('Constant Approach  Case %d', s);
% title([{fileName}; {str}]);
% hold on
% xlabel('Lag Distance (m)');
% ylabel('Autocorrelation Function');
% grid;
% set(gcf,'color','w');

%Utilizing four autocovariance function and evaluating spatial correlation
%length.

syms a x
f=exp(-x/a) ;
summ=0;
for k=1:size(lagDis,1)
 x0=lagDis(k);
subs(f,x,x0);
summ=summ+(autoCor(k)-subs(f,x,x0))^2;
end
err=sqrt(summ);
eqnF = matlabFunction(err);
a_exp=fminbnd(eqnF,lagDis(1),  lagDis(end));
corrLengthExpConstant=2*a_exp;
curveValue1=exp(-(1/a_exp).*lagDis);
R1Constant=1-sum((autoCor-curveValue1).^2)/sum((autoCor-mean(autoCor)).^2);
% k=lagDis(1):0.1:lagDis(end);
% l=exp(-(1/a_exp).*k);
% plot(k,l,'--');
% hold on
```

```
syms a x
f=exp(-(x/a)^2) ;
summ=0;
for k=1:size(lagDis,1)
 x0=lagDis(k);
subs(f,x,x0);
summ=summ+(autoCor(k)-subs(f,x,x0))^2;
end
err=sqrt(summ);
eqnF = matlabFunction(err);
a_sqr=fminbnd(eqnF,lagDis(1),  lagDis(end));
corrLengthSqrConstant=a_sqr*sqrt(pi);
curveValue2=exp(-(lagDis./a_sqr).^2);
R2Constant=1-sum((autoCor-curveValue2).^2)/sum((autoCor-mean(autoCor)).^2);
% k=lagDis(1):0.1:lagDis(end);
% l=exp(-(k/a_sqr).^2);
% plot(k,l,':k');
% hold on


syms a x
f=exp(-x/a).*cos(x/a) ;
summ=0;
for k=1:size(lagDis,1)
 x0=lagDis(k);
subs(f,x,x0);
summ=summ+(autoCor(k)-subs(f,x,x0))^2;
end
err=sqrt(summ);
eqnF = matlabFunction(err);
a_Autoreg=fminbnd(eqnF,lagDis(1),  lagDis(end));
corrLengthExpCosConstant=a_Autoreg;
curveValue3=exp(-(lagDis)/a_Autoreg).*cos((lagDis)/a_Autoreg);
R3Constant=1-sum((autoCor-curveValue3).^2)/sum((autoCor-mean(autoCor)).^2);
% k=lagDis(1):0.1:lagDis(end);
% l=exp(-k/a_Autoreg).*cos(k/a_Autoreg);
% plot(k,l,'-.');
% hold on


syms a x
f=exp(-x/a).*(1+x/a) ;
summ=0;
for k=1:size(lagDis,1)
 x0=lagDis(k);
subs(f,x,x0);
summ=summ+(autoCor(k)-subs(f,x,x0))^2;
end
err=sqrt(summ);
eqnF = matlabFunction(err);
a_4=fminbnd(eqnF,lagDis(1),  lagDis(end));
corrLengthSecOrAutoregressionConstant=4*a_4;
curveValue4=exp(-(lagDis)./a_4).*(1+(lagDis)./a_4);
R4Constant=1-sum((autoCor-curveValue4).^2)/sum((autoCor-mean(autoCor)).^2);
% k=lagDis(1):0.1:lagDis(end);
% l=exp(-k/a_4).*(1+k/a_4);
% plot(k,l);
```

```
% hold on
% legend('Data','Exponential','Squared Exponential','Cosine of Exponential','Second Order
Autoregressive');


%Second part-"Trend Approach". The mean of data is assumed to have a trend
%with depth.

nValue=A(:,1);
depth=A(:,2);

p = polyfit(A(:,2),A(:,1),1);       %the ax+b linear function is fitted to the data.
aTrend=p(1);
bTrend=p(2);
curveValueData=aTrend.*depth+bTrend;
RTrend=1-sum((nValue-curveValueData).^2)/sum((nValue-mean(nValue)).^2);

meanCPT=p(1).*depth+p(2);
dif1=(A(:,1)-meanCPT);

for k=0:size(A,1)-1  ;
    dif12=zeros((size(A,1)-k),1);
for m=1:size(A,1)-k
  dif2(m,:)=(A((m+k),1)-meanCPT(m+k));
  dif12(m,:)=dif1(m).*dif2(m);
end
autoCor(k+1,:)=sum(dif12,1)/sum((dif1.^2),1);
lagDis(k+1,:)=k*z;
end
% figure
% scatter(lagDis,autoCor);
% str=sprintf('Trend Approach  Case %d', s);
% title([{fileName}; {str}]);
% hold on
% xlabel('Lag Distance (m)');
% ylabel('Autocorrelation Function');
% grid;
% set(gcf,'color','w');

%Utilizing four autocovariance function and evaluating spatial correlation
%length.

syms a x
f=exp(-x/a) ;
summ=0;
for k=1:size(lagDis,1)
 x0=lagDis(k);
subs(f,x,x0);
summ=summ+(autoCor(k)-subs(f,x,x0))^2;
end
err=sqrt(summ);
eqnF = matlabFunction(err);
a_exp=fminbnd(eqnF, lagDis(1),  lagDis(end));
corrLengthExpTrend=2*a_exp;
curveValue1=exp(-(1/a_exp).*lagDis);
R1Trend=1-sum((autoCor-curveValue1).^2)/sum((autoCor-mean(autoCor)).^2);
% k=lagDis(1):0.1:lagDis(end);
% l=exp(-(1/a_exp).*k);
```

```
% plot(k,l,'--');
% hold on


syms a x
f=exp(-(x/a)^2) ;
summ=0;
for k=1:size(lagDis,1)
 x0=lagDis(k);
subs(f,x,x0);
summ=summ+(autoCor(k)-subs(f,x,x0))^2;
end
err=sqrt(summ);
eqnF = matlabFunction(err);
a_sqr=fminbnd(eqnF,lagDis(1),  lagDis(end));
corrLengthSqrTrend=a_sqr*sqrt(pi);
curveValue2=exp(-(lagDis./a_sqr).^2);
R2Trend=1-sum((autoCor-curveValue2).^2)/sum((autoCor-mean(autoCor)).^2);
% k=lagDis(1):0.1:lagDis(end);
% l=exp(-(k/a_sqr).^2);
% plot(k,l,':k');
% hold on


syms a x
f=exp(-x/a).*cos(x/a) ;
summ=0;
for k=1:size(lagDis,1)
 x0=lagDis(k);
subs(f,x,x0);
summ=summ+(autoCor(k)-subs(f,x,x0))^2;
end
err=sqrt(summ);
eqnF = matlabFunction(err);
a_Autoreg=fminbnd(eqnF,lagDis(1),  lagDis(end));
corrLengthExpCosTrend=a_Autoreg;
curveValue3=exp(-(lagDis)/a_Autoreg).*cos((lagDis)/a_Autoreg);
R3Trend=1-sum((autoCor-curveValue3).^2)/sum((autoCor-mean(autoCor)).^2);
% k=lagDis(1):0.1:lagDis(end);
% l=exp(-k/a_Autoreg).*cos(k/a_Autoreg);
% plot(k,l,'-.');
% hold on


syms a x
f=exp(-x/a).*(1+x/a) ;
summ=0;
for k=1:size(lagDis,1)
 x0=lagDis(k);
subs(f,x,x0);
summ=summ+(autoCor(k)-subs(f,x,x0))^2;
end
err=sqrt(summ);
eqnF = matlabFunction(err);
a_4=fminbnd(eqnF,lagDis(1),  lagDis(end));
corrLengthSecOrAutoregressionTrend=4*a_4;
curveValue4=exp(-(lagDis)./a_4).*(1+(lagDis)./a_4);
R4Trend=1-sum((autoCor-curveValue4).^2)/sum((autoCor-mean(autoCor)).^2);
```

```
% k=lagDis(1):0.1:lagDis(end);
% l=exp(-k/a_4).*(1+k/a_4);
% plot(k,l);
% hold on
% legend('Data','Exponential','Squared Exponential','Cosine of Exponential','Second Order
Autoregressive');


SCL{i,Focus-1}={'Depths',y(1),y(end)...
;'Column',Focus,''...
;'Constant Approach','',''...
;'Correlation Function','Spatial Correlation Length','R-Squared'...
;'Exponential',corrLengthExpConstant,R1Constant...
;'Squared exponential',corrLengthSqrConstant,R2Constant...
;'Cosine of Exponential',corrLengthExpCosConstant,R3Constant...
;'Second Order Autoregressive',corrLengthSecOrAutoregressionConstant,R4Constant...
;'Trend Approach','',''...
;'Trend Line Inclination and R-Squared',aTrend,RTrend ...
;'Correlation Function','Spatial Correlation Length','R-Squared'...
;'Exponential',corrLengthExpTrend,R1Trend...
;'Squared exponential',corrLengthSqrTrend,R2Trend...
;'Cosine of Exponential',corrLengthExpCosTrend,R3Trend...
;'Second Order Autoregressive',corrLengthSecOrAutoregressionTrend,R4Trend...
;'Classification',M,Ratio };


warning('off','MATLAB:xlswrite:AddSheet');

end
end
end
end
```

```
function []=WriteExcel(SCL,NumFile,fileName)

Sheet=NumFile;
Row=3;

%The row number of SCL is analysed by for loop.
for i=1:size(SCL,1)

    %The starting row is defined.
    if i>1
    Row=Row+size(SCL{1},1)+1;
    end

    %The starting Column is defined.
    RowAdd=num2str(Row);
    StartColumn1='A';
    Start1 = strcat(StartColumn1,RowAdd);
    StartColumn2='E';
    Start2 = strcat(StartColumn2,RowAdd);
    StartColumn3='I';
    Start3 = strcat(StartColumn3,RowAdd);

    StartCell={Start1,Start2, Start3};
```

```
  %The cell of SCL is written to excel file
   ResultsFileName='ResultsCPT';
   for j=1:3
   Temp=SCL(i,j);
   xlswrite(ResultsFileName,Temp{1},Sheet,StartCell{j})
   end

end

   %Name of boring is written.
   StartName='A1';
   fileName={fileName};
   xlswrite(ResultsFileName,strcat(fileName),Sheet,StartName)

end
```

APPENDIX B

FIELD DATA

B.1. Examples of SPT Data at Shallow Water

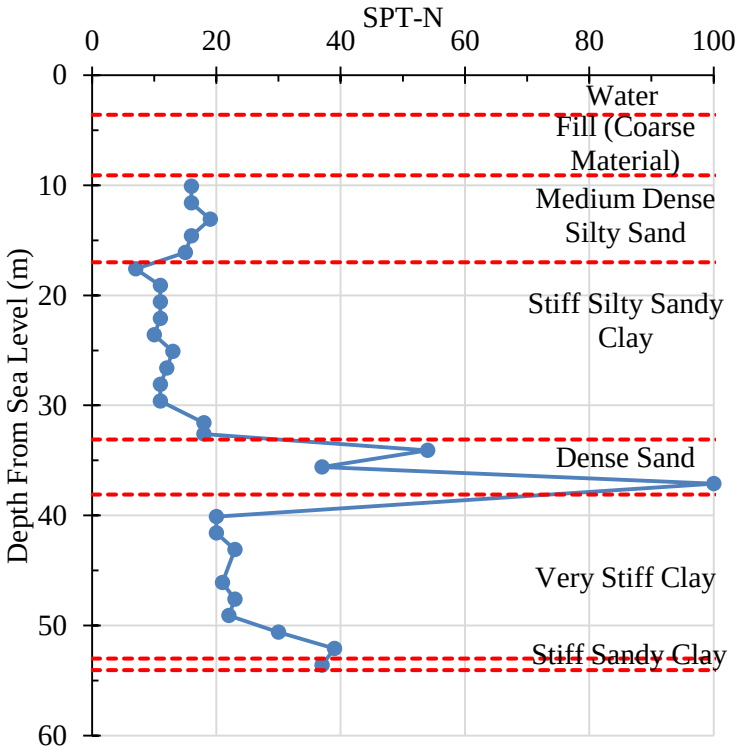

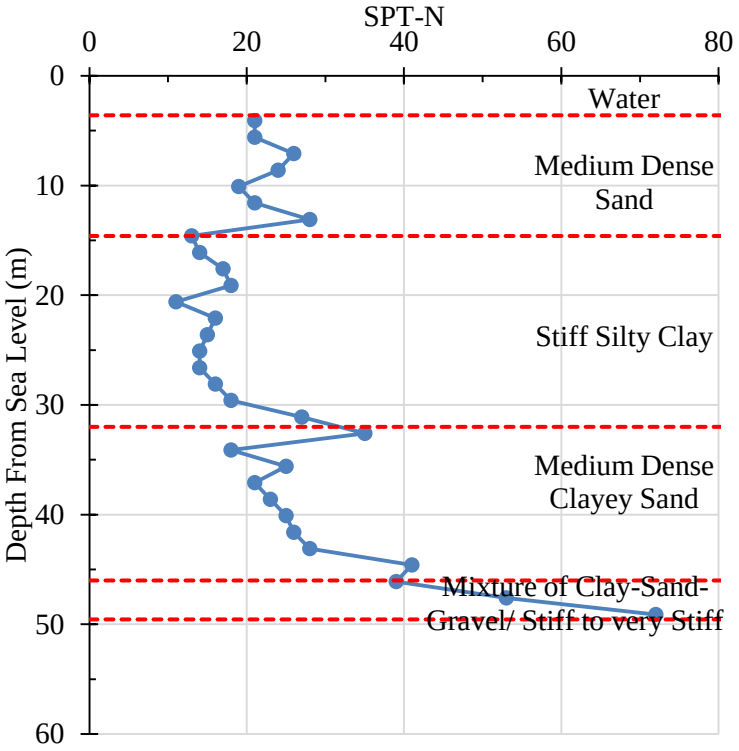
SPT-N
0
20
40
60
80
0
10
20
30
40
50
60
Depth From Sea Level (m)
Water
Medium Dense
Sand
Stiff Silty Clay
Medium Dense
Clayey Sand
Mixture of Clay-Sand-
Gravel/ Stiff to very Stiff

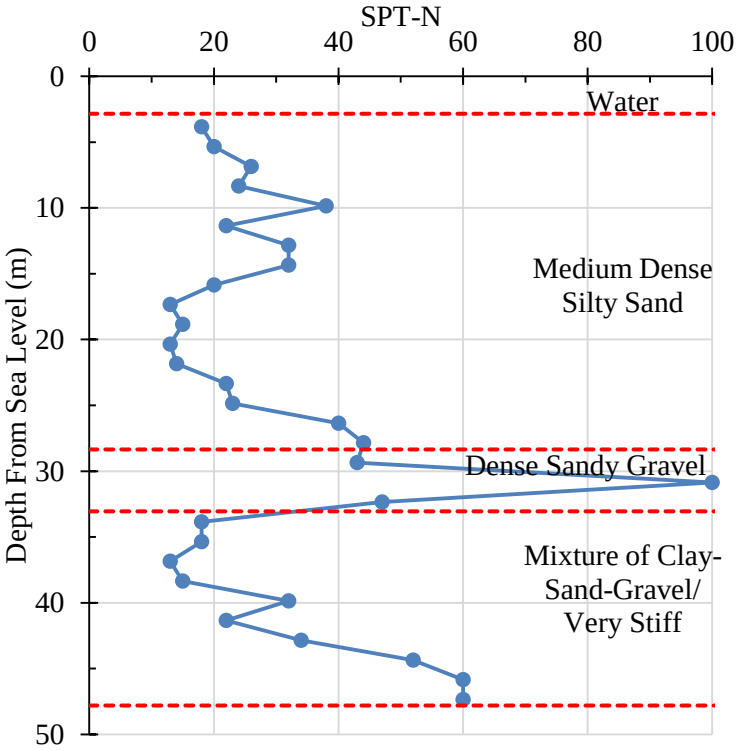
SPT-N
0
20
40
60
80
100
0
10
20
30
40
50
Depth From Sea Level (m)
Water
Medium Dense
Silty Sand
Dense Sandy Gravel
Mixture of Clay-
Sand-Gravel/
Very Stiff

B.2. Examples of CPT Data at Deep Water Locations